VISCOELASTIC BEHAVIOR OF FILLED AND UNFILLED ELASTOMERS IN MODERATELY LARGE DEFORMATIONS

Thesis by

Ricardo Bloch

In Partial Fulfillment of the Requirements

for the Degree of

Doctor of Philosophy

California Institute of Technology

Pasadena, California

1976

(submitted March 1, 1976)

To my wife Remie and my daughter Jennifer

ACKNOWLEDGMENTS

I would like to thank Professor N.W. Tschoegl, my advisor, for the invaluable help and guidance he provided during the entire course of this work. The several discussions and the assistance provided by W.V. Chang, which made this research possible, are gratefully acknowledged.

Dr. G. Kraus of Phillips Petroleum Company was very helpful and cooperated in both the testing and analysis phase of this project. The company also provided several samples for which I am grateful.

The generous fellowship provided by Phillips Petroleum Co. over a period of three years is deeply appreciated.

Finally, I want to express my gratitude to Dr. S. Sharda, Dr. R. Fillers, G. Ward, N. Panagiotacopulos and K. Engel for their assistance at various stages of this thesis.

The work was partially supported by the National Science Foundation whose financial support is gratefully acknowledged.

ABSTRACT

A constitutive model was developed for the description of the viscoelastic (time-dependent) behavior of soft rubberlike materials in moderately large deformations. The model assumes that time shift invariance is preserved in such deformations. Hence, the Boltzmann superposition integral remains valid and time-dependent behavior can be described by incorporating a nonlinear stress-strain law into it. The elastic potential of Blatz, Sharda, and Tschoegl, which is based on a generalized measure of strain, was used for this purpose.

A slightly plasticized styrene-butadiene copolymer rubber (SBR) was subjected to various modes of deformation in simple tension. The experimental data were compared with the theoretical predictions of the model. The agreement was unprecedentedly good.

In the course of this work a curious anomaly was discovered in the behavior of emulsion polymerized compression molded dicumyl-peroxide cured SBR. This material showed lack of time shift invariance in the region of very small strains in which elastomers generally follow a linear stress-strain law. Normally, non-preservation of time shift invariance is linked with stress-strain nonlinearity. In the anomalous SBR the former effect can be studied free of interference from the other.

To test the applicability of the model to filled elastomers, experiments were made on both crosslinked and uncrosslinked SBR

filled with a high-structure carbon black. The model, and several generalizations of it, failed to predict the behavior of the filled materials in response to small (theoretically infinitesimal) deformations superposed on a finite stretch. Such experiments may be considered looked upon as sensitive probes with which the behavior of the material may be explored in large deformations. The superposition tests confirmed that in carbon black filled rubbers there exists a network of secondary aggregates of the filler particles which is held together by Van der Waals forces. This network imparts to the filled rubber a thixotropic character with a rebuilding time of about 15 minutes at room temperature. Successful prediction of the properties of such a filled system must await the development of a new constitutive model which incorporates the thixotropic behavior.

TABLE OF CONTENTS

Chapter		Page
	Acknowledgments	iii
	Abstract	iv
1	INTRODUCTION	1
	References	3
2	THE BEHAVIOR OF RUBBERLIKE MATERIALS IN MODERATELY LARGE VISCOELASTIC DEFORMATIONS	5
	Introduction	6
	Theory of the Application of the Solid Model	8
	Theory of the Application of the Liquid Model	21
	Materials	21
	Experimental Methods	23
	Results	25
	Discussion	31
	References	39
3	STRAIN INDEPENDENT NONLINEARITIES IN PEROXIDE CURED SBR	59
	Introduction	60
	Theory	61
	Materials	62
	Experimental Methods	66
	Results	66
	Discussion	74
	References	77
4	VISCOELASTIC AND THIXOTROPIC BEHAVIOR IN CARBON BLACK FILLED SBR	89
	Introduction	90
	Theory	92
	Materials	100
	Results	105
	Discussion	112
	References	118

Appendix		Page
I	THE TIME-DEPENDENT RESPONSE OF SOFT POLYMERS IN MODERATELY LARGE DEFORMATIONS - A NEW APPROACH	135
	Abstract	136
	References	144
II	EXPERIMENTAL PROCEDURES	148
	Specimen Preparation	149
	Measurements of Mechanical Properties	152
	References	164

CHAPTER 1

INTRODUCTION

The subject of this thesis is the experimental investigation of the viscoelastic behavior of certain classes of filled and unfilled polymers. It is primarily concerned with the experimental verification of a new constitutive equation for soft (rubberlike) viscoelastic materials in moderately large deformations. We call moderately large deformations those in which time shift invariance is preserved, so that nonlinear effects arise solely from stress-strain nonlinearity (see Appendix I). As explained more fully in Appendix I, we can then write

$$\bar{\sigma}_\alpha(t) = - P + (2/3n) \int_o^t E(t-u) \frac{d\, \lambda_\alpha^n(u)}{du} du \qquad \alpha = 1,2,3 \qquad (1)$$

where $\bar{\sigma}_\alpha$ are the principal true stresses (force over deformed area), P is a hydrostatic pressure (present in the equation due to the assumption of incompressibility), E(t) is the tensile relaxation modulus, t is the current time, u is the past time, λ_α are the principal stretch ratios (deformed length over undeformed length), and n is a material parameter which characterizes the generalized strain

$$\underline{b}_\alpha = (\lambda_\alpha^n - 1)/n \qquad (2)$$

This generalized strain was used successfully by Blatz, Sharda, and Tschoegl[1,2,3,4] to describe the large elastic deformation of rubberlike materials. Equation (1) was developed by the author in collaboration with V. Chang, following a suggestion by Professor Tschoegl. This thesis discusses the applicability of Eq. (1) for describing deformations of crosslinked rubbers in general, and styrene-butadiene rubber (SBR)

in particular. It also discusses efforts made to adapt it to carbon black filled elastomers. Chang's thesis[5] will elaborate further on the basis and the development of our new approach to modelling the constitutive behavior of soft (rubberlike) materials and will discuss the applicability of Eq. (1) to uncrosslinked rubbers.

Chapter 2, and 3 of this thesis are written in the form of self-contained manuscripts ready for submission to Transactions of the Society of Rheology. Chapter 2 describes the viscoelastic behavior of crosslinked rubberlike materials in moderately large deformations. Chapter 3 deals with the anomalous behavior of peroxide cured SBR in which time shift invariance is not preserved even at quite small deformations in which the stress-strain behavior is linear. Chapter 4 is in the form of a manuscript to be submitted to Rubber Chemistry and Technology. It describes work on the viscoelastic behavior of carbon black filled rubber in moderately large deformations.

Appendix I is a copy of a manuscript already accepted for publication by the Proceedings of the National Academy of Sciences. This manuscript briefly describes the derivation of Eq. (1). Appendix II describes the experimental methods and procedures used by the author in more detail than is contained in the experimental parts of Chapters 2, 3, and 4.

References

1. P.J. Blatz, S.C. Sharda, and N.W. Tschoegl, *Proc. Nat. Acad. Sci.* 70, 3041(1973).

2. P.J. Blatz, S.C. Sharda, and N.W. Tschoegl, *Trans. Soc. Rheol.* 18

18, 145(1974).

3. S.C. Sharda, P.J. Blatz, and N.W. Tschoegl, *Letters* Appl. Eng. Sci., 2, 53(1974).

4. S.C. Sharda and N.W. Tschoegl, in Press, *Trans. Soc. Rheol.*

5. W.V. Chang, Ph.D. Dissertation, 1976, California Institute of Technology, Pasadena, California 91125.

CHAPTER 2

THE BEHAVIOR OF RUBBERLIKE MATERIALS IN MODERATELY LARGE VISCOELASTIC DEFORMATIONS

INTRODUCTION

A three-dimensional constitutive equation capable of describing the viscoelastic behavior of elastomers under finite deformations is indispensible for a rational study of their mechanical response. In a recent publication[1] we concluded that theories based on integral expansions of a functional with respect to a fixed strain measure usually suffer the same shortcomings as elastic constitutive equations based on the Taylor expansion of a strain energy density function: the rate of convergence of the expansion is so slow that prediction of the response of a material under different modes of deformation requires more terms than the number which can be uniquely determined[2].

However, the situation is somewhat more favorable if one does not attempt to describe the mechanical response of all materials but rather limits oneself to some particular class. Published data indicate[1] that the effects of time and strain are separable at moderate strains in both uniaxial and multiaxial stress relaxation or creep curves obtained on crosslinked or uncrosslinked soft (rubberlike) polymeric materials, i.e. in regions of the response which are not too close to the glassy region. This experimental fact implies[1] that a three-dimensional single integral constitutive equation is more appropriate than a multiple integral constitutive equation.

Furthermore, if the effects of time and strain are uncoupled, then time shift invariance is preserved in the appropriate range of finite strains. We have called[1,3] deformations to which these observations

apply *moderately large viscoelastic deformations*. In such deformations any nonlinear behavior results only from stress-strain nonlinearity. In a series of earlier publications[1,3-7] we had introduced a simple single-term strain energy density function based on the idea of a generalized strain measure characterized by a single material parameter, n, which successfully described the *elastic moderately large deformations* of several elastomers. We later showed[1,3] that introduction of this strain measure into the Boltzmann Superposition integral allows the phenomenological description and prediction of viscoelastic moderately large deformations of rubberlike materials. In this paper we present a detailed examination of this theory on hand of our own as well as literature data on crosslinked elastomers. Another paper[8] presents a similar examination on uncrosslinked rubberlike materials.

Two models were proposed[1]: one is designed for polymeric solids such as crosslinked and uncrosslinked rubberlike materials and the other for polymeric liquids such as polymer melts. These models contain a single time dependent material function (the relaxation modulus of linear viscoelastic theory) and the material constant n which characterizes the strain measure. Both of these two pieces of information can be obtained by conducting stress relaxation experiments under small as well as moderate strains[1,3].

To examine the range of validity of our models, we must check their predictions against the experimentally determined responses of a variety of materials to different time-dependent loading histories under different homogeneous and nonhomogeneous states of strain. Before proceeding to complex loading geometries, we first investigate the

applicability of the models to different strain histories in simple tension.

THEORY OF THE APPLICATION OF THE SOLID MODEL

Our solid model (model S of reference 1), designed for an isotropic incompressible rubberlike material, yields

$$\bar{\sigma}_\alpha(t) = -P + (2/3n)\int_o^t E(t-u)\,\frac{d\lambda_\alpha^n(u)}{du}\,du \qquad \alpha = 1,2,3 \qquad (1)$$

as the equation for the principal true stress components in an orthogonal deformation, i.e. in directions remaining unchanged. In eq. (1) $\bar{\sigma}_\alpha(t)$ is the principal true stress in the α-direction at the current time t, P is an unspecified hydrostatic pressure, n is the material constant characterizing the strain measure, E(t) is the small deformation tensile relaxation modulus, and $\lambda_\alpha(u)$ is the principal stretch ratio in the α-direction at the past time u. Eq. (1) is limited to isothermal deformations, although it can be modified to cover non-isothermal conditions. In an isothermal deformation (the case we are interested in) $\lambda_\alpha(u)$ is defined as

$$\lambda_\alpha(u) = L_\alpha(u,T)/L_{\alpha o}(T) \qquad (2)$$

where $L_{\alpha o}(T)$ is the length of the specimen in the α-direction at zero stress at the test temperature T, and $L_\alpha(u,T)$ is the length of the specimen in the same direction at time u at the same temperature. Eliminating P we obtain the true stress in uniaxial tension as

$$\bar{\sigma}(t) = (2/3n)\int_0^t E(t-u)d\frac{[\lambda^n(u) - \lambda^{-n/2}(u)]}{du}\,du \qquad (3)$$

If $\lambda(u)$ is continuous, we may use

$$\bar{\sigma}(t) = (2/3)\int_0^t E(t-u)[\lambda^{n-1}(u) + 0.5\lambda^{-(n+2)/2}(u)]\,\frac{d\lambda(u)}{du}\,du \qquad (4)$$

We now develop special forms of eqs. (3) or (4) for different strain histories in uniaxial tension.

Ramp Function of Strain

We begin by considering the imposition of a constant rate of strain, i.e. a ramp function. The stretch ratio becomes

$$\lambda(u) = 1 + \dot{\varepsilon}u \qquad (5)$$

where $\dot{\varepsilon}$ is the rate of strain. Thus

$$d\lambda(u) = \dot{\varepsilon}du \qquad (6)$$

and eq. (4) yields

$$\bar{\sigma}(t) = (2\dot{\varepsilon}/3)\int_0^t E(t-u)](1 + \dot{\varepsilon}u)^{n-1} + 0.5(1 + \dot{\varepsilon}u)^{-(n+2)/2}]\,du \qquad (7)$$

The nominal stress results as

$$\sigma(t) = [2\dot{\varepsilon}/3(1 + \dot{\varepsilon}t)]\int_o^t E(t-u)[(1 + \dot{\varepsilon}u)^{n-1} + 0.5\ (1 + \dot{\varepsilon}u)^{-(n+2)/2}]du \quad (8)$$

Evaluation of the integral requires numerical integration.

Exponential Stretch Ratio

Let the excitation function be given by

$$\lambda(u) = \exp(ku) \quad (9)$$

where k is a constant. Then

$$d\lambda(u) = k \exp(ku)du \quad (10)$$

and substitution into eq. (4) yields

$$\bar{\sigma}(t) = (2k/3\int_o^t E(t-u)\ \exp(ku)[(\exp(ku))^{n-1} + 0.5\ (\exp(ku))^{-(n+2)/2}]\ du \quad (11)$$

Again, numerical integration is necessary to evaluate $\bar{\sigma}(t)$.

Ramp Followed by a Constant Strain

If the strain history consists of the imposition of a constant rate of strain to $t = t_1$ at which time the extension is held constant, we have

$$\lambda(u) = 1 + \dot{\varepsilon}uh(u) - \dot{\varepsilon}(u - t_1)h(u - t_1) \tag{12}$$

where $h(u)$ is the unit step function. Then

$$d\lambda(u) = \dot{\varepsilon}[h(u) - h(u - t_1) + u\delta(u) - (u - t_1)\delta(u - t_1)]\, du \tag{13}$$

where $\delta(u)$ is the delta function. Inserting this into eq. (4) we see that the delta function terms contribute nothing so that we may write

$$d\lambda(u) = \begin{cases} \dot{\varepsilon}du & \text{for} \quad u < t_1 \\ \\ o & \text{for} \quad u > t_1 \end{cases} \tag{14}$$

for convenience. Consequently

$$\bar{\sigma}(t) = (2\dot{\varepsilon}/3)\int_o^{t_1} E(t-u)[(1 + \dot{\varepsilon}u)^{n-1} + 0.5(1 + \dot{\varepsilon}u)^{-(n+2)/2}]\, du \tag{15}$$

which differs from eq. (7) only in the upper limit of integration. We note that eq. (15) is not a convolution integral.

Trapezoidal Function of Strain

We now consider the previous strain history but follow it with a descending ramp. Thus, we impose a constant rate of strain $\dot{\varepsilon}_1$ to $t = t_1$, hold the strain constant until $t = t_2$, and then impose another constant rate of strain $\dot{\varepsilon}_2$ but with the direction of travel of the crosshead reversed. The excitation function thus has the shape of a trapezoid. We have

$$\lambda(u) = 1 + \dot{\varepsilon}_1 u h(u) - \dot{\varepsilon}_1 (u - t_1) h(u - t_1) - \dot{\varepsilon}_2 (u - t_2) h(u - t_2) \tag{16}$$

and

$$d\lambda(u) = [\dot{\varepsilon}_1 h(u) - \dot{\varepsilon}_1 h(u - t_1) - \dot{\varepsilon}_2 h(u - t_2) + \dot{\varepsilon}_1 u \delta(u) - \dot{\varepsilon}_1 (u - t_1)\delta(u - t_1) - \dot{\varepsilon}_2 (u - t_1)\delta(u - t_1)]\, du \tag{17}$$

Again, the delta function terms will contribute nothing. Hence

$$d\lambda(u) = \begin{cases} \dot{\varepsilon}_1\, du & \text{for} \quad u < t_1 \\ 0 & \text{for} \quad t_1 < u < t_2 \\ -\dot{\varepsilon}_2\, du & \text{for} \quad u > t_2 \end{cases} \tag{18}$$

Substitution into eq. (4) yields

$$\bar{\sigma}(t) = \bar{\sigma}(t;t_1,\dot{\varepsilon}_1) - (2\dot{\varepsilon}_2/3)\int_{t_2}^{t} E(t-u)[\lambda_p^{n-1}(u) + 0.5\ \lambda_p^{-(n+2)/2}(u)]\ du \tag{19}$$

where $\bar{\sigma}(t;t_1,\dot{\varepsilon}_1)$ is the stress given by eq. (15) and

$$\lambda_p(u) = 1 + \dot{\varepsilon}_1 t_1 - \dot{\varepsilon}_2(u - t_2) \tag{20}$$

Step Function of Strain

For an excitation represented by a step function of strain we may write

$$\lambda^n(u) = 1 + (\lambda_o^n - 1)h(u) \tag{21}$$

where λ_o is the stretch ratio corresponding to the constant strain ε_o imposed at $t = 0$. Substitution into eq. (3) yields

$$\bar{\sigma}(t) = (2/3n)\ E(t)(\lambda_o^n - \lambda_o^{-n/2}) \tag{22}$$

as the sought-for expression for the stress. As $t \to \infty$, eq. (22) reduces to the equation of Blatz, Sharda, and Tschoegl[5]

$$\bar{\sigma}(\infty) = (2G/n)(\lambda_o^n - \lambda_o^{-n/2}) \tag{23}$$

if we let $E(\infty) = 3G$, where G is the (equilibrium) shear modulus.

Equation (23) is applicable to purely elastic behavior in moderately large deformations.

From Eq. (22) we obtain the nominal stress as

$$\sigma(t) = (2/3n)\ E(t)[\lambda_o^{n-1} - \lambda_o^{-(n+2)/2}] \tag{24}$$

We note that it is not possible experimentally to impose a finite strain instantaneously. In practice a step function of strain consists invariably of a ramp followed by a step as discussed earlier. However, if t_1 is much smaller than the first time of interest, the "ramp transients" will have effectively decayed and the response will have become sensibly indistinguishable from the response elicited by the imposition of a true step function.

Small Step Function Superposed on a Finite Step of Strain

We now consider a small deformation superposed on a moderately large one. Let the small strain superposed at t_r be given by ε_s and the large stretch ratio by λ_r. Further, assume that the stress due to the finite deformation has substantially relaxed when the small deformation is superimposed. Then

$$\lambda = \lambda_r + \varepsilon_s \tag{25}$$

and we have

$$\lambda^n = \lambda_r^n + \lambda_r^{n-1}\, n\varepsilon_s \tag{26}$$

because, by stipulation, $\varepsilon_s << (\lambda_r - 1)$. Thus, for a superposed step function of small strain we may write

$$\lambda^n(u) = 1 + (\lambda_r^n - 1)h(u) + (\lambda^n - \lambda_r^n)h(u - t_r) \tag{27}$$

or, using eq. (26),

$$\lambda^n(u) = \lambda_r^n(u) + n\varepsilon_s \lambda_r^{n-1} h(u - t_r) \tag{28}$$

where

$$\lambda_r^n(u) = 1 + (\lambda_r^n - 1)h(u) \tag{29}$$

Note that $\lambda_r(u)$ is a function of time. We consider that the stress induced by it has largely relaxed but it is not necessary to assume that it has reached elastic equilibrium. Now, the incremental true stress at $t > t_r$ arising from the superposition of the small deformation at $t = t_r$ is

$$\Delta\bar{\sigma}(t-t_r) = \bar{\sigma}(t) - \bar{\sigma}_r(t) \tag{30a}$$

where $\bar{\sigma}(t)$ is obtained from eq. (3) using eq. (28), and $\bar{\sigma}_r(t)$ is obtained similarly but using eq. (29). Consequently,

$$\Delta\bar{\sigma}(t-t_r) = (2/3n)\int_o^t E(t-u)d[\lambda_s^n(u) - \lambda_s^{-n/2}(u)] \tag{30b}$$

where

$$\lambda_s^n(u) = \lambda^n(u) - \lambda_r^n(u) = n\varepsilon_s\lambda_r^{n-1}h(u-t_r) \tag{31}$$

Substituting eq. (31) into (30b) we find

$$\Delta\bar{\sigma}(t-t_r) = \varepsilon_s f(\lambda_r)E(t-t_r) \tag{32}$$

where

$$f(\lambda_r) = (2/3)[\lambda_r^{n-1} + 0.5\ \lambda_r^{-(n+2)/2}] \tag{33}$$

The relaxation modulus, $E_s(t)$, obtained from the superposed deformation results as

$$E_s(t-t_r) = \Delta\bar{\sigma}(t-t_r)/\varepsilon_s = f(\lambda_r)E(t-t_r) \tag{34}$$

Since the imposition of a step function of strain in practice consists of a rapid extension at constant rate (ramp function) to the desired strain which is then held constant, it is necessary to assume that the effect of the ramp excitation has become negligible when the first value of $E_s(t)$ is calculated from the experimentally observed response. The effect of the ramp excitation required to impose the finite elongation, λ_r, is, of course, considered to have become sensibly negligible

at t_r.

The superposition of small strains on an effectively relaxed finite deformation may be regarded as a tool with which it is possible to probe the induced anisotropy of a material subjected to a finite elastic deformation as if the deformed body represented a new material. In simple tension our theory predicts these changes through the function $f(\lambda_r)$ which may be looked upon as the ratio of the relaxation modulus of the deformed material to that of the undeformed one.

The function $f(\lambda_r)$ is plotted in Fig. 1 for several values of n. For $n \leq 1$ the function decreases monotonically with λ_r, indicating strain softening. When $n > 1$, the function has a minimum at

$$\lambda_{r,min} = [(n + 2)/4(n - 1)]^{2/3n} \tag{35}$$

For n close to unity the minimum is so shallow that, for practical purposes, the material may be considered strain softening. As n moves close to 2, the minimum moves close to $\lambda_r = 1$ so that the material appears as purely strain hardening. The minimum lies at $\lambda_r = 1$ for $n = 2$ and moves to $\lambda_r < 1$ (simple compression) for $n > 2$.

Small Ramp Superposed on a Finite Step Function of Strain

Superposing a small ramp function of strain (constant rate of strain) on a sensibly relaxed finite elongation, eq. (25) becomes

$$\lambda(u) = \lambda_r + \dot{\varepsilon}(u-t_r)h(u-t_r) \tag{36}$$

and $\lambda_s^n(u)$ becomes

$$\lambda_s^n(u) = n\dot{\varepsilon}\lambda_r^{n-1}(u-t_r)h(u-t_r) \tag{37}$$

Consequently, when $t > t_r$, the incremental stress resulting from the superposed small ramp function of strain is obtained from eq. (30) as

$$\Delta\bar{\sigma}(t-t_r) = \dot{\varepsilon}f(\lambda_r)\int_o^{t-t_r} E(t-t_r-w)\ dw \tag{38}$$

by a change of variable from $u-t_r$ to w. We may then write

$$F_s(t-t_r) = \Delta\bar{\sigma}(t-t_r)/\dot{\varepsilon}(t-t_r) = f(\lambda_r)F(t-t_r) \tag{39}$$

where

$$F(t) = (1/\dot{\varepsilon}t)\int_o^t E(t-u)\ du \tag{40}$$

is the time dependent secant modulus extensively used by T.L. Smith[9].

Small Sinusoidal Oscillation Superposed on a Finite Step Function of Strain

For this case we have

$$\lambda(u) = \lambda_r + \varepsilon_s \exp[j\omega(u-t_r)]h(u-t_r) \tag{41}$$

where ε_s is the peak amplitude of the oscillation and ω is its radian frequency. We obtain

$$\lambda_s^n(u) = n\varepsilon_s \lambda_r^{n-1} \exp[j\omega(u-t_r)]h(u-t_r) \tag{42}$$

and the incremental true stress at $t > t_r$ becomes

$$\Delta\bar{\sigma}(t-t_r) = \varepsilon_s f(\lambda_r) j\omega \int_o^{t-t_r} E(t-t_r-u)\, \exp(j\omega u)\, du \tag{43}$$

by substitution into eq. (30). for the steady state eq. (43) yields

$$E_s'(\omega) = f(\lambda_r)E'(\omega) \tag{44a}$$

and

$$E_s''(\omega) = f(\lambda_r)E''(\omega) \tag{44b}$$

where $E'(\omega)$ and $E''(\omega)$ are the real and imaginary components of the complex tensile modulus. To see this, we set

$$L j\omega \int_o^t E(t-u)\, \exp(j\omega u)\, du = \frac{j\omega \bar{E}(s)}{s-j\omega} \tag{45}$$

where the right hand side represents the Laplace transform of the

expression on the left, s being the transform variable. $\bar{E}(s)$, the transform of E(t), may be represented by the ratio of two polynomials in s. Thus we may write

$$\frac{j\omega\bar{E}(s)}{s-j\omega} = \frac{j\omega\bar{e}(s)}{(s-j\omega)\bar{r}(s)} = \frac{A}{s-j\omega} + \frac{\bar{B}(s)}{\bar{r}(s)} \quad . \tag{46}$$

The second equation on the right results from decomposition into partial fractions, A being a constant, and $\bar{B}(s)$ being an (unspecified) polynomial in s. The first term on the far right results from the response to the driving transform while the second term represents the response arising from the material transform. Thus, the first term represents the steady state response and the second the transient response. By the theory of partial fraction decomposition

$$A\bar{r}(s) + (s-j\omega)\bar{B}(s) = j\omega\bar{e}(s) \tag{47}$$

and we find

$$A = \frac{j\omega\bar{e}(s)}{\bar{r}(s)}\bigg|_{s=j\omega} = s\bar{E}(s)\bigg|_{s=j\omega} = E^*(\omega) \tag{48}$$

where $E^*(\omega)$ is the complex tensile modulus by definition.

It follows that

$$\frac{\Delta\bar{\sigma}(\omega)}{\varepsilon_s} = E^*_s(\omega) = f(\lambda_r)E^*(\omega) \tag{49}$$

Sample Preparation

Samples were prepared according to the following recipe:

SBR 1502	100 parts
N-phenyl-2-naphtyl amine (antioxidant)	1 part
Dicumyl peroxide	1 part

The dicumyl peroxide was Hercules, Inc., Di-Cup®. The ingredients were cold-milled on a two-roll laboratory mill. The milled material was placed in 15.2 x 15.2 x 0.2 cm (6 x 6 x 0.08 inch) molds and cured for fifteen minutes at about 1750 bar (25000 psi) pressure at a temperature of about 160°C(325°F).

The sol fraction of the samples never exceeded 6%. The number average molecular weight of the network chains was 13000 as determined by equilibrium swelling measurements at 23°C in n-heptane, using [10] a χ-value of 0.589.

Dow Corning series 200 silicone oil (10 centistokes) was used as plasticizer. Unplasticized peroxide cured SBR gave anomalous results as described in the companion paper[11]. When plasticized with the silicone oil (to about 1.5%) the behavior was normal and conformed with results obtained on other rubbers.

Specimen Preparation

All experiments were made on tab bonded strip specimens. The strips were cut from molded sheets using a knife-edged mill blade. U-shaped phosphorus bronze tabs were glued to the ends using a poly(cyano acrylate) (Devcon Corp. Zip Grip 10®).

Two kinds of specimen were used. Specimen A had dimensions of about 12 x 0.5 x 0.2 cm. To minimize end effects, the area of contact between the strips and the tabs (i.e. the bonded area) was kept as small as possible. The length of overlap on each side at both ends of the strips was 1.5 mm. Specimen B was a short specimen with dimensions of about 1.0 x 0.5 x 0.2 cm. The tabs overlapped one third of the length on each side at both ends. In such a short specimen a uniaxial tension produces a nonhomogeneous biaxial stress-strain field.

For some experiments, the specimens (A) were extracted with toluene for at least two days before bonding. The toluene extracted and unextracted specimens gave identical results. The specimens were plasticized after bonding by immersion in the silicon oil at 23°C for at least forty-eight hours to ensure equilibrium uptake.

The exact width and length of the specimens were measured with a travelling microscope. Thicknesses were determined with a micrometer. When not in use, the specimens were kept in a refrigerator at 0°C.

EXPERIMENTAL METHODS

Experiments were made in uniaxial tension on a Model TTB Instron Testing machine fitted with a Missimers temperature control chamber. Special baffles were installed to reduce the effect of the air currents which tended to shake the specimen, thus superposing random oscillations on the force recorded. The temperature was monitored through a thermocouple placed close to the specimen. The temperature could be

controlled to about $\pm$0.1°C in the operative range from -20 to 23°C. At temperatures below -20°C, the specimens (A) tended to fail at the rubber-bronze interface of the tabs.

The range of crosshead speeds covered the entire operative range of the instrument from 0.00508 to 50.8 cm (0.002 to 20 inches) per minute. Stretch ratios were kept below 3 for the reasons given in the discussion. No appreciable heat built up in the specimen even at the highest crosshead speed over the short time interval required. Careful experiments[12] showed that strains calculated from cathetometer readings of bench marks placed on specimens of type A agreed with those calculated from the recorded trace of force against time.

To increase the precision of the measurements, most of the work reported in detail was made on a single specimen of type A. Ample time (never less than five times the previous duration of the experiment) was allowed between experiments so that the sample would recover its original properties. During these recovery periods the specimen was removed from the grips. To decrease the recovery time between experiments, each series of experiments was carefully planned and tests requiring smaller deformations were made before those in which larger deformations were applied. The length of the optimum recovery times was established in a series of tests not reported here[12].

Upon installation the specimen was first attached to the upper grip so that it would hang by its own weight (about 1.5 g). The force registering on the load cell was then balanced to zero, and the specimen was connected to the lower grip. Since this operation normally introduced some stress in the specimen, the crosshead was now

adjusted until the force reading again returned to zero, and the specimen was rested for at least thirty minutes. Bending or buckling of the specimen was minimized by proper alignment. This problem is discussed in detail elsewhere[12].

Below room temperature the evaporation of silicone oil from the plasticized specimens was negligible. Hence, the specimen could be considered thermodynamically as a closed system. After concluding a set of experiments the specimen was restored to room temperature and several small deformation ramp tests were made to ascertain that no noticeable change had occured in the mechanical properties.

RESULTS

Our first task was the determination of the small deformation tensile relaxation modulus, E(t), at the reference temperature, 23°C. This was accomplished by the standard procedure, using time-temperature superposition to widen the experimental window. At each temperature several isothermal segments were obtained to attain different final strains. Data were read for times longer than $10t_1$ (where t_1 is the time required to impose the final strain) so the ramp transient behavior had effectively decayed away. The maximum strain always remained in the region within which the true stress was linear in the strain. The results at different final strains were averaged and the isothermal segments were shifted into superposition. For the sake of increased accuracy, the ordinates were amplified and the abscissae were compressed to maximize the curvature and facilitate shifting. No vertical shifts

from which eqs. (44) follow in turn.

THEORY OF THE APPLICATION OF THE LIQUID MODEL

Our liquid model (model L of reference 1) yields the equation

$$\bar{\sigma}_{\alpha}(t) = - P + (2/3n)\int_{o}^{t} E(t-u)d[\lambda(t)/\lambda(u)]^{n}\, du \qquad (50)$$

for the principal true stress components in the homogeneous deformation of an incompressible material eq. (50) should be compared with eq. (1). The theory of the liquid model is fully developed elsewhere[1]. As far as its application is concerned, we are here interested only in its response to a small ramp function superposed on a finite step of strain. As shown elsewhere[8], this response is

$$F_{s}(t-t_{r}) = \frac{\Delta\bar{\sigma}(t-t_{r})}{\dot{\varepsilon}(t-t_{r})} = \lambda_{r}^{-1}F(t-t_{r}) + (2/3)f(\lambda_{r})E(t) - \lambda_{r}^{-1}E(t) \qquad (51)$$

which should be compared with the corresponding equation for the solid model, eq. (39).

MATERIALS

The work described in this paper was carried out on a styrene-butadiene rubber, using Phillips ® SBR 1502 as gum stock.

($T_o\rho_o/T\rho$) were required. This matter is discussed further elsewhere[13]. The parameters of the WLF equation were $c_1 = 4.9$ and $c_2 = 121$ °C.

The master curves thus obtained on the unplasticized and the plasticized sample are displayed in Fig. 2 using different origins for the ordinates for convenience.

The differences between the two samples do not show up in relaxation tests[11]. Consequently, the two master curves, which cover essentially the region between the entanglement and rubbery plateau, are closely similar.

Although numerical data could have been used, it was deemed convenient to represent the relaxation function by an equation. We used the equation[14]

$$E(t) = E_e + \frac{E}{1 + (t/\tau)^k} \tag{51}$$

For the plasticized sample the coefficients in eq. (51) were found by nonlinear least squares fitting to be: $E_e = 6.27$ bar*, $E = 37.74$ bar, $\tau = 6.8 \times 10^{-7}$ minutes, and $k = 0.1848$. This equation fitted the data within $\pm$ 2% over the range from $t = 10^{-6}$ to 10^3 minutes.

The second piece of information which our theory requires is the strain parameter n. To obtain it, relaxation tests were first made as described before but imposing strains which are outside of the linear true stress-strain range. Such curves are shown in Fig. 3, plotted as log $\sigma(t)$ vs. log t. They are parallel, vindicating our basic assumption that time shift invariance is preserved in these deformations. We next selected a suitable isochronal time, t_r (in our case $t_r = 10$ min.),

---

*One bar equals 10^6 dyne/cm^2 or 14.5 psi.

and crossplotted the stress σ_r as a function of λ_r as shown in Fig. 4, in which each solid circle represents a separate experiment. The parameter n is then obtained from a nonlinear least squares fit to the data. In our case n = 1.22 and the solid line represents the isochronal form of eq. (24)

$$\sigma_r = (2/3n)E(t_r)[\lambda_r^{n-1} - \lambda_r^{-(n+2)/2}] \tag{52}$$

with $E(t_r)$ taken from the master curve, Fig. (2). The insert shows the linear true stress-strain region and the corresponding nominal stress-strain values. We remark that our theory implies that any t_r will produce the same n (cf. Fig. 3) if it is chosen correctly experimentally, i.e. if care is taken that ramp transients have died out and the strains do not exceed the region within which the theory is applicable. We point out that we calculate t_r from the moment the specimen is first deformed, i.e. from t = 0 and not from $t = t_1$. We do this because relaxation proceeds throughout the imposition of the ramp required to produce the constant strain.

The basic assumption underlying our theory, that of the preservation of time shift invariance in moderately large deformation, was further verified in a set of experiments involving the short specimen B. Relaxation experiments at various extension ratios (the strain is not known with this specimen) produced log f vs. log t curves (where f is the force in the direction of the stretch) which were not only parallel to each other, but were parallel also to the curves obtained in true uniaxial tension. As mentioned before, specimen B produces a

nonhomogeneous biaxial stress-strain field. The experiments, which we have not reported here in detail, indicate that time shift invariance is preserved not only in homogeneous uniaxial stress-strain fields.

We can now begin the presentation of the experimental results which verify the validity of our theory. Figure 5 shows stress-strain data obtained using specimen A at four strain rates spanning three and a half decades of time. The solid lines represent eq. (8). The necessary calculations were performed on a computer, replacing the integration by summation, dividing the time interval into 100 identical steps. Finer divisions, as many as 500, showed almost no change in the results. Several trials showed that single precision sufficed for these calculations. We followed the same procedure in all our other integral evaluations. The lower limit of integration (0) does not present any problem because eq. (51) does not diverge for $t = 0$. This is not the case with other possible representations of $E(t)$ as, e.g., the Nutting equation[15]

$$E(t) = E_e[1 + (t/\tau)^{-k}] \tag{53}$$

The fit of the predictions to the experimental data is unprecedentedly good. The worst deviation, which occurs at the highest strain rate at the highest strains, is still only of the order of 2%. It should be noted that this deviation is not due to the appearance of the upswing in the stress-strain curve because this would have made the experimental points lie above the solid curve, not below it. We consider the most likely source of this slight discrepancy to be a possible inadequacy of

either eq. (51) or of the data themselves at short times.

Figure 6 plots the same data but in a way which emphasizes the behavior at small strains. It shows clearly that the behavior becomes linear at small strains. The envelope represents the function

$$\eta(t) = tF(t) = \sigma(t)/\dot{\varepsilon} \tag{54}$$

of linear viscoelastic theory.

Prediction of the response to the removal or reversal of a strain is generally regarded[16] to be a more severe test than the prediction of the response to an imposition of strain. Accordingly, we tested our theory in a trapezoidal excitation. The response (solid circles) is shown as well as the prediction (solid lines) in Fig. 7. The first, ascending portion of the curve represents the data at the highest strain rate shown in Fig. 5. The very slight deviation around the point where the crosshead was stopped is the same as that apparent in Fig. 5. Clearly, eq. (19) rather well predicts not only the first (ascending) ramp ($\dot{\varepsilon}$ = 4.536 min^{-1}) and the constant strain ($\dot{\varepsilon}$=0) data, but also those in the second (descending) ramp deformation ($\dot{\varepsilon}$ = -1.134 min^{-1}). Figure 8 displays the same data as stress vs. strain, emphasizing the excellent prediction in the descending ramp region. If the slight deviation in the ascending ramp prediction as the highest stress results from partial failure of eq. (51) as suggested earlier, then the similar deviation in the descending ramp at the smallest strains follows automatically. The observed behavior thus appears to support this hypothesis.

Figure 9 shows relaxation modulus data on the unplasticized sample. The ordinate is represented as $3n\bar{\sigma}(t)/2(\lambda_o^n - \lambda_o^{-n/2})$ to avoid confusion with the small deformation relaxation modulus E(t). The full circles (only a few are shown at the upper and lower end) represent E(t) obtained from the master curve, Fig. 2, shifted to 10°C using the WLF equation given in the companion paper[11]. The deviations (fanning out) at the shorter times are due to the ramp transients. Figure 9, which contains essentially the same kind of information as Fig. 3, indicates that eq. (24) is obeyed even in the unplasticized material. These data were obtained at 10°C, and required n = 1.06.

Figure 10 is the equivalent of Fig. 4 for the unplasticized sample but includes different temperatures. Again, each circle represents a separate experiment, and the solid lines represent fits to eq. (52). $E(t_r)$ was obtained from the master curve shifted to the appropriate temperature. The fit is equally good at all temperatures.

The dependence of n on temperature is shown in Fig. 11. The parameter n is seen to increase with temperature. The point at -45°C results from only two experiments which are not included in Fig. 10. The error bars in Fig. 11 represent ± 1 standard deviation as obtained from the least squares estimation of n from Fig. 10. The increase in standard deviation at -16.5°C reflects the higher precision required at lower temperatures in the experimental data because of the increasing steepness of the relaxation and its temperature dependence. At 23°C the values of n for the plasticized and unplasticized samples agreed to within the second decimal.

DISCUSSION

The data presented in the preceding section lend strong support to our assumption that time shift invariance is preserved in moderately large deformations. Our solid model utilizes this basic contention in a particularly simple and elegant way. Other models could exploit it equally well but are not likely to be simpler. This matter has been discussed in a more fundamental way elsewhere[1]. We remark here only that combination of the concept of the preservation of time shift invariance with, e.g., the approach developed by Valanis and Landel[17] to take into account stress-strain nonlinearity is perfectly feasible. In terms of our theory, Valanis and Landel's empirical function $w'(\lambda_\alpha)$ becomes simply[4]

$$w'(\lambda_\alpha) = (2E/3)\lambda_\alpha^{n-1} \tag{55}$$

A series development of our strain measure gives

$$(\lambda_\alpha^n - 1)/n = \Sigma_i a_i \ln^i \lambda_\alpha \qquad i=1,2... \tag{56}$$

where

$$a_i = n^{i-1}/i! \tag{57}$$

i.e. the strain measure can be viewed in terms of a polynomial expansion in the natural, or Hencky, strain. Thus, the strain energy density

function proposed by Valanis and Landel for natural rubber[17]

$$w(\lambda_\alpha) = 2\mu \ln \lambda_\alpha \tag{58}$$

corresponds to the first term in the expansion of the strain energy density function of Blatz, Sharda, and Tschoegl[5] if we equate μ with G/n.

Among other possible models, we are particularly interested in our liquid model[1,8]. Although this model was developed primarily for polymer melts, it describes the data on crosslinked SBR presented so far almost equally as well as does the solid model, albeit with unnecessary elaboration. We must turn to superposed small deformations as a more sensitive test to discriminate between the predictions of the two models. Figure 12 presents, as a function of λ_r, the incremental stress resulting from the superposition of small ramps upon a substantially relaxed finite extension for the isochronal time $t = t_r + t'$ where t_r = 10 min. and t' = 0.1 min. For convenience we calculated the incremental stress from

$$\Delta\bar{\sigma}(t-t_r) = \bar{\sigma}(t) - \bar{\sigma}_r(t_r) \tag{59}$$

instead of eq. (30a). This is admissible because $\bar{\sigma}_r(t)$ is closely the same as $\bar{\sigma}_r(t_r)$ since the stress induced by the finite deformation has substantially relaxed. The data presented in Fig. 12 clearly favor the solid model.

Another matter that requires discussion is the separability of strain and time effects in viscoelastic deformations. Elastic molecular

theories such as the Gaussian statistical theory of rubber elasticity must be tested against data obtained in elastic equilibrium. In practice, this equilibrium can only be approached asympototically. The concept of isochronal time substitutes measurements referred to the same state of relaxation for equilibrium data. Isochronal measurements require that the effects of strain and of time be separable. We have adduced strong evidence here and elsewhere[1,8] in support of the contention that time shift invariance is preserved in moderate deformations of rubberlike materials. This assumption leads directly to eq. (24) which states that the effects of strain and time should factor in stress relaxation, i.e. in the response to a step function of strain. According to eq. (8) these effects should not uncouple in the response to a constant rate of strain (ramp) excitation. Experimental evidence, particularly the work of T.L. Smith[9], shows, however, that in such experiments the effects of strain and time offen appear to be separable. We must consider, therefore, under what circumstances our theory would reconcile these two seemingly conflicting observations. To see the matter more clearly we rewrite eq. (4) as

$$\bar{\sigma}(t) = \int_0^t E(t-u) f[\lambda(u)]\, d\lambda(u) \tag{60}$$

where $f[\lambda(u)]$ is given by eq. 33. Evidently, if

$$f[\lambda(u)]\Big|_0^t \simeq \text{constant} \tag{61}$$

i.e. if $f(\lambda)$ is nearly constant in the time interval $(0,t)$, it can be taken out from under the integral sign. Specializing the remaining integral for the case of a constant rate of strain, i.e. using eq. (6), we then obtain

$$\bar{\sigma}(t) = f(\lambda)\dot{\varepsilon}\eta(t) = f(\lambda)\dot{\varepsilon}tF(t) \tag{62}$$

by eq. (54). But $\dot{\varepsilon}t = \lambda - 1$, and therefore

$$\sigma(t) = \Gamma(\lambda)F(t) \tag{63}$$

where

$$\Gamma(\lambda) = \lambda^{-1}(\lambda-1)f(\lambda)$$

Equation (63) is the equation of T.L. Smith[9,18]. His empirical strain function $\Gamma(\lambda)$ receives mathematical form through eq. (64) which establishes the relation between $\Gamma(\lambda)$ and $f(\lambda)$, i.e. between our theory and the procedure developed by him. In terms of our theory the validity of Smith's procedure rests on the validity of eq. (61). Figure 1 shows that eq. (61) is likely to be valid with good approximation for values of n close to unity but even at higher values $f(\lambda)$ can easily be "flat" enough to allow empirical factorization according to eq. (63).

The particular distinction of our theory is its simplicity. It differs significantly in this respect from any other theory proposed so far for the description of viscoelastic behavior in large deformations.

We shall concern ourselves here only with the theory of Bernstein, Kearsley, and Zapas[19] (BKZ theory) and the approach advocated by Lianis[20] which is essentially a simplification of the theory of Coleman and Noll[21]. Instead of applying these theories to our data, however, we use the much simpler way of applying our theory to the data of others.

Figure 13 shows data of Goldberg, Bernstein, and Lianis[22] showing (full circles) the response of a crosslinked SBR to an exponential stretch ratio excitation. To apply our theory to these data we used eq. (11). The small deformation relaxation modulus, E(t), can be found in the original reference. This did not, however, contain the data required to define n by our procedure. Since the SBR in question has a modulus similar to our sample's, we simply read the value of n = 1.0 appropriate for the experimental temperature of 0°C from our Fig. 11. As off-hand as this procedure might be, it produced the excellent fit to the data shown by the solid lines in Fig. 13. This fit is as good, if not better, as that obtained by the authors with either the BKZ or the Lianis theory.

Again, a more sensitive test is obtained by the use of superposed small deformations. Lianis and Goldberg[23] superposed small sinusoidal oscillations on a finite stretch. Their data on SBR and their predictions calculated by the BKZ and Lianis theories are shown in Fig. 14. Both theories give a rather unsatisfactory fit, particularly for $E_s''(\omega)$. We were not able to calculate the predictions of our theory exactly because we lacked the necessary input [E(t), or $E'(\omega)$, and n]. However,

it can easily be ascertained that the data conform to the simple shift by $f(\lambda_r)$ implied by our Eqs. (44). This would be seen even more convincingly if the ordinate represented log $E_s'(\omega)$ and $E_s''(\omega)$ rather than $E_s'(\omega)$ and $E_s''(\omega)$.

Formulation of a molecular interpretation of the parameter n requires knowledge of its dependence on the different thermodynamical and molecular variables that characterize the behavior of crosslinked polymers. The work of Blatz, Sharda and Tschoegl[5] indicates that for a moderately crosslinked natural rubber sample n may be sensibly independent of the temperature. Figure 11 shows some experimental data on the dependence of n on temperature for SBR. The large error bar at -16.5°C indicates that at temperatures at which the relaxation is steep, small variations in temperature will be reflected in relatively large variations in n. No error bar is shown at -45°C because this value of n was determined from two points only.

According to Fig. 11, n for SBR increases sigmoidally with temperature, the transition occurring roughly near -10°C. At low temperatures (which, however, still lie above the glass temperature) n has the characteristic value found independently of temperature in the uncrosslinked gum stock[8].

Comparison of E(t) for the crosslinked material (see Fig. 2) with that for the uncrosslinked material[8] shows that at temperatures where n is similar for the two materials, the relaxation curves naturally coincide in the time interval from 10^{-2} to 10^{2} minutes. Thus, in moderately large deformations the crosslinked and uncrosslinked materials respond identically in the appropriate time and temperature regions.

In large deformations they would, of course, be distinguishable by the upswing occurring in the crosslinked system.

We suspect that n may approach the value 2 asympotically if measurements were carried out under a nitrogen blanket to avoid oxidation. Clearly, further work is needed to clarify the temperature dependence of n.

Values of the parameter n estimated from the isochronal ramp data of Smith[24] on Viton A-HV are plotted as function of temperature for two crosslink densities in Fig. 15. According to Fig. 15, n is clearly a function of crosslink density as well as temperature. The large values of n at low temperatures are possibly explained by the fact that these temperatures lie close to the glass temperature of Viton A-HV (~-20°C) or by the fact that n was derived from isochronal ramp instead of step data.

The data of Gumbrell, Mullins and Rivlin[25] on the dependence of n on crosslink density for natural rubber at 25°C are shown in Fig. 16. The figure shows that n increases with the crosslink density which is here represented by $\rho RT/2M_c$ where ρ is the density, M_c is the molecular weight between crosslinks determined from swelling measurements in various solvents and R and T have their usual significance. Figure 17 shows n as a function of the volume fraction, v_r, of the rubber with $\rho RT/2M_c = 1.31$, swollen in benzene at different degrees of saturation at 25°C. The figure displays the well established fact that n=2 for a highly swollen system. We obtained n for these data from the authors' values of C_2/C_1 using a nomogram presented elsewhere[8]. C_2/C_1 are the parameters in the equation

$$\bar{\sigma} = (\lambda^2 - \lambda^{-2})(2C_1 + 2C_2\lambda^{-1}) \tag{65}$$

Arenz, Landel and Tsuge[26] presented uniaxial and biaxial tension data on a series of SBR crosslinked to differing degrees with sulfur. We calculated n from their isochronal step response data as required by our theory and plotted the values against their values of $\nu_e = 1/M_c$ in Fig. 18. Again n increases with crosslink density, except at the highest values of ν_e. We have no explanation for the fall in n at the highest values at this time. We remark that we obtained the same n from the uniaxial and the biaxial data at the same crosslink density.

References

1. W.V. Chang, R. Bloch, and N.W. Tschoegl, (to be submitted to *Rheol. Acta*).
2. N.W. Tschoegl, Unpublished Result.
3. W.V. Chang, R. Bloch, and N.W. Tschoegl, *Proc. Nat. Acad. Sci.* (in press).
4. P.J. Blatz, S.C. Sharda, and N.W. Tschoegl, *Proc. Nat. Acad. Sci.* 70, 3041 (1973).
5. P.J. Blatz, S.C. Sharda, and N.W. Tschoegl, *Trans. Soc. Rheol.* 18, 145 (1974).
6. S.C. Sharda, P.J. Blatz, and N.W. Tschoegl, *Letters Appl Eng. Sci.* 2, 53(1974).
7. S.C. Sharda and N.W. Tschoegl, *Trans. Soc. Rheol.* (in press).
8. W.V. Chang, R. Bloch, and N.W. Tschoegl, (to be submitted to *J. Polymer Sci.*).
9. T.L. Smith, *Trans. Soc. Rheol.* 6, 61 (1962).
10. G.M. Bristow and W.F. Watson, *Trans. Faraday Soc.* 54, 1731 (1958).
11. R. Bloch, W.V. Chang, and N.W. Tschoegl, (to be submitted to *Trans. Soc. Rheol*).
12. R. Bloch, Ph.D. Dissertation (Appendix 2), California Institute of Technology, Pasadena, California 91125 (1976).
13. W.V. Chang, R. Bloch, and N.W. Tschoegl, (to be submitted to *Macromolecules*).
14. T.L. Smith, *J. Polymer Sci.*, Part C, No. 35, pp. 39 (1971).
15. T.G. Nutting, J. Franklin Inst. 191, 679 (1921).

16. E.H. Lee and L.E. Hulbert, in: H.H. Kausch, J.A. Hassell, and R.I. Jaffe, eds., *Deformation and Fracture of High Polymers*, Plenum Press, New York, 1973, p. 447.

17. K.C. Valanis and R.F. Landel, *J. Appl. Phys.* 36, 2997 (1967).

18. T.L. Smith and R.A. Dickie, *J. Polymer Sci.* Part A-2, 7, 635 (1969).

19. B. Bernstein, E.A. Kearsley, and L.J. Zapas, *Trans. Soc. Rheol.* 7 391 (1963).

20. G. Lianis, Purdue University Report AAEES 63-11, 1963.

21. B.D. Coleman and W. Noll. *Rev. Mod. Phys.* 33, 239 (1961); 36, 1103 (1964).

22. W. Goldberg, B. Bernstein and G. Lianis, *Int. J. Non-Linear Mechanics* 4, 277 (1969).

23. W. Goldberg and G. Lianis, *J. Appl. Mech.* 35, 433 (1968).

24. T.L. Smith, *J. Polymer Sci.*, Part C, 16, 841(1967).

25. S.M. Gumbrell, L. Mullins and R.S. Rivlin, *Trans. Faraday Soc.* 49, 1495 (1953).

26. R.J. Arenz, R.F. Landel and K. Tsuge, private communication.

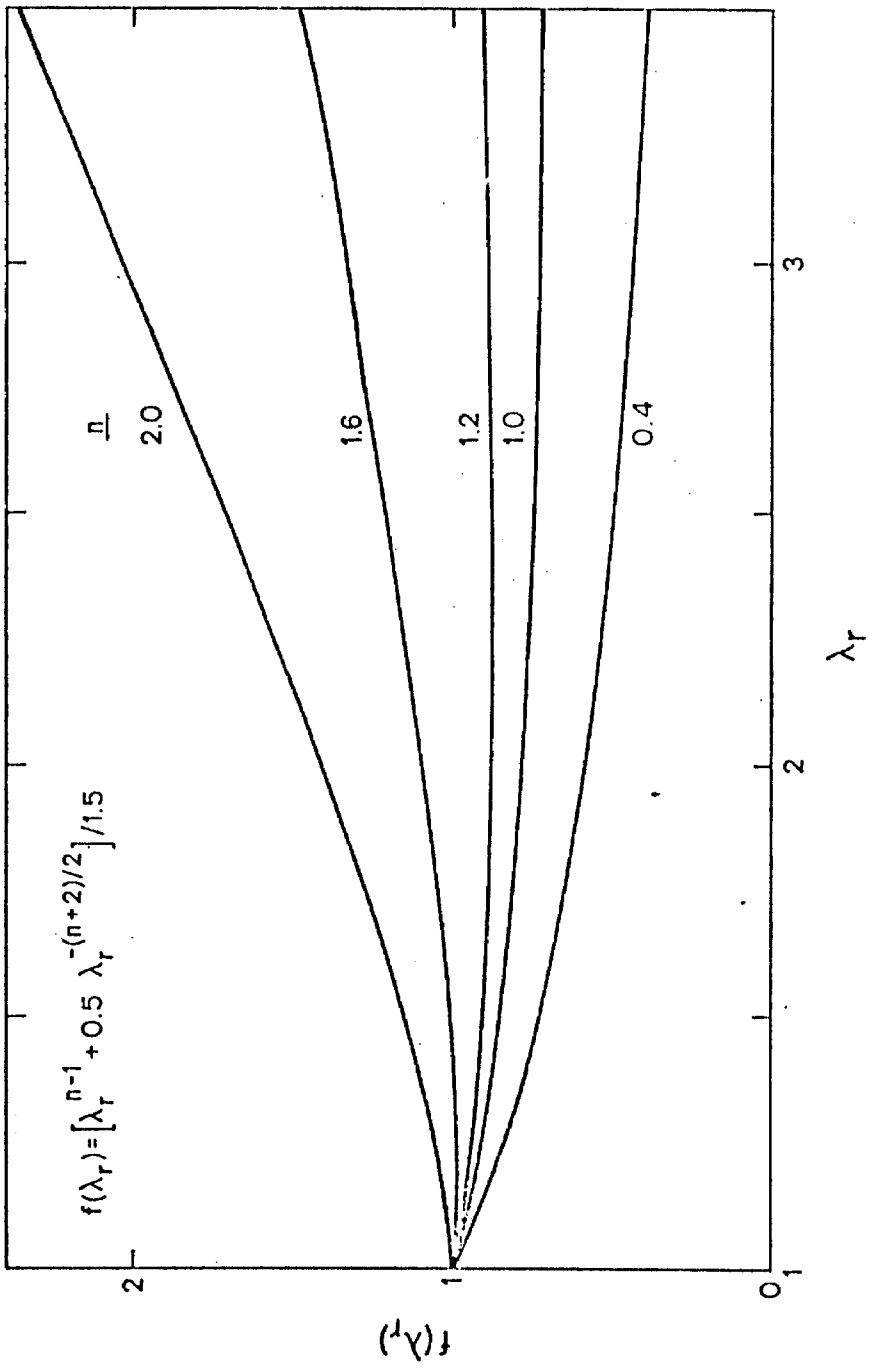

Figure 1. The function $f(\lambda_r)$ as a function of the stretch ratio for various values of n.

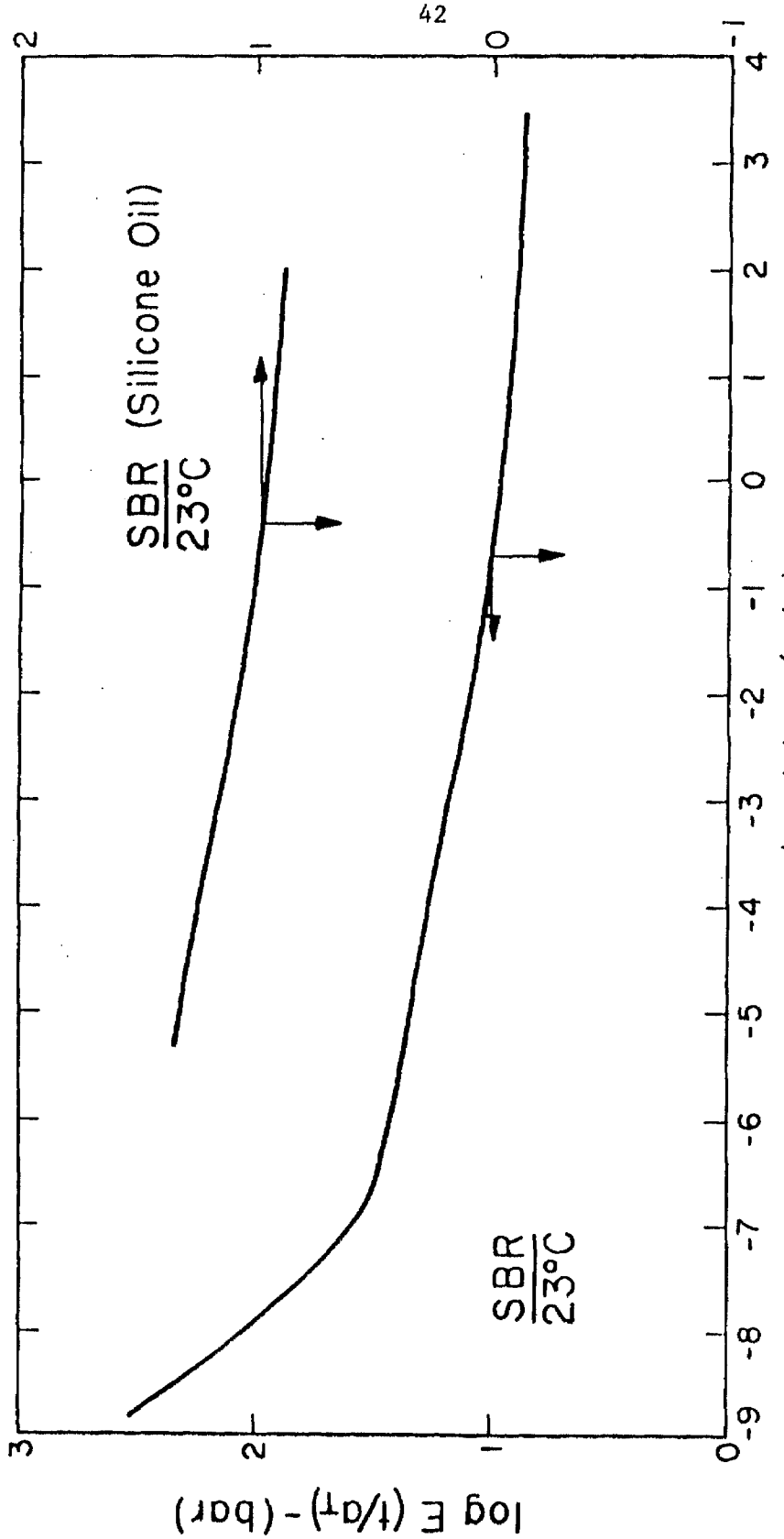

Figure 2. Relaxation master curves of SBR at 23°C with and without plasticization by silicone oil.

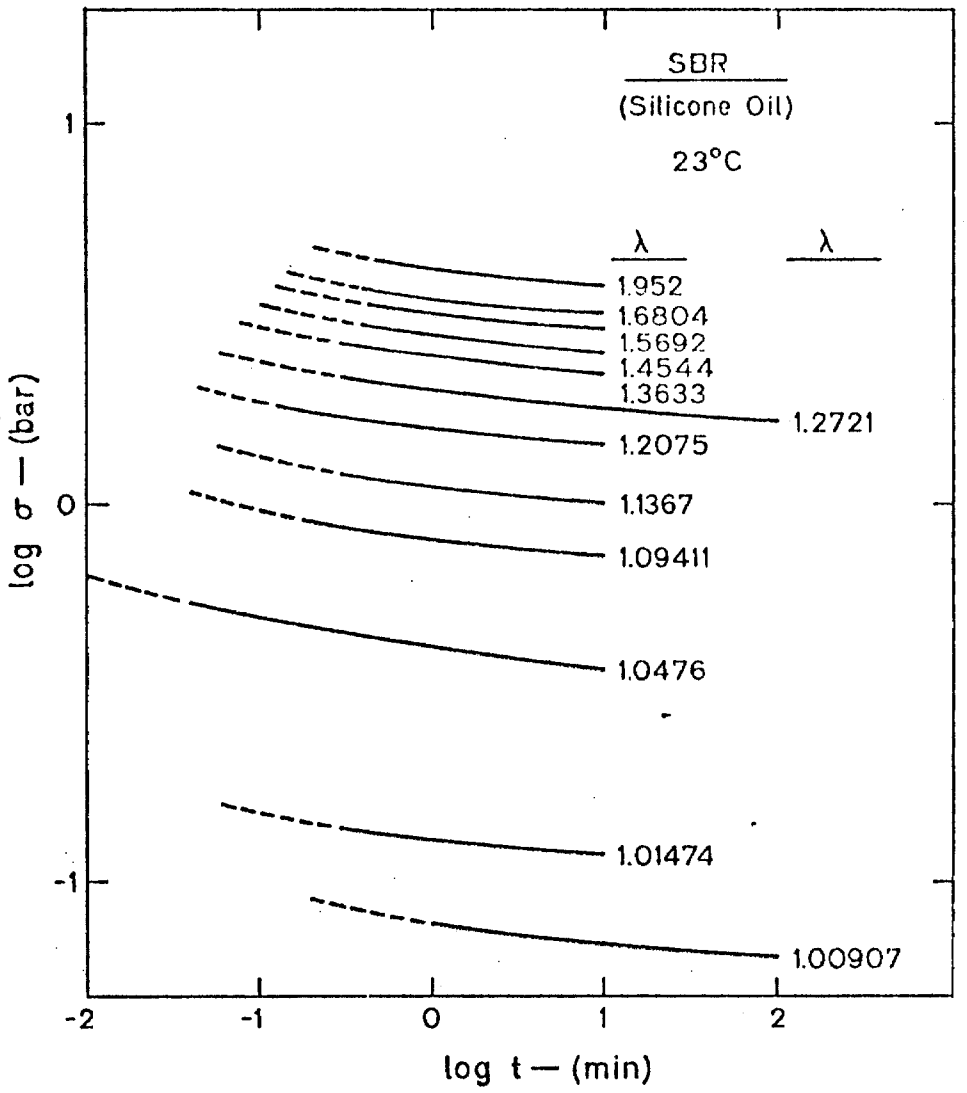

Figure 3. Response of plasticized SBR at 23°C to step functions of strain at various stretch ratios as function of time.

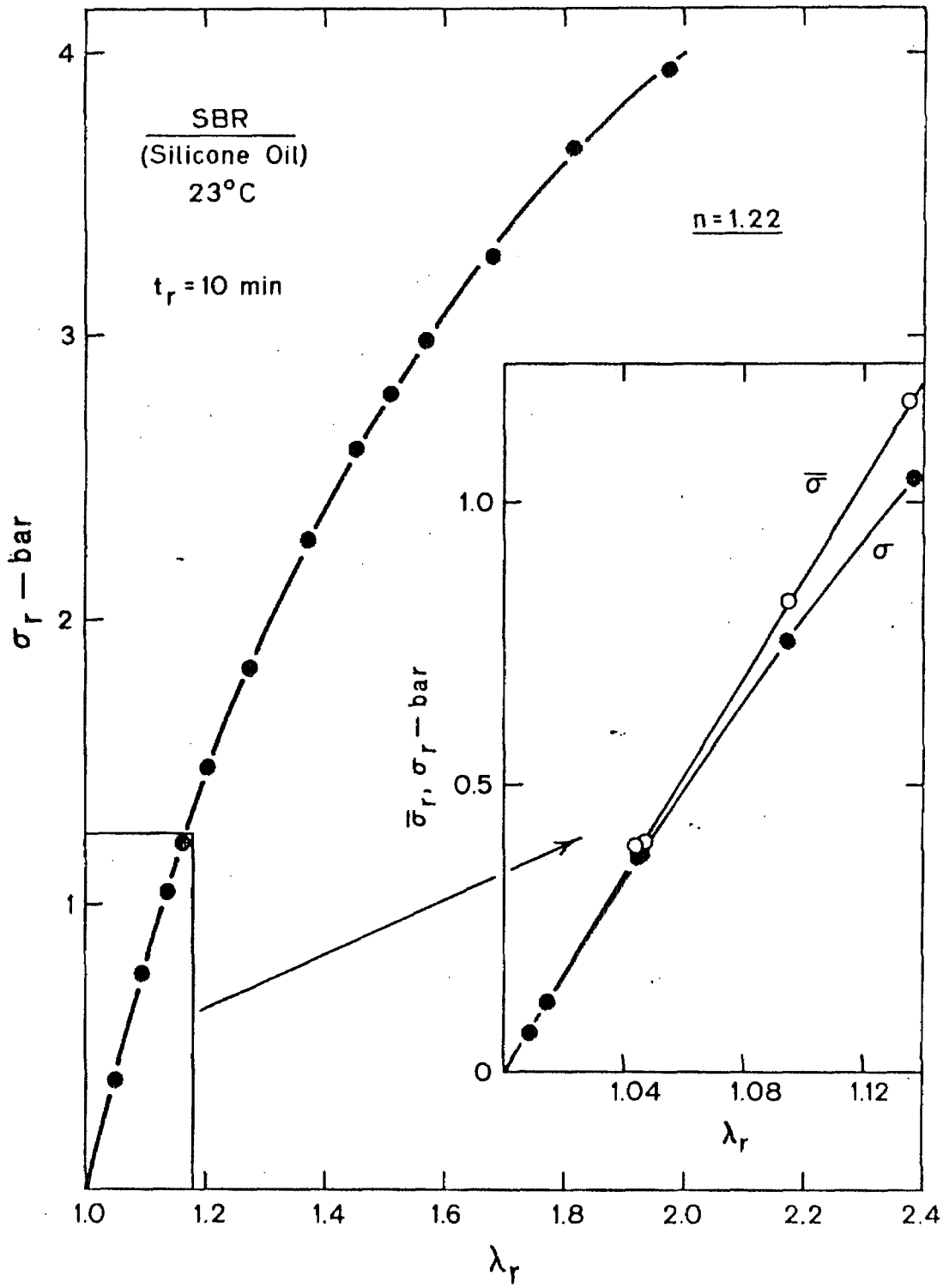

Figure 4. Isochronal stress-strain curve for plasticized SBR at 23°C.

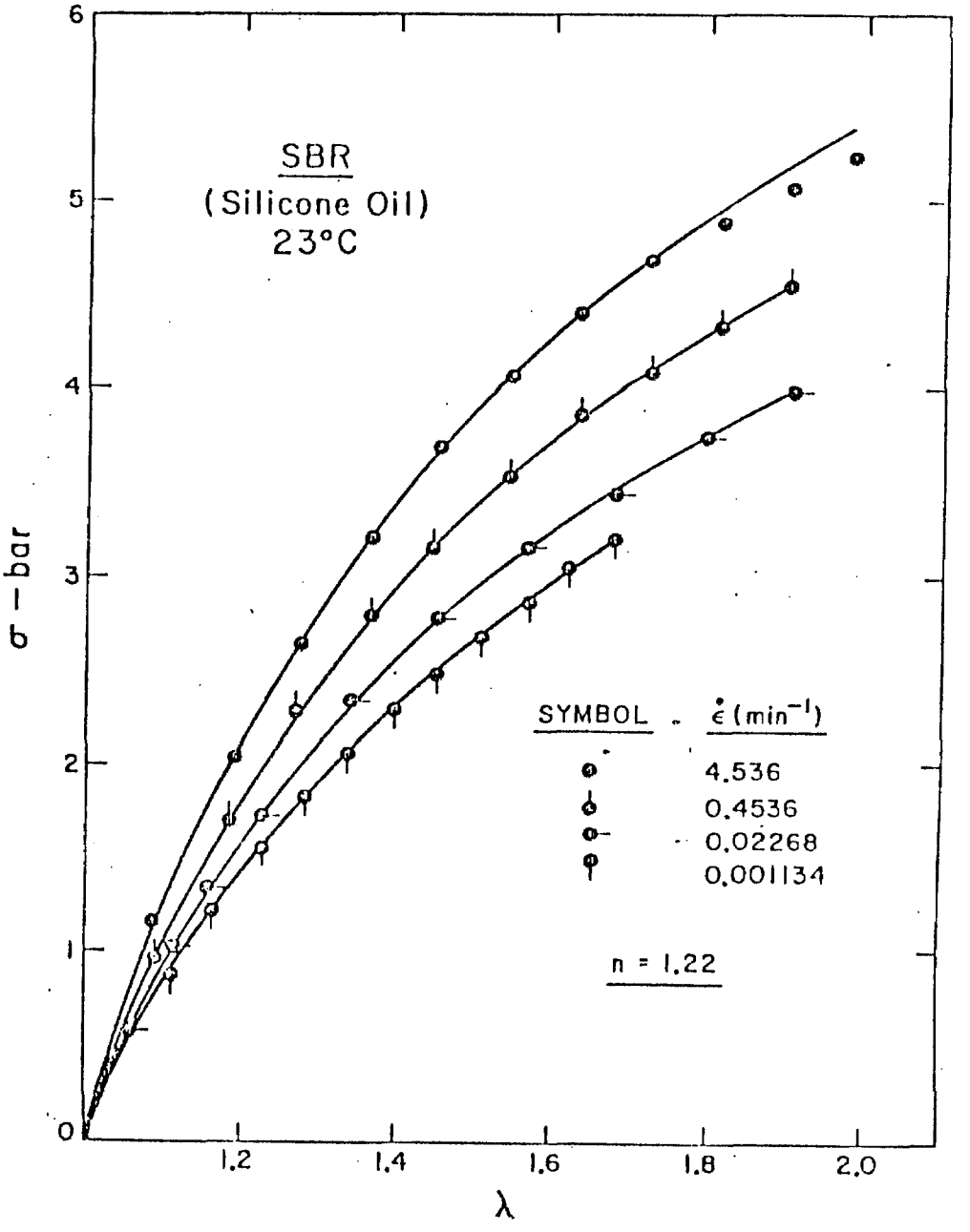

Figure 5. Response of plasticized SBR at 23°C to ramp functions of strain at various rates of strain as function of the stretch ratio.

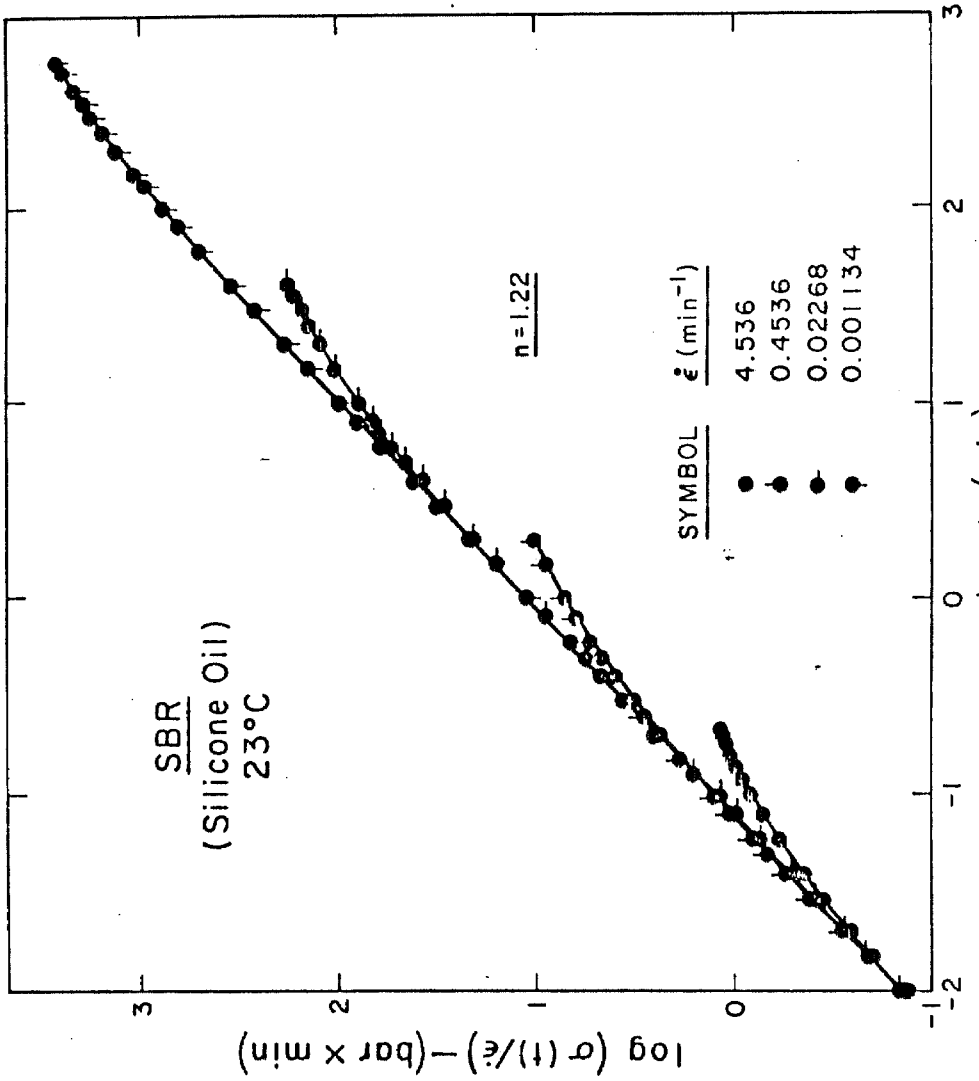

Figure 6. Response of plasticized SBR at 23°C to ramp functions of strain at various rates of strain as function of time.

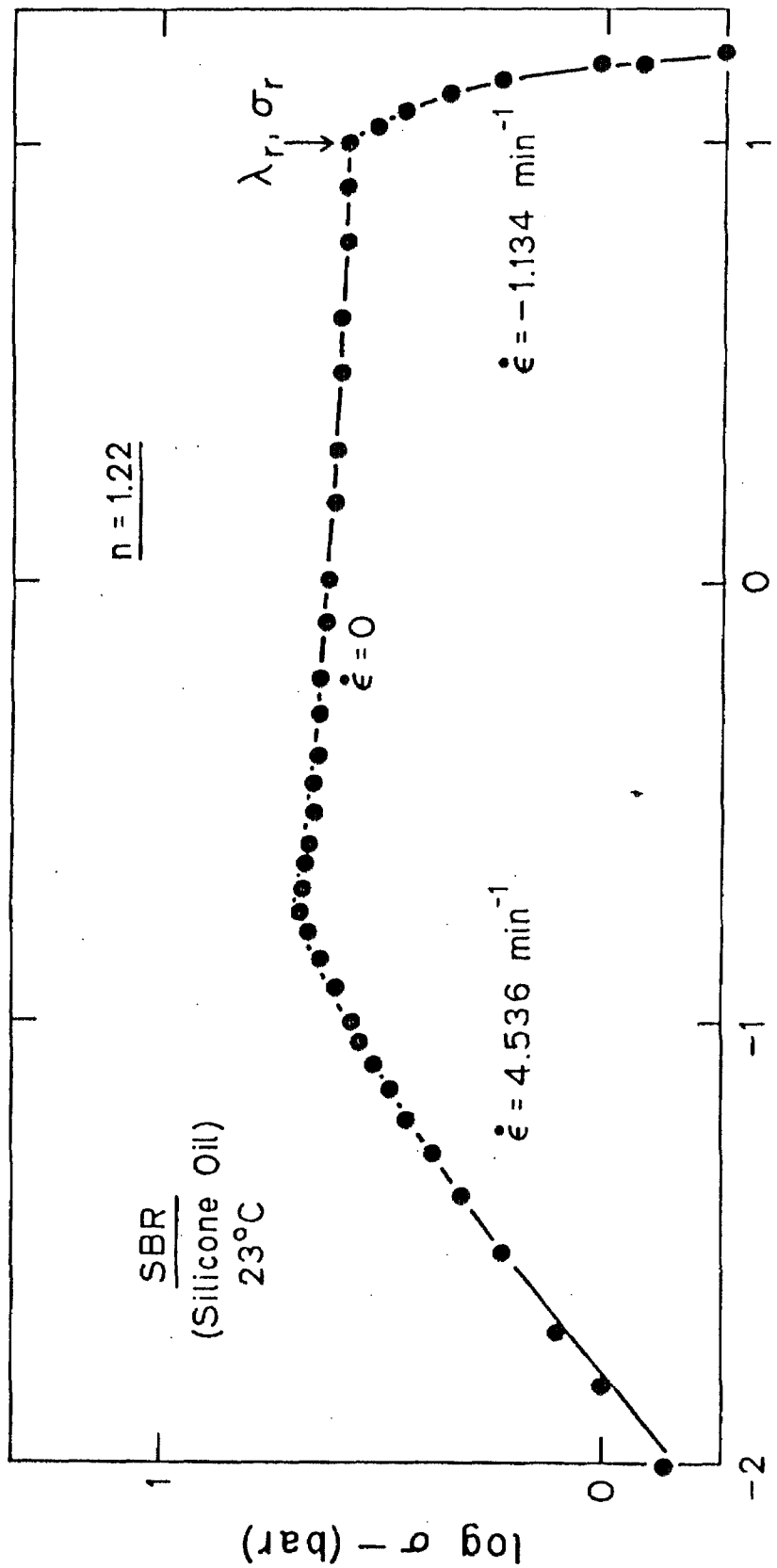

Figure 7. Response of plasticized SBR at 23°C to a trapezoidal function of strain as function of time.

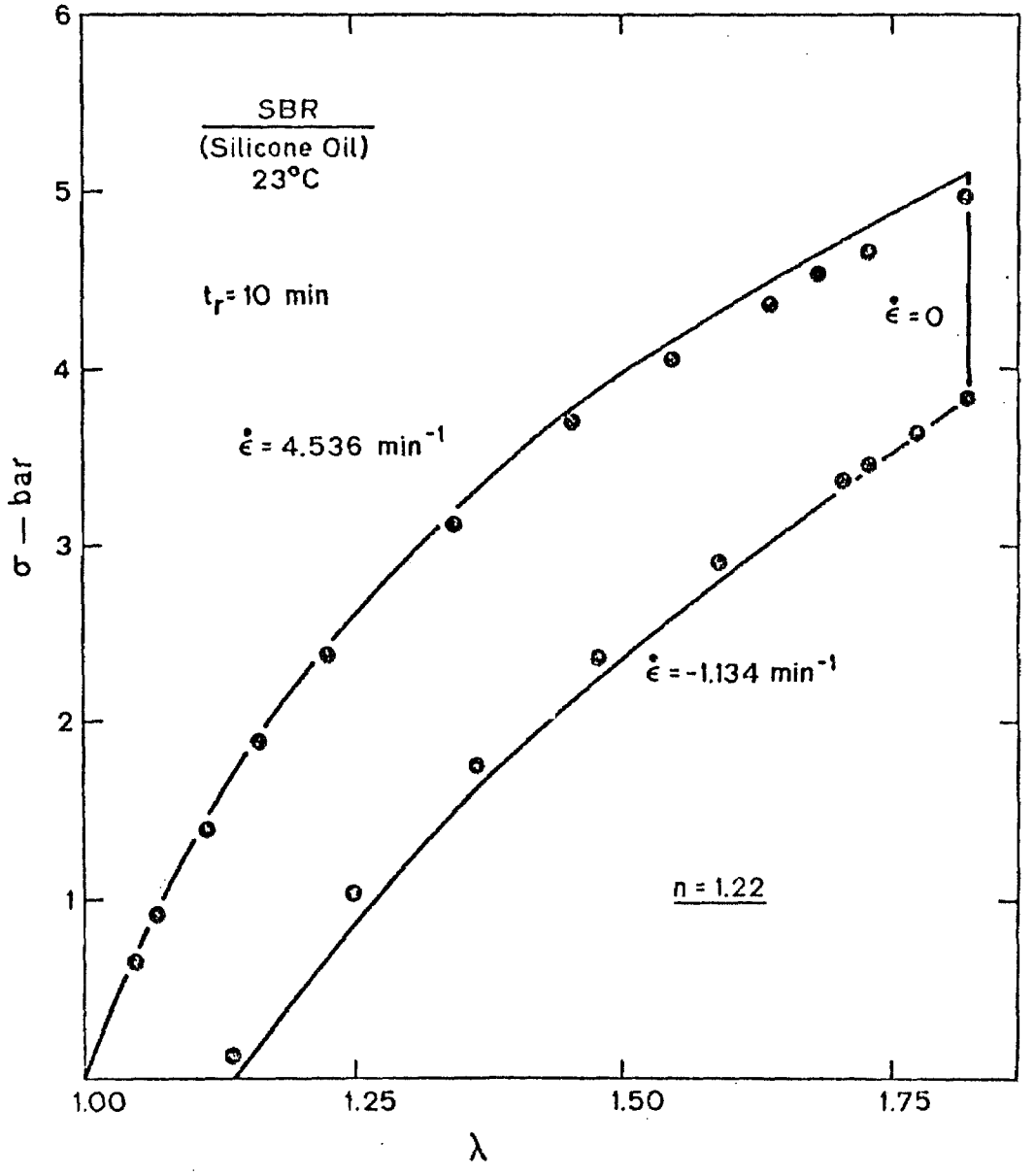

Figure 8. Response of plasticized SBR at 23°C to a trapezoidal function of strain as function of the stretch ratio.

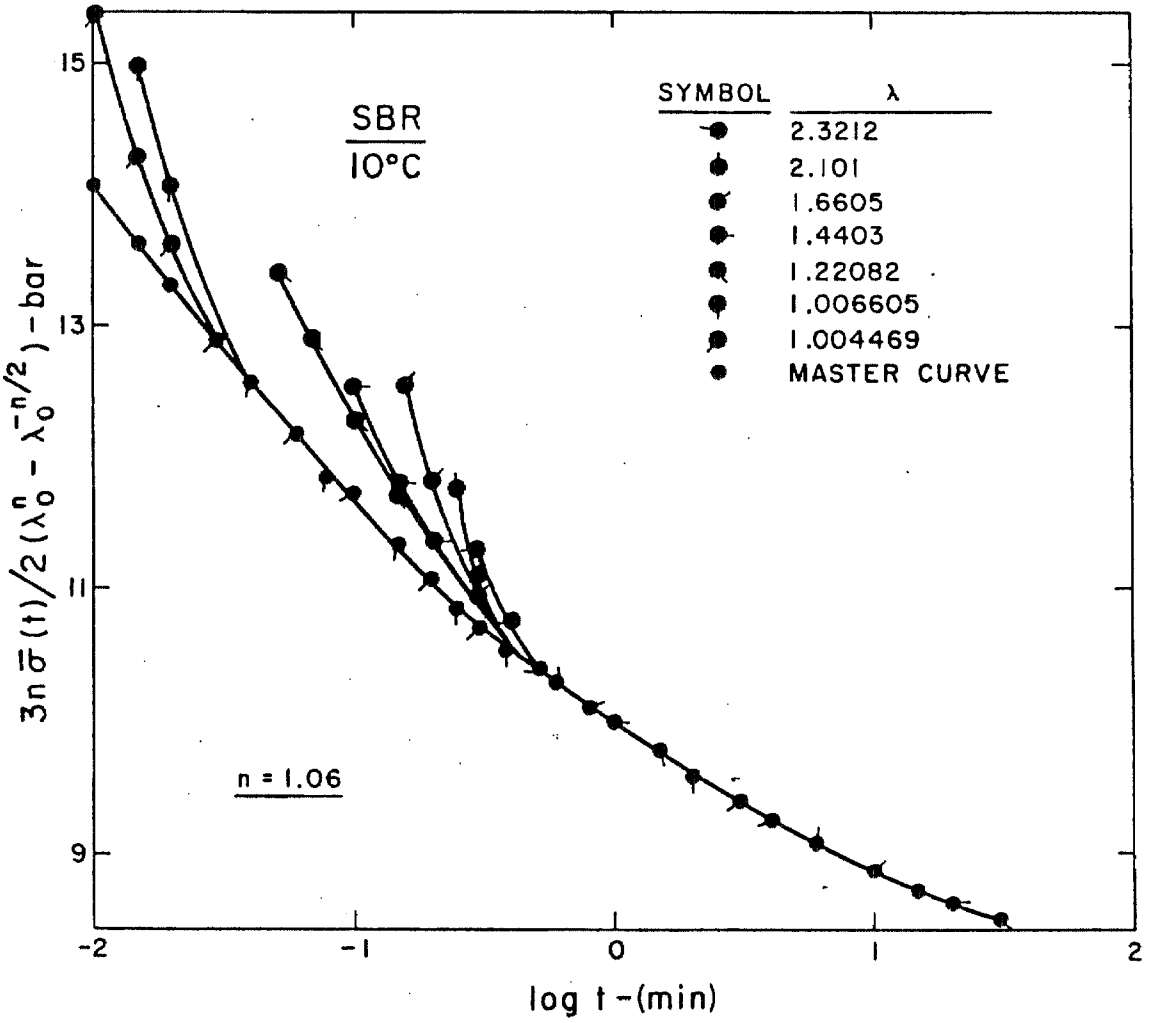

Figure 9. Response of unplasticized SBR at 10°C to step functions of strain at various stretch ratios as function of time.

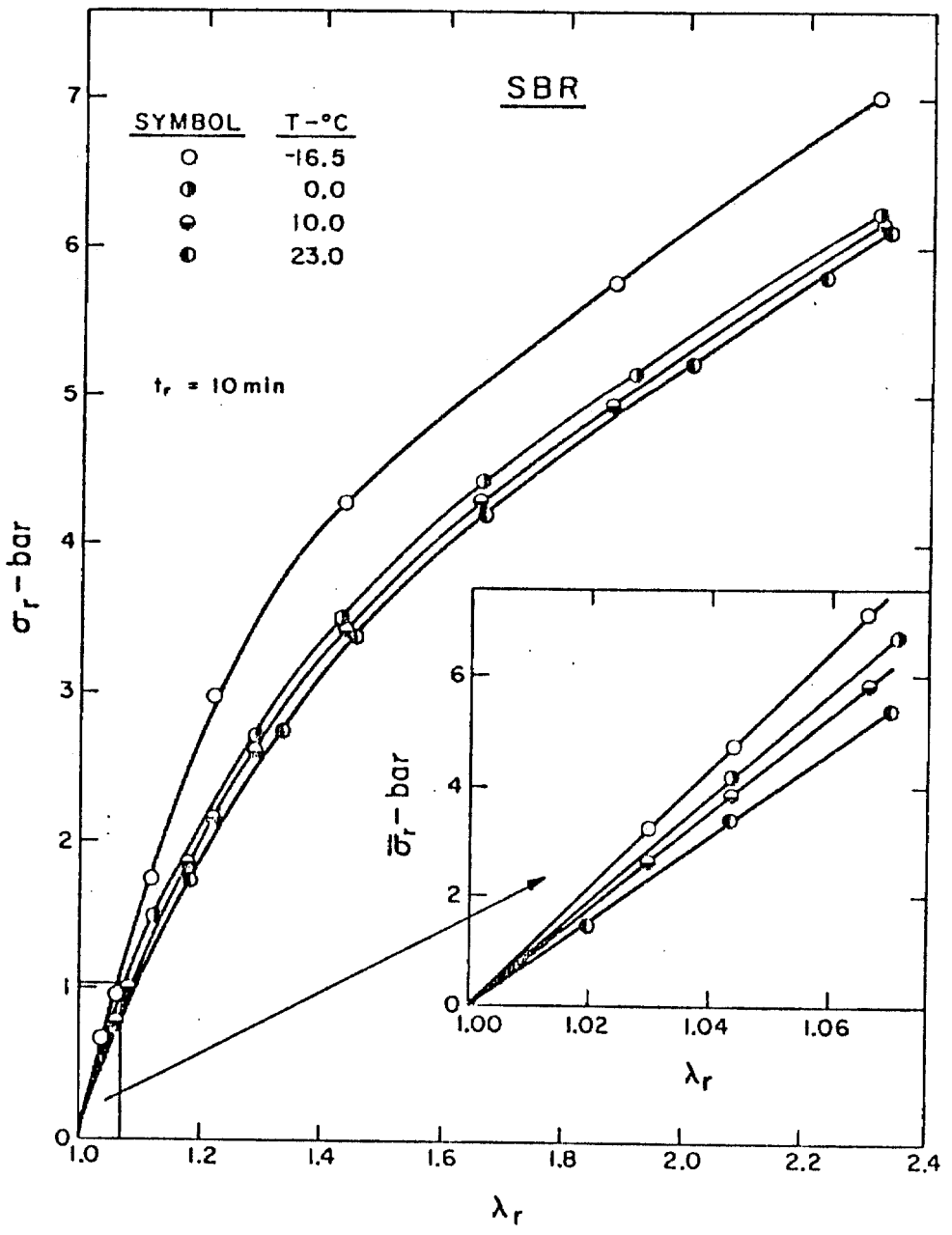

Figure 10. Isochronal stress-strain curve for unplasticized SBR at various temperatures as function of the stretch ratio.

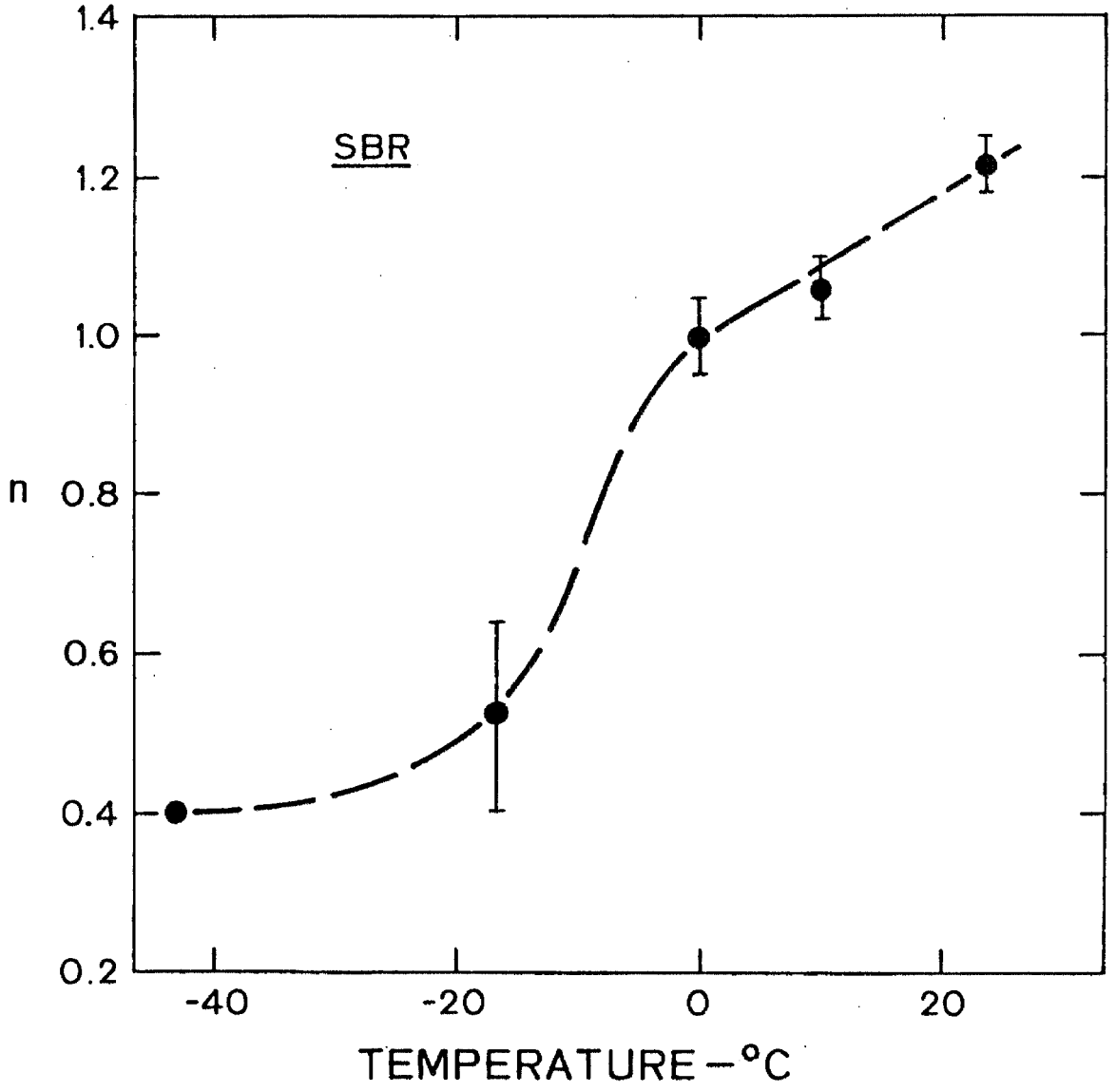

Figure 11. The parameter n as a function of temperature for SBR.

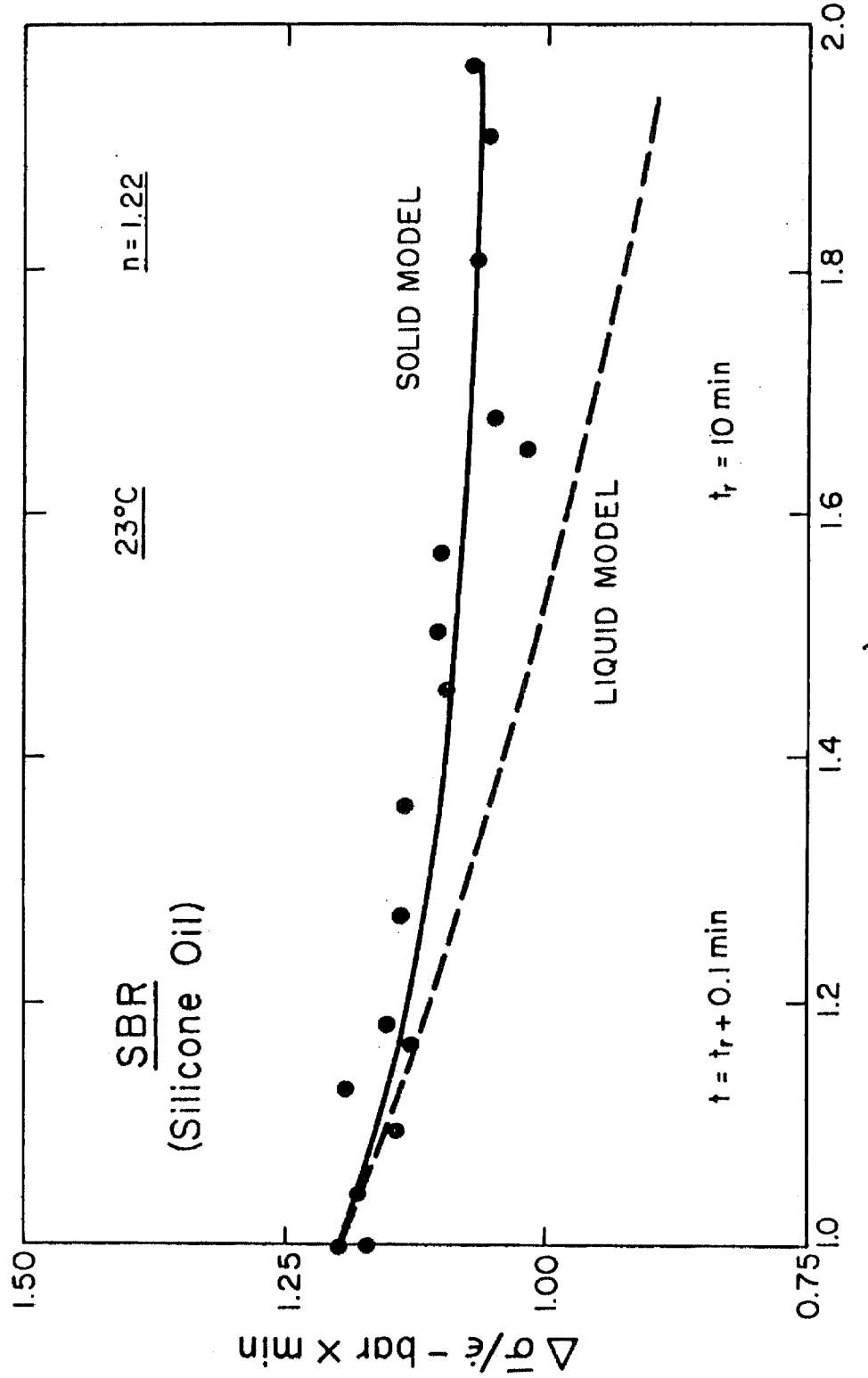

Figure 12. Comparison of the predictions of the solid and liquid models. $\Delta\bar{\sigma}/\dot{\varepsilon}$ as function of the stretch ratio.

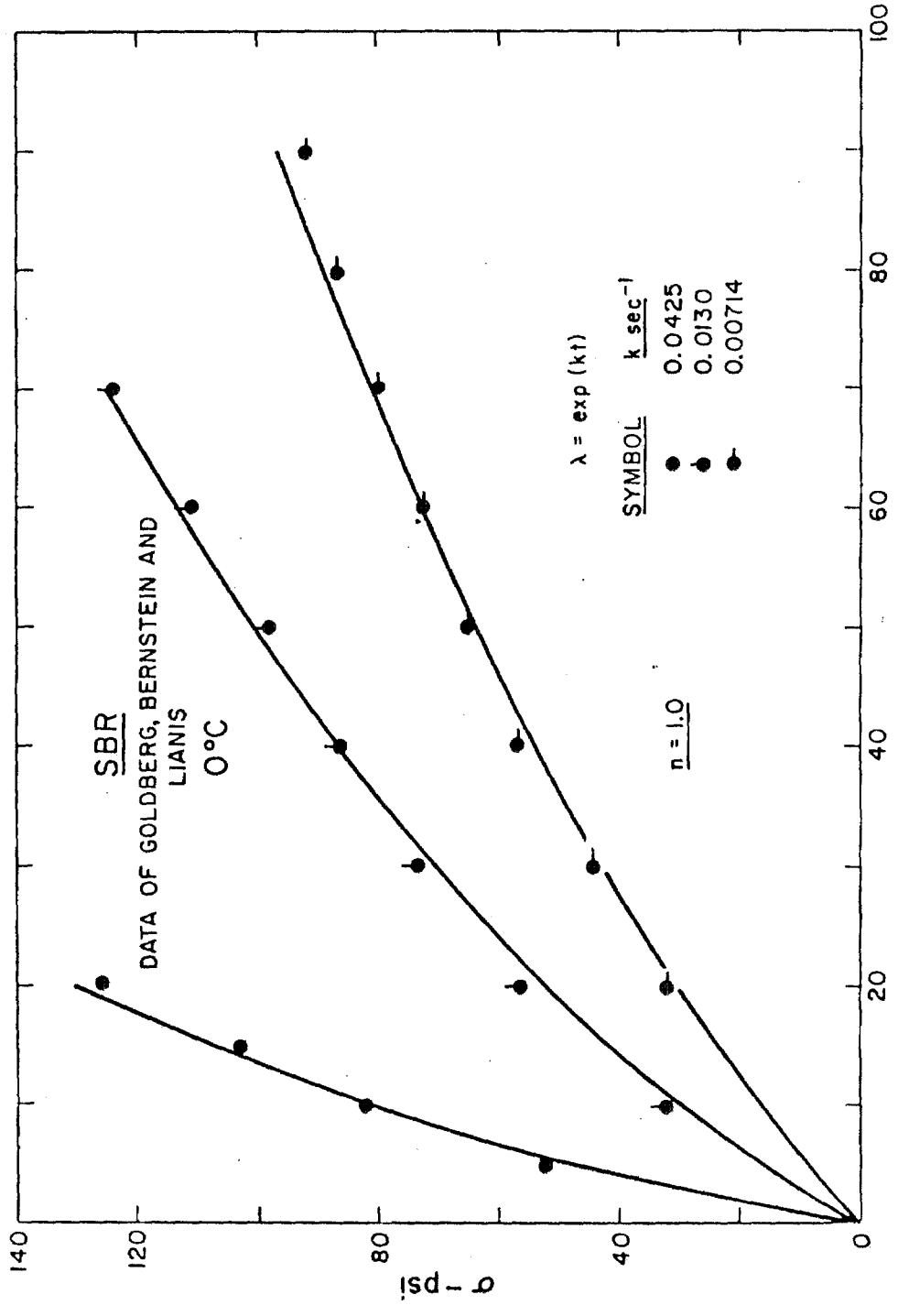

Figure 13. Response of SBR at 0°C to different exponential stretch ratio excitations as function of time. Data of Goldberg et al[22].

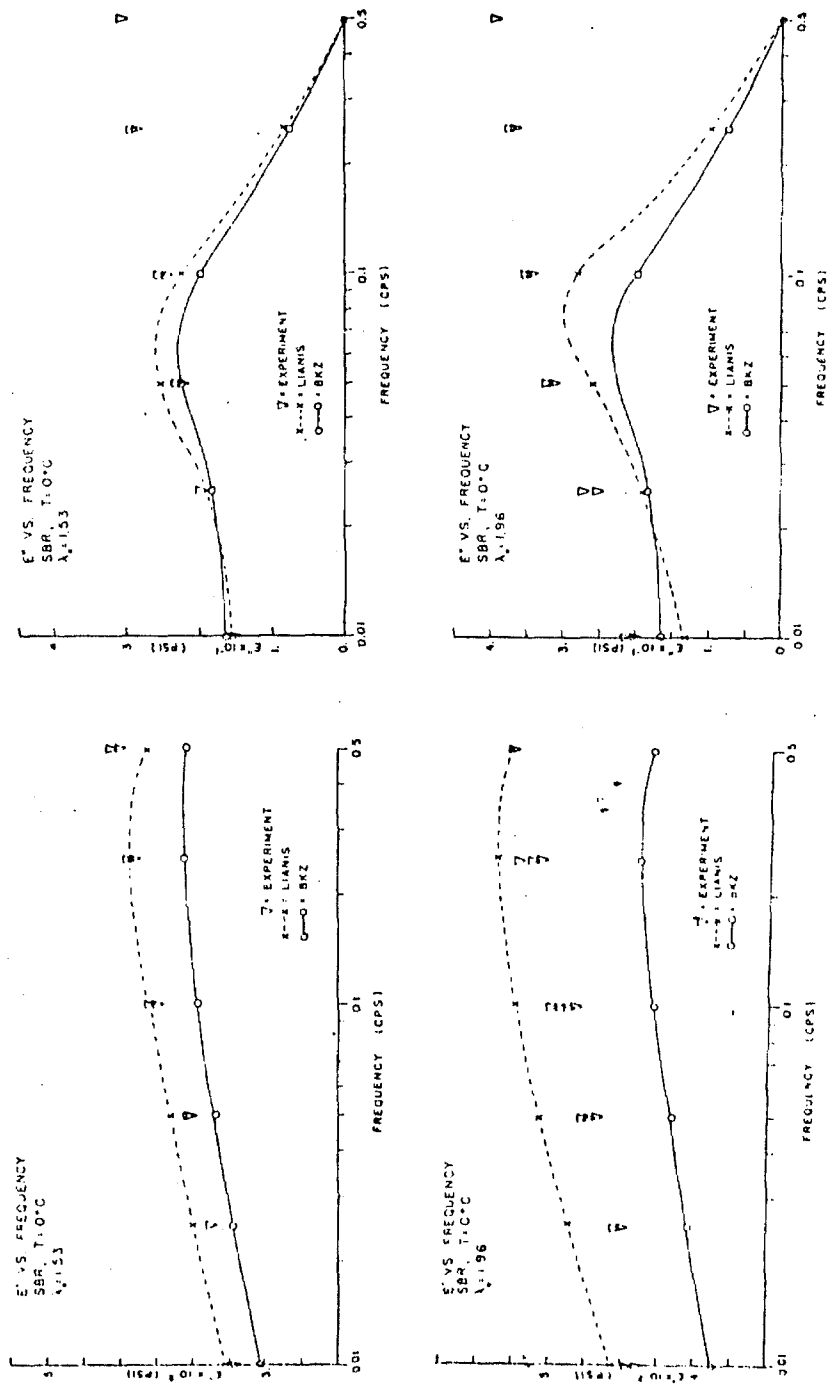

Figure 14. Small sinusoidal oscillations superposed on a finite stretch. Data on SBR at 0°C of Lianis and Goldberg[23].

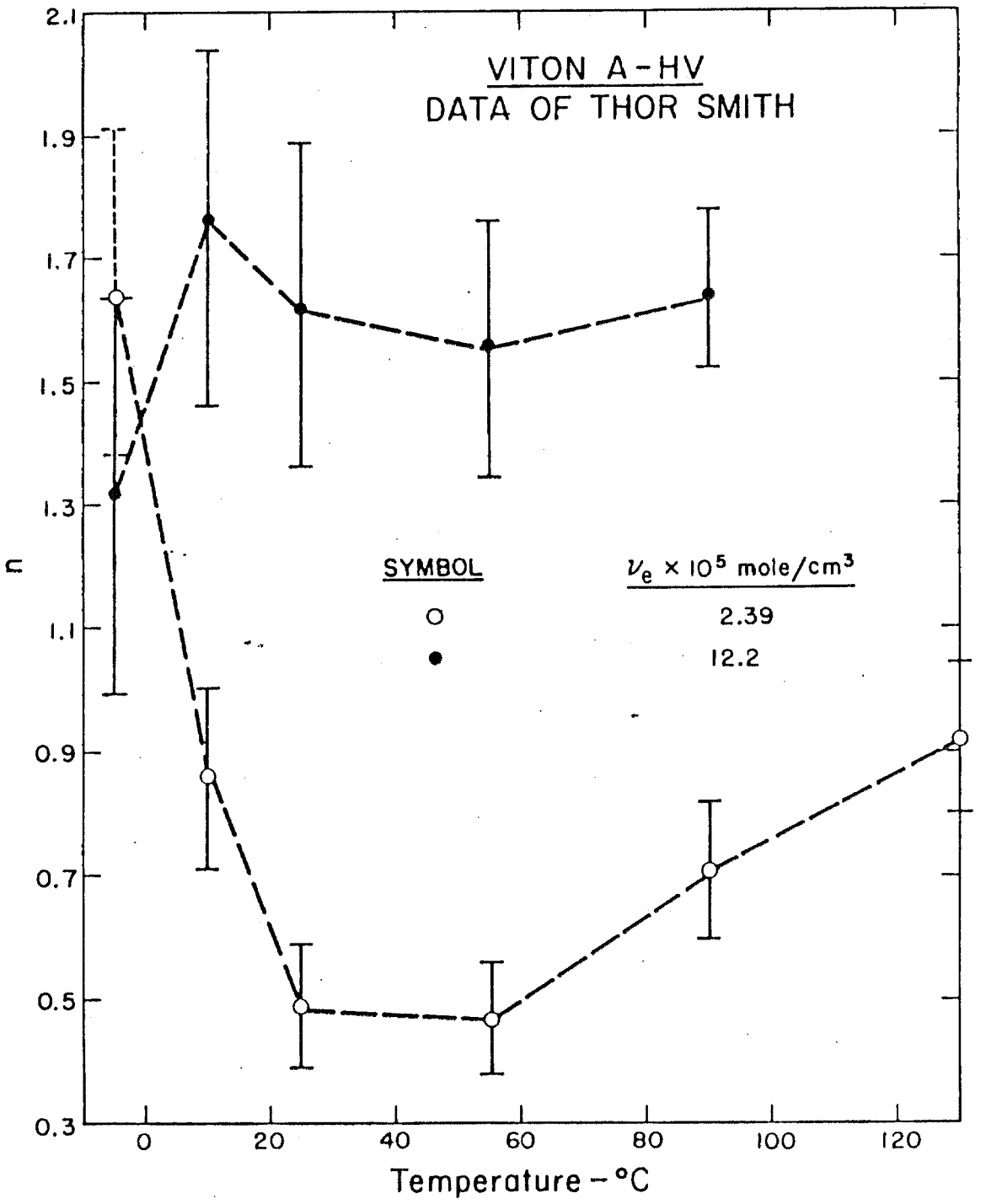

Figure 15. The parameter n as a function of temperature for Viton A-HV at two crosslink densities. Data of T.L. Smith[24].

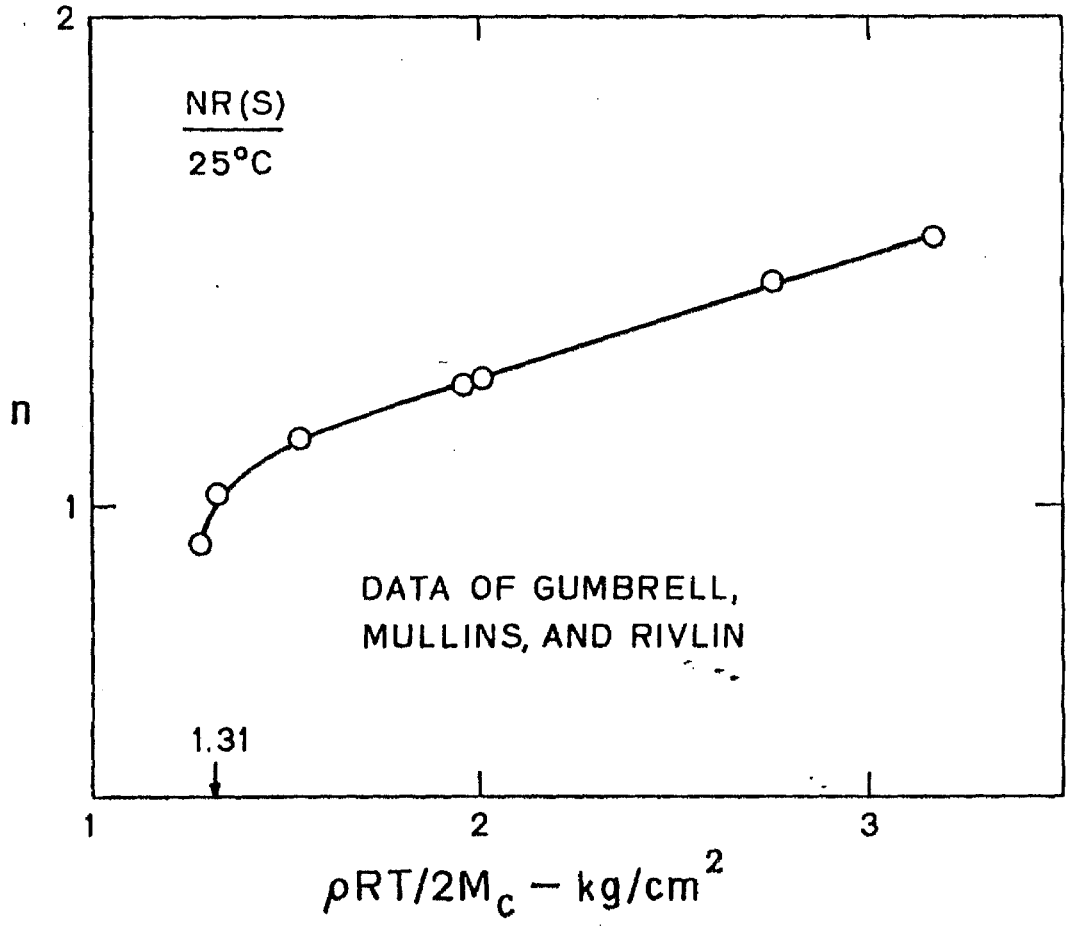

Figure 16. The parameter n as a function of crosslink density of NR at 25°C. Data of Gumbrell et al.[25].

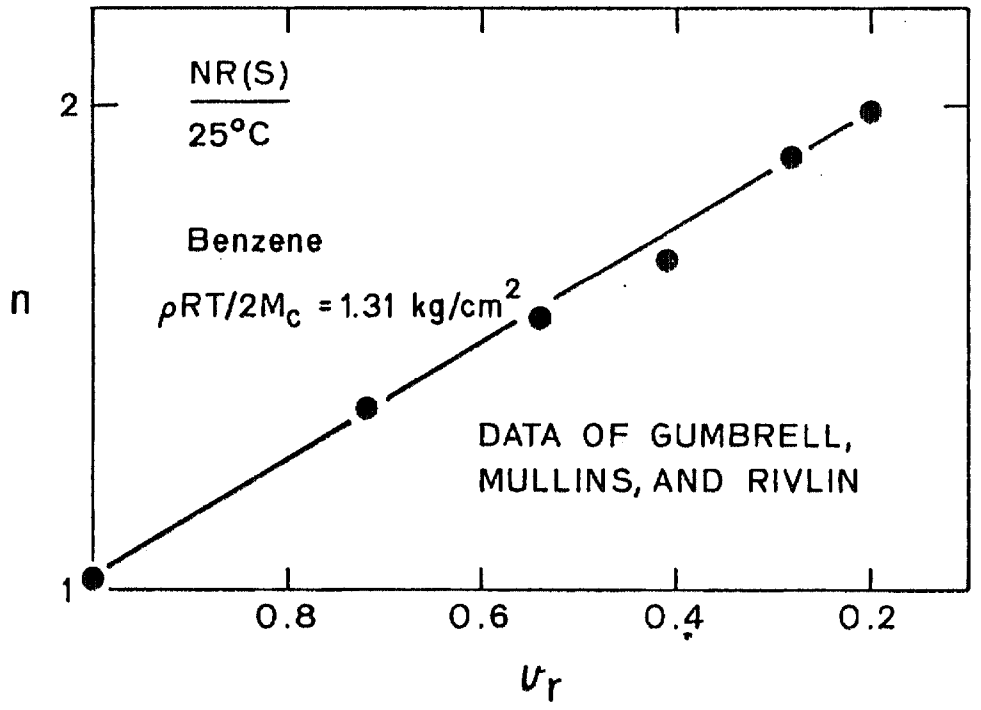

Figure 17. The parameter n as a function of volume fraction for NR swollen in benzene at 25°C. Data of Gumbrell et al.[25].

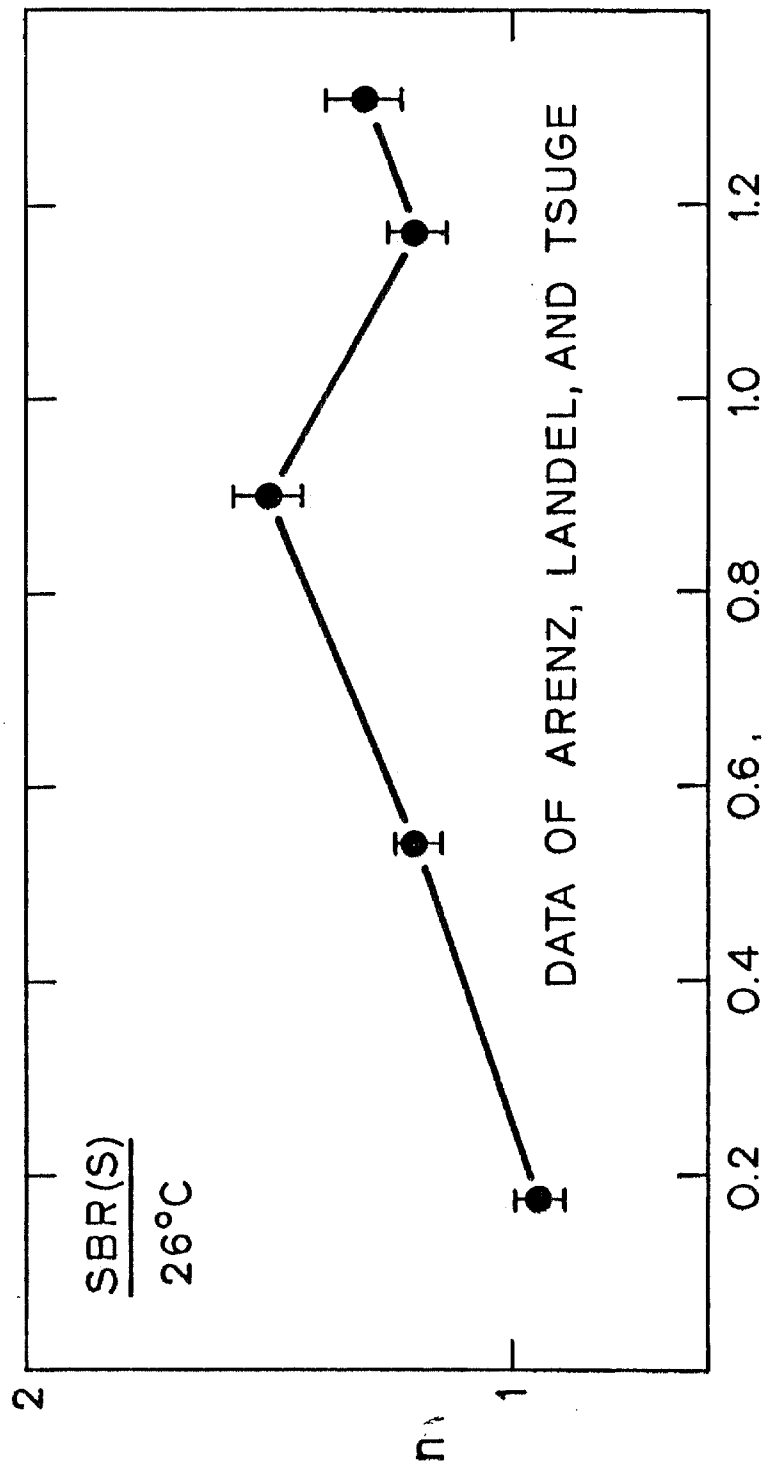

Figure 18. The parameter n as a function of crosslink density for SBR at 26°C. Data of Arenz et al.[26].

CHAPTER 3

STRAIN INDEPENDENT NONLINEARITIES IN PEROXIDE CURED SBR

INTRODUCTION

In a companion paper[1] we introduced a method for the description of the viscoelastic behavior of soft (rubberlike) materials in time-dependent moderately large deformations. We defined a moderately large deformation of a soft material as one which does not change the distribution of relaxation times. In such a deformation, therefore, time-shift invariance is preserved and any observed nonlinear mechanical behavior arises solely from stress-strain nonlinearity. We showed[2] that in this case the Boltzmann superposition principle remains applicable and time-dependent mechanical behavior can be described by combining the superposition principle with any suitable method for handling stress-strain nonlinearity. In particular, we introduced a generalized measure of strain[3] into the Boltzmann integral and demonstrated the success of the theory on hand of experimental data[1,4].

In the course of this work we came across a curious anomaly in the behavior of a dicumyl peroxide cured styrene-butadiene rubber (SBR). In this material time-shift invariance is not preserved at strains at which the true stress-strain behavior is definitely linear. The lack of time shift invariance is not apparent in stress relaxation measurements but can be demonstrated easily in experiments at constant rates of strain. Furthermore, it can be removed reversibly by lightly plasticizing the sample with silicone oil. In this paper we describe our efforts to track down this anomalous behavior. The work reported here clearly shows that one may not infer that a material is linearly viscoelastic simply because it behaves linearly in stress relaxation tests.

THEORY

We assume that the reader is familiar with the theory developed in the companion paper[1]. Here, we present only the theory of the application of our solid model[1,2,4] to a triangular function of strain.

Triangular Function of Strain

Let a specimen be deformed in simple tension at a constant rate of strain $\dot{\varepsilon}_1$ from $t = 0$ to $t = t_r$ at which time another constant rate of strain $\dot{\varepsilon}_2$ is imposed with the direction of travel of the crosshead reversed. The strain thus appears as a triangular function of time. The triangular strain function is similar to the trapezoidal function discussed in the companion paper[1]. It differs from it in that the strain is not held constant between the ascending and descending branches of the function.

We have

$$\lambda(u) = 1 + \dot{\varepsilon}_1 u h(u) - (\dot{\varepsilon}_1+\dot{\varepsilon}_2)(u-t_r)h(u-t_r) \tag{1}$$

and

$$d\lambda(u) = [\dot{\varepsilon}_1 h(u) - (\dot{\varepsilon}_1+\dot{\varepsilon}_2)h(u-t_r) + \dot{\varepsilon}_1 u\delta(u) - (\dot{\varepsilon}_1+\dot{\varepsilon}_2)(u-t_r)\delta(u-t_r)]\, du \tag{2}$$

The delta function terms will contribute nothing. Hence, we may set

$$d\lambda(u) = \begin{cases} \dot{\varepsilon}_1 \, du & \text{for} \quad u<t_1 \\ -\dot{\varepsilon}_2 \, du & \text{for} \quad u>t_1 \end{cases} \tag{3}$$

Substitution of eq. (3) into eq. (4) of the companion paper[1] yields

$$\begin{aligned} \bar{\sigma}(t) = (2\dot{\varepsilon}_1/3)\int_0^{t_r} E(t-u)[(1+\dot{\varepsilon}_1 u)^{n-1} + 0.5\,(1+\dot{\varepsilon}_1 u)^{-(n+2)/2}]\,du \\ -(2\dot{\varepsilon}_2/3)\int_{t_r}^{t} E(t-u)]\lambda_p^{n-1}(u) + 0.5\,\lambda_p^{-(n+2)/2}(u)]\,du \end{aligned} \tag{4}$$

where

$$\lambda_p(u) = 1 + \dot{\varepsilon}_1 t_r - \dot{\varepsilon}_2(u-t_r) \tag{5}$$

MATERIALS

Most of the work described here was carried out on dicumyl peroxide (DCP) cured styrene-butadiene rubber (SBR). Various other materials were also examined, albeit in less detail. Series of samples with different crosslink densities were prepared from most materials. The main characteristic of the materials we used are presented in Table I. In particular, this table lists the equilibrium swelling ratios, q, of

the samples in toluene at 23°C, as a measure of crosslink density. Because of its crystallinity, the trans-1,4-polybutadiene sample was refluxed in toluene to facilitate swelling and subsequently cooled to 23°C.

Sample Preparation

Except for some cast samples, all crosslinked samples were compression molded as described previously[1].

A series of samples with three different crosslink densities were prepared from Phillips SBR 1502 gum stock with DCP. The work reported in detail in this paper was carried out on the sample with swelling ratio 8.3. Since this sample will be compared chiefly with the same material lightly plasticized with silicone oil described in the companion paper, it will be referred to here as the unplasticized SBR, or simply as SBR.

Cast samples were prepared by dissolving 100 parts of SBR 1502 cold-milled with 1 part of DCP in toluene. Solution was complete, indicating that milling of SBR in the presence of DCP does not lead to crosslinking. The 5% solution was evaporated at room temperature over a period of about one week. Samples with different crosslink densities were produced by heating, under a nitrogen blanket, varying the time and temperature in the oven.

A sulfur-cured sample of the same SBR was prepared using the recipe:

SBR 1502	100 parts
Sulfur	1 part
Zinc oxide	2 parts
Methazate	0.5 parts
Stearic acid	0.5 parts
MBTS	0.5 parts
N-phenyl-2-naphthylamine (antioxidant)	1 part

Methazate® is zinc dimethyl dithiocarbamate. MBTS® is benzothiazyl disulfide. Both chemicals are manufactured by Naugatuck Chemical.

A series of samples with varying crosslink densities were also prepared from Shell® SBR 1500 using DCP. These samples did not contain antioxidant. Some samples with different crosslink densities were made from another SBR, Phillips Solprene® 1204. These samples were also cured with DCP. No antioxidant was used.

Two samples with different crosslink densities were prepared from natural rubber (smoked sheet).

In addition, DCP-crosslinked samples were prepared from cis-1,4-polybutadiene. Samples of trans-1,4-polybutadiene were prepared in a similar way but were milled at about 100°C on hot rolls. Both gum stocks were graciously supplied by Phillips Petroleum Company.

Samples with different crosslink density were also made of Exxon® 305 butyl rubber. Exxon supplied this material free of charge for our research. The samples were sulfur cured by the following recipe:

Butyl 305	100 parts
Sulphur	2 parts
ZnO	4 parts
Methazate	1 part
Stearic acid	1 part
MBTS	1 part

We also prepared samples of acrylonitrile-butadiene (nitrile) rubber by milling 100 parts of the gum with 1 part of DCP.

Uncrosslinked samples were also compression molded but at lower temperatures than the crosslinked ones. We used SBR 1502 with one part of N-phenyl-2-naphthylamine as antioxidant, and two samples of uncrosslinked polybutadiene (PBD). The PBD samples were prepared in the Research Laboratory of Phillips Petroleum Co. from Phillips Solprene® 235. Their characteristics are given elsewhere[4]. They were intended to be ultralightly crosslinked with sulfur, but dissolved completely in toluene. Stress relaxation measurements pointed to a possible bimodal distribution of molecular weights. Thus, these samples in all likelihood contained highly branched structures.

Specimen Preparation

All experiments were made on tab bonded strip specimens as described earlier[1]. Several specimens were extracted with various solvents as listed in Table I.

EXPERIMENTAL METHODS

Experiments were made in uniaxial tension on a model TTB Instron testing machine fitted with a Missimers temperature control chamber. Further details are given elsewhere[1].

RESULTS

The stress relaxation modulus master curve for our main sample, the unplasticized SBR, is shown in Fig. 2 of the companion paper[1] and is there compared with the master curve for the plasticized sample. Determination of the strain parameter n from stress relaxation measurements on the unplasticized sample according to our theory gives n = 1.22 at 23°C, identical with the value obtained on the plasticized sample[1]. Figure 1 shows stress-strain data on the unplasticized SBR for three different strains rates. These data could not be fitted with n = 1.22. The solid lines represent the fit with n = 1.4, obtained from nonlinear least squares fitting to the data with $\dot{\varepsilon} = 4.42\ \text{min}^{-1}$. Such a fit to the data at $\dot{\varepsilon} = 0.0011\ \text{min}^{-1}$ gives n = 1.7. Clearly, our theory does not apply to this material.

Figure 2 shows the response to a triangular function of strain at two different strain rates. The stress is plotted as function of time. The solid lines represent the predictions of the theory. The stretch ratio λ_r corresponds to the strain at t_r. Deviations at the highest strain result from the upswing in the stress-strain curve to which our theory does not apply. The response to the ascending branch of the

excitation function is otherwise well predicted with n = 1.4. In fact, the two ascending branches are identical with the two uppermost curves in Fig. 1. Clearly, however, our theory fails to predict the response to the descending branches correctly. The experimental point on the time axis at zero stress is common to both experiments. Its distance along the time axis from the common zero-stress point predicted by the theory is the same. Hence Fig. 2 indicates that the failure of the theory may not be related to the magnitude of the strain.

Further corroboration comes from Fig. 3. Here, the full and empty circles represent a continuous ramp function of strain and a triangular strain function respectively. The reproducibility of the data in both ascending branches is excellent. Because of the very small maximum strain (0.61%) reached in the triangular test, we may predict the descending branch from linear viscoelastic theory. In general, we may forego the use of the generalized strain measure whenever the strain falls into the isochronal linear stress strain (or true stress-strain) region[1]. We will show later that for the unplasticized SBR the isochronal true stress-strain relations are linear below about 1.3% strain.

Since, in our case, the same strain rate was used in both the ascending and descending branches, we have $\dot{\varepsilon}_1 = \dot{\varepsilon}_2 = \dot{\varepsilon}$ and eq. 1 gives

$$\varepsilon(t) = \dot{\varepsilon} t h(t) - 2\dot{\varepsilon}(t-t_t)h(t-t_r) \tag{6}$$

Hence, the stress is

stress relaxation experiments. Figure 6 shows E(t) as a function of log t for different strains, all less than 1.5%. The fanning-out at short times results from the ramp transients which, in turn, derive from the fact that experimentally a constant strain cannot be achieved instantaneously. Part of this fanning-out is no doubt due to the non-preservation of time shift invariance in the ramp portion. The envelope in Fig. 6 represents the true step response which is seen to be independent of strain over about two decades of time. We also note that the maximum strain in Fig. 4 is well within the range of strains covered in Fig 6. Clearly, the isochronal stress-strain behavior[1] is linear at least below 1.34% strain and any observed nonlinear behavior is due to lack of time shift invariance.

So far we have discussed only data at 23°C. We obtained data at different temperatures between about -40 and 23°C in both step and ramp experiments. For a thermorheologically simple material we should have[5]

$$\log a_T = - c_1 \Delta T/(C_2+\Delta T) \tag{10}$$

where c_1 and c_2 are the WLF parameters and ΔT is the difference between the test and reference temperatures. The bottom curve in Fig. 7 shows the usual plot of $\Delta T/\log a_T$ against ΔT for the experiments at constant strain, ε_o. The top curve represents a similar plot for experiments at the same constant rate of strain, $\dot{\varepsilon} = 0.0011\ \text{min}^{-1}$. The shift distances, $\log a_T$, were obtained by diagonal shifting as required by theory. In experiments at constant strain, we have

$$\sigma(t)/\varepsilon_o = E_{T_o}(t) \tag{11}$$

at the reference temperature T_o, and

$$\sigma(t)/\varepsilon_o = E_{T_1}(t) = E_{T_o}(t/a_T) \tag{12}$$

at the test temperature T_1. In eq. (12) a_T is the shift factor which changes the time scale at T_1 to that at T_o. In experiments at constant rate of strain we have

$$\sigma(t)/\dot{\varepsilon} = \int_o^t E_{T_o}(t-u)\, du = \eta_{T_o}(t) \tag{13}$$

at the reference temperature, and

$$\sigma(t)/\dot{\varepsilon} = \int_o^t E_{T_1}(t-u)\, du = \eta_{T_1}(t) \tag{14}$$

at the test temperature. Substituting eq. (12) into eq. (14) we obtain

$$\sigma(t)/\dot{\varepsilon} = \int_o^t E_{T_o}[(t-u)/a_T]\, du \tag{15}$$

A change of variable yields

$$\sigma(t)/\dot{\varepsilon} = a_T \int_o^{t/a_T} E_{T_o}(t/a_T - w)\, dw = a_T\, \eta_{T_o}(t/a_T) \tag{16}$$

Hence,

$$\eta_{T_1}(t) = a_T \, \eta_{T_o}(t/a_T) \tag{17}$$

and it is seen that time-temperature superposition in ramp experiments requires both a horizontal and a vertical shift, i.e. a shift along a diagonal in logarithmic coordinates. Equation (17) further implies that the shift factor a_T should be the same in step and in ramp experiments. The latter is a consequence of the use of the Boltzmann superposition principle in the derivation of the equation.

In deriving eq. (17) we have neglected the customary temperature-density correction[5] because we did not need it with our unplasticized SBR sample. This matter is more fully discussed elsewhere[6].

Although the constant rate of strain data at different temperatures could be superposed by a diagonal shift, and were found to obey the WLF equation as shown by the top curve in Fig. 7, the shift distances in the two sets of experiments were not identical.

We remark parenthetically that the unplasticized SBR appeared to be thermorheologically complex in either step or ramp experiments in the temperature range between 30 and 60°C. No data were obtained at still higher temperatures.

As prepared, the sample on which the experiments described here were performed, contains about 6% sol fraction. The data presented in Figs. 1, 2, 5 and 7 were obtained on this sample. Uncrosslinked SBR 1502 is time shift invariant. Hence, after these experiments were completed, the specimen was exhaustively extracted with toluene at 23°C to remove the

sol fraction. The data presented in Figs. 3, 4, and 6 were obtained with the extracted specimen. Removal of the sol fraction appeared to make the anomalous lack of time shift invariance in the crosslinked SBR 1502 more prominent.

Strikingly, plasticization with about 1.5% silicone oil (Dow Corning 200, either 10 or 2 centistokes) completely removed the anomaly, as described in the companion paper[1]. An illustration of this is given in Fig. 8 which should be compared with Fig. 4. The effect is reversible. Extraction of the silicone oil with toluene restored the anomalous behavior. Replasticization again removed it.

So far we have presented results obtained on the unplasticized DCP-cured SBR 1502 with swelling ratio 8.3. We remark that similar results were obtained with different specimens cut from the same sheet and with specimens from different sheets. Another sample with a swelling ratio of 6.5 showed the same lack of time shift invariance; however, a highly crosslinked sample with swelling ratio 1.7 did not.

The samples prepared from SBR 1500 also showed lack of time shift invariance at all the crosslink densities studied (see Table I). No correlation was found between swelling ratio and the amount of deviation from time shift invariance as measured by the separation between two ramp responses (see Fig. 4). To ascertain whether mixing inhomogenities were involved, we prepared and examined the cast samples. These showed perfect preservation of time shift invariance. So did the compression molded samples prepared from Solprene 1204. The composition and structural characteristics of Solprene 1204, SBR 1500, and SBR 1502 are compared in Table II.

The tabulation is due to Hanmer and Railsback[7]. The solution polymerized Solprene 1204 differs both in composition and structural characteristics from the emulsion polymerized SBR 1500 and SBR 1502 which differ from each other only in their content of fatty and rosin acids apart from polymerization conditions[8] which are not included in Table II.

Removal of the fatty and rosin acids through Soxhlet extraction with toluene-ethanol azeotrope (TEA)[9] had no effect on the anomalous behavior. We found that the TEA extraction also removes unreacted DCP and antioxidant. Hence, the presence of these compounds in the sample is unrelated to the anomalous behavior.

The main difference between the solution and emulsion polymerized SBRs is in their microstructure. We found that DCP-cured cis-1,4-polybutadiene (at 23°C) did not show the anomaly. The behavior of DCP-cured trans-1,4-polybutadiene was regular at 23°C but anomalous at 60°C in the sense of showing lack of time shift invariance but this was accompanied by stress-strain nonlinearity.

SBR 1502 when crosslinked with sulfur (see Table I) evinced regular behavior as shown in Fig. 9 which should be compared with Fig. 3. To ascertain that this was not due to a possible plasticizing effect of the stearic acid required by the compounding recipe, the unreacted acid was removed by extraction with TEA. This had no effect on the behavior.

Sulfur cured butyl rubber and natural rubber as well as nitrile rubber crosslinked with DCP behaved regularly. Hence, DCP is not responsible for the anomaly.

Another difference between the solution and emulsion polymerized SBRs is the degree of long chain branching. Solprene 1204 contains fewer branches[7] than SBR 1500 and 1502. That long chain branches are unlikely to be responsible for the anomaly is indicated by the regular behavior of the two highly branched uncrosslinked PBD samples and of the already discussed cis-1,4-polybutadiene which is also highly branched[9].

DISCUSSION

In the preceding section we have shown that compression molded dicumyl peroxide cured emulsion polymerized SBR shows anomalous viscoelastic behavior inasmuch as its mechanical response to a ramp function of strain is not time shift invariant in a region of small strains in which the isochronal stress-strain relation is perfectly linear. We know of no other unfilled material which would not obey the Boltzmann superposition principle under these circumstances. This anomalous behavior is reflected also in the temperature dependence of the response to step and to ramp functions of strain. We believe that this is a consequence of the fact that the temperature function a_T can only be identical in the two responses if the material satisfies the superposition principle.

According to linear viscoelastic theory the step and ramp responses are given by

$$\sigma(t) = E(t)\varepsilon_o \tag{18}$$

and

$$\sigma(t) = \eta(t)\dot{\varepsilon} \tag{19}$$

where

$$\eta(t) = \int_o^t E(u)\ du \tag{20}$$

We showed that our material satisfies eq. (18), but does not satisfy either eq. (19) or (20). As shown by Farris[10] similar behavior is encountered in solid propellants for strains which are small enough so that the effect, if any, of vacuole formation can be neglected. Farris developed a method which preserves eqs. (18) and (19) but substitutes an equation based on Lebesgue norms for eq. (20). Farris did not present data to show whether his propellant satisfied eq. (19). Since our material does not, his method fails in our case. Farris's approach[10] is, in principle, more general than the specific form which he used to describe his propellant. We hope to examine at a later date the possibilities which the more general approach offers.

Farris's observation on a solid propellant suggests that our SBR may, in some way, behave as a two-phase system. Deviations from linear viscoelastic behavior may be expected in such materials[11]. Now, trans-1,4-polybutadiene is highly crystalline[12] and melts (Form II) at 145°C.

It undergoes a crystalline phase transition[12] to Form I which is stable below 75°C. Cis-1,4-polybutadiene also crystallizes but melts at 2°C. At 25°C the degree of crystallinity[13] is zero, and is less that 20% at -16°C in this material. It is known that in butadiene polymers prepared with AlR_3-$TiCl_4$ catalyst the non-cis units occur in blocks[12]. According to Mandelkern, Tryon, and Quinn[14] a polybutadiene having a similar composition to that of the butadiene in our SBR, shows a crystalline melting range between -25°C and room temperature. It seems at least possible, therefore, that the 74% of trans-1,4 isomer in the butadiene contained in DCP-cured SBR 1500 and 1502 occurs partly in blocks which may form crystallites whose melting range extends from about -25°C to room temperature. On the basis of this hypothesis we might consider that main chain modifications introduced by a sulfur cure would decrease the length of regular segments along the chain and thus prevent crystallite formation. The role of silicone oil in removing the anomoly would still remain unexplained. Neither can we explain the difference in behavior between the compression molded and the cast samples. It is possible that compression molding promotes the formation of crystallites by aligning regular segments.

In conclusion we point out that compression molded dicumyl peroxide cured emulsion polymerized SBR might be a suitable material for studying time shift invariance free of possible complications arising from nonlinear stress-strain behavior.

References

1. R. Bloch, W.V. Chang and N.W. Tschoegl, submitted to this journal.
2. W.V. Chang, R. Bloch and N.W. Tschoegl, submitted to *Rheol. Acta.*
3. P.J. Blatz, S.C. Sharda and N.W. Tschoegl, *Trans. Soc. Rheol.* 18, 145 (1974).
4. W.V. Chang, R. Bloch, and N.W. Tschoegl, submitted to *J. Polymer Sci.*
5. J.D. Ferry, *Viscoelastic Properties of Polymers*, 2nd ed., Wiley New York 1970.
6. W.V. Chang, R. Bloch, and N.W. Tschoegl, submitted to *Macromolecules.*
7. R.S. Hanmer and H.E. Railsback, *Rubber Age* 96, 73 (1964).
8. G.S. Whitby, "*Synthetic Rubber*", Wiley, New York, 1954.
9. G. Kraus, Phillips Petroleum Co., private communication.
10. R.J. Farris, Ph.D. Dissertation, University of Utah, 1970.
11. R. Bloch, W.V. Chang and N.W. Tschoegl, submitted to *Rubber Chem. Tech.*
12. W.W. Saltman, *Encyclopedia of Polymer Science and Technology*, H. Mark, ed., Wiley-Interscience, Vol. 2, p. 727.
13. L.E. Alexander, S. Ohlberg and G.R. Taylor, *J. Appl. Phys.* 26, 1068 (1955).
14. L. Mandelkern, M. Tryon, and F.A. Quinn, *J. Polym. Sci.* 19, 77 (1956).

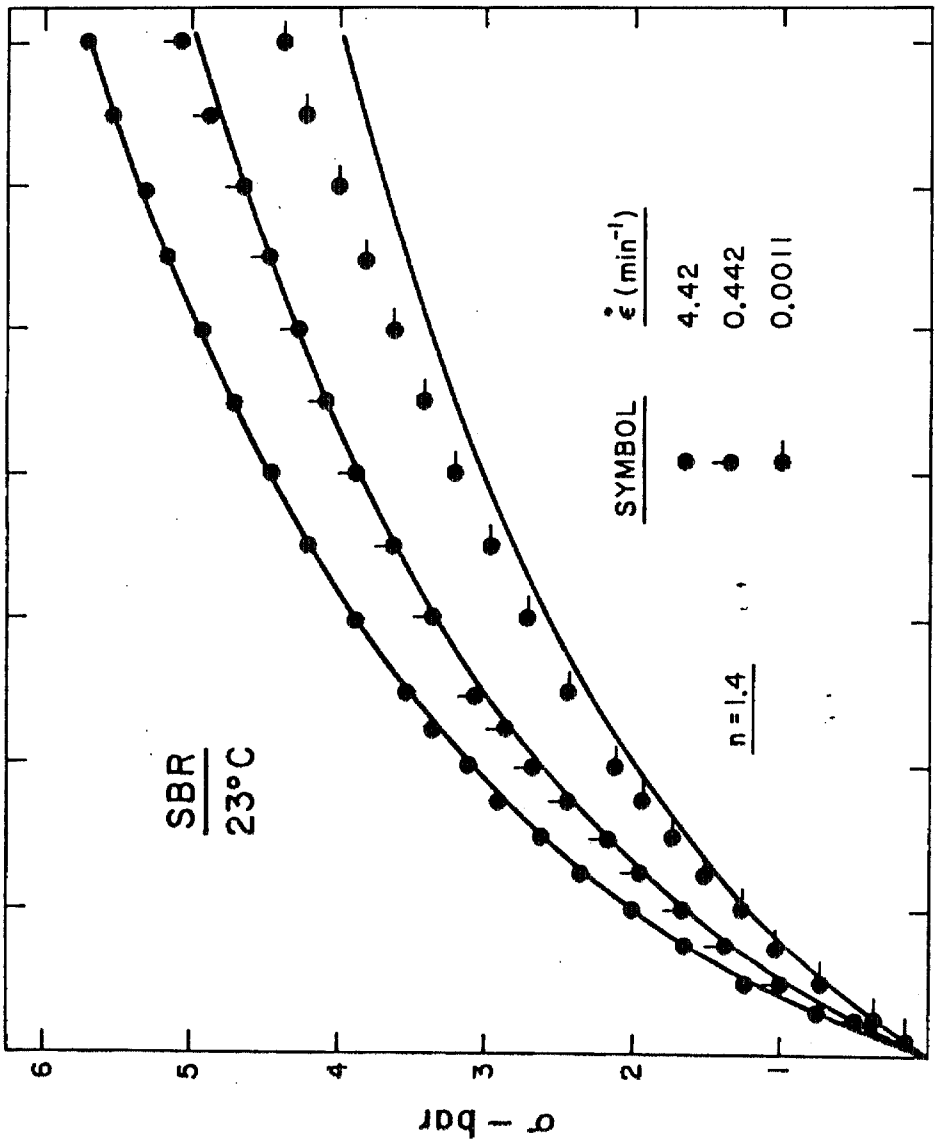

Figure 1 Response of unplasticized SBR at 23°C to ramp functions of strain at various strain rates as a function of stretch ratio.

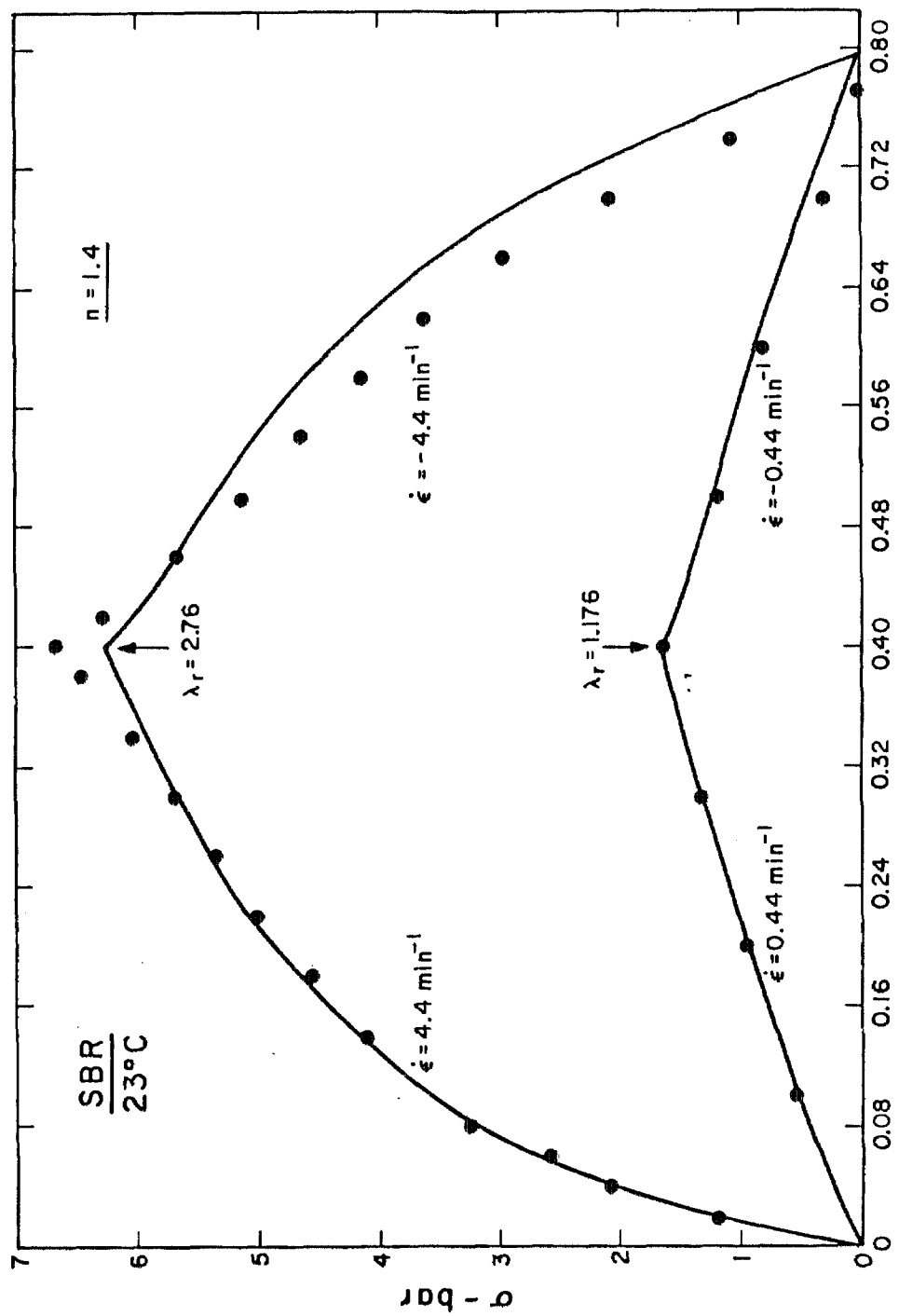

Figure 2 Response of unplasticized SBR at 23°C to two triangular functions of strain as function of time.

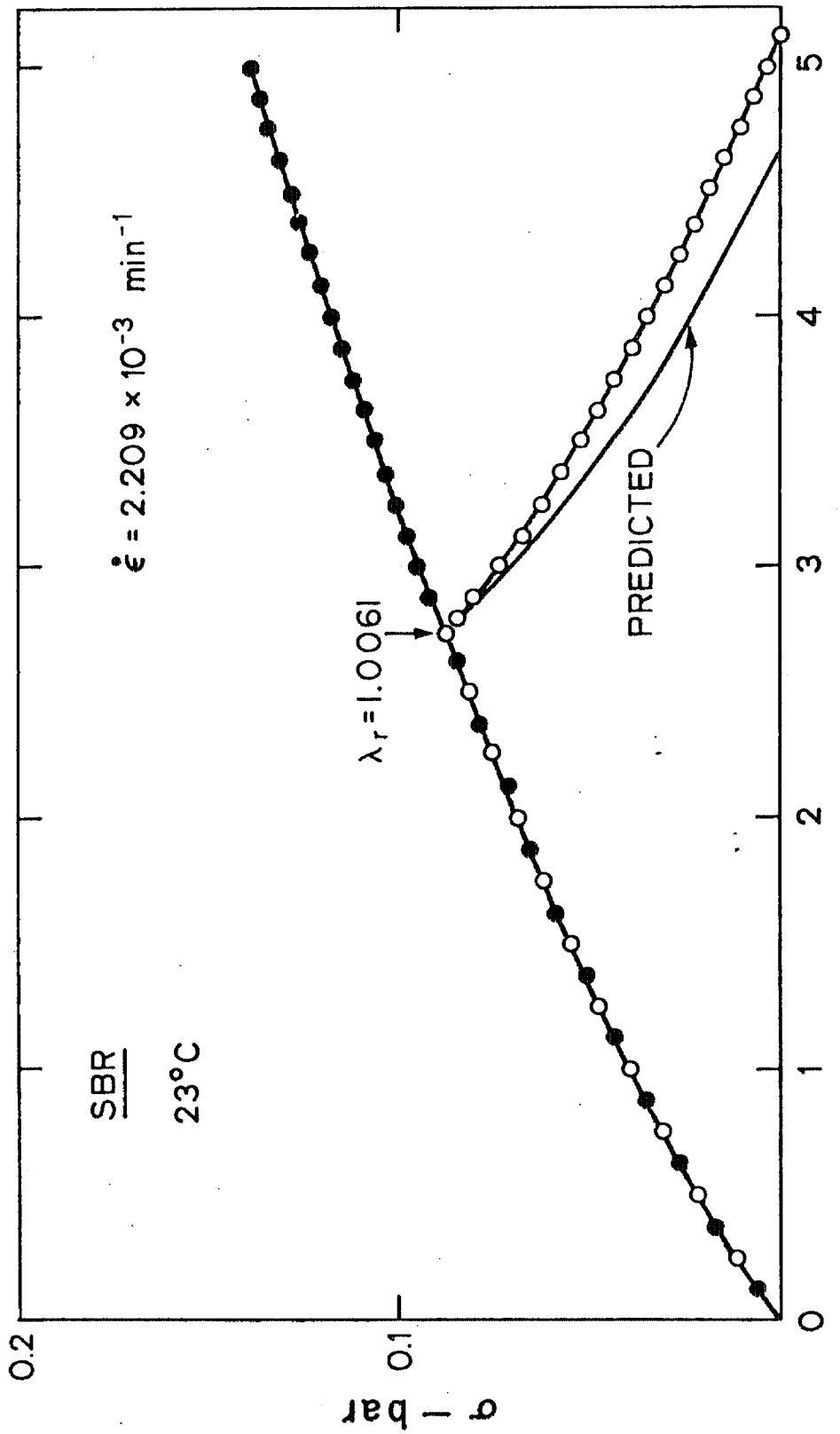

Figure 3 Response of unplasticized SBR at 23°C to a ramp function and to a triangular function of strain as function of time.

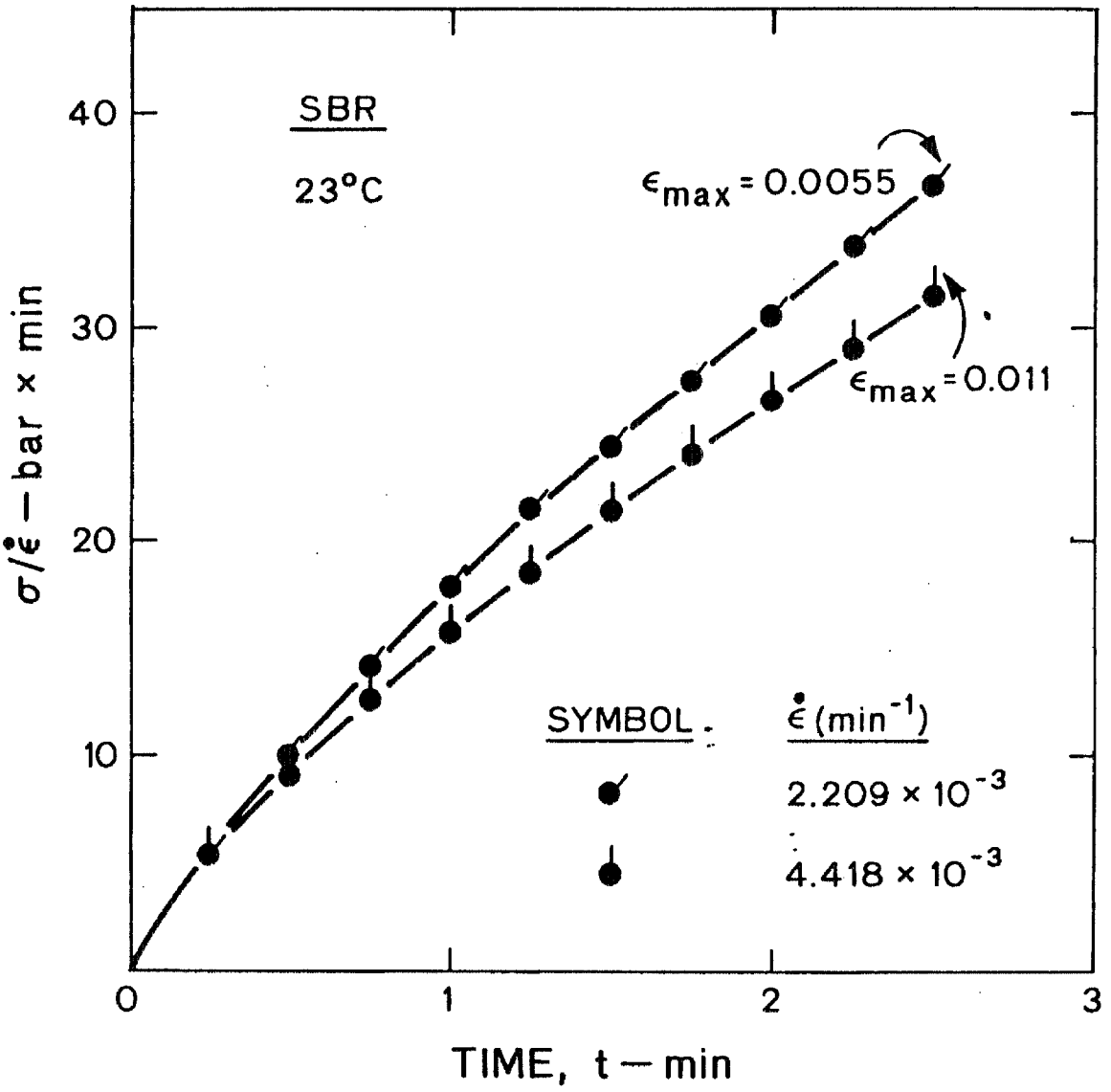

Figure 4 Response of unplasticized SBR at 23°C to two ramp functions of strain as function of time.

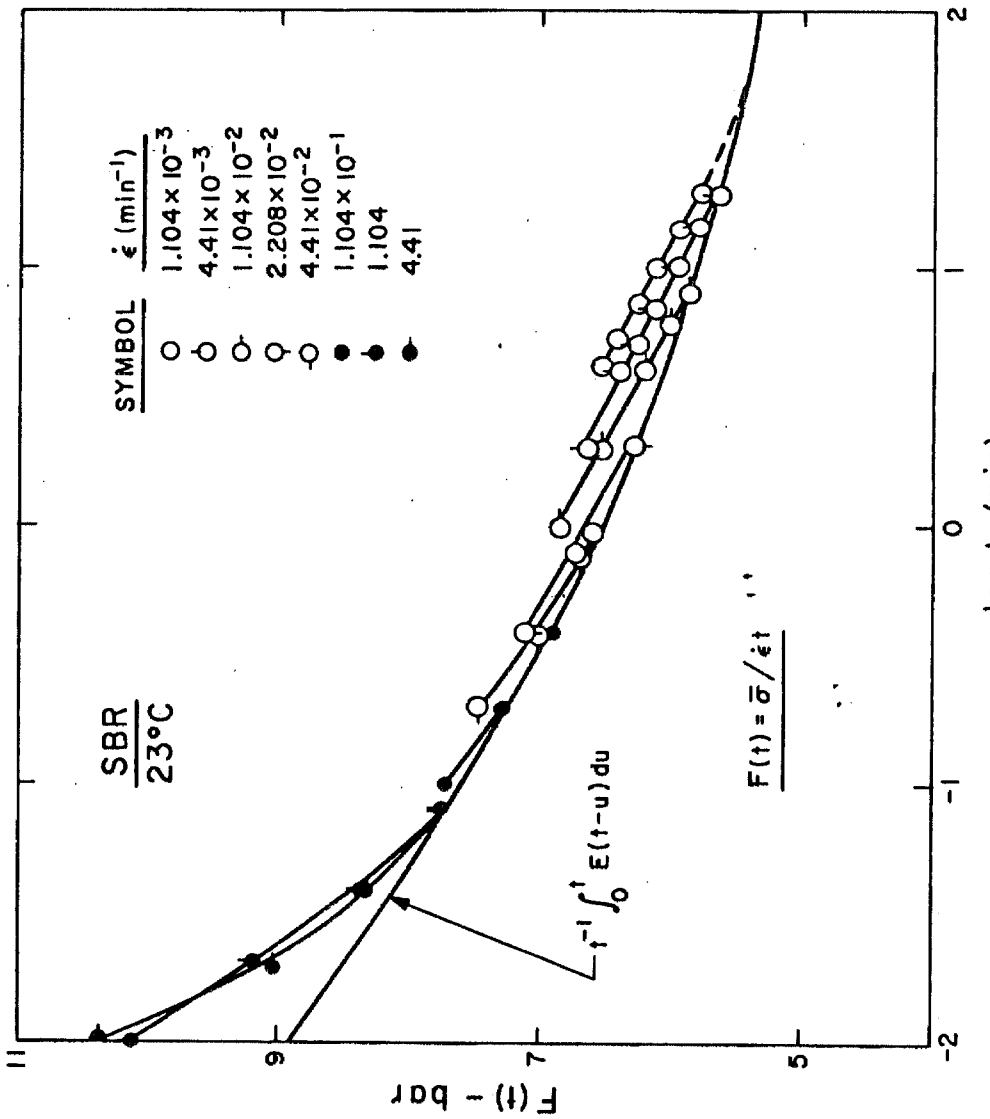

Figure 5 Secant moduli of unplasticized SBR at 23°C for various strain rates as function of time.

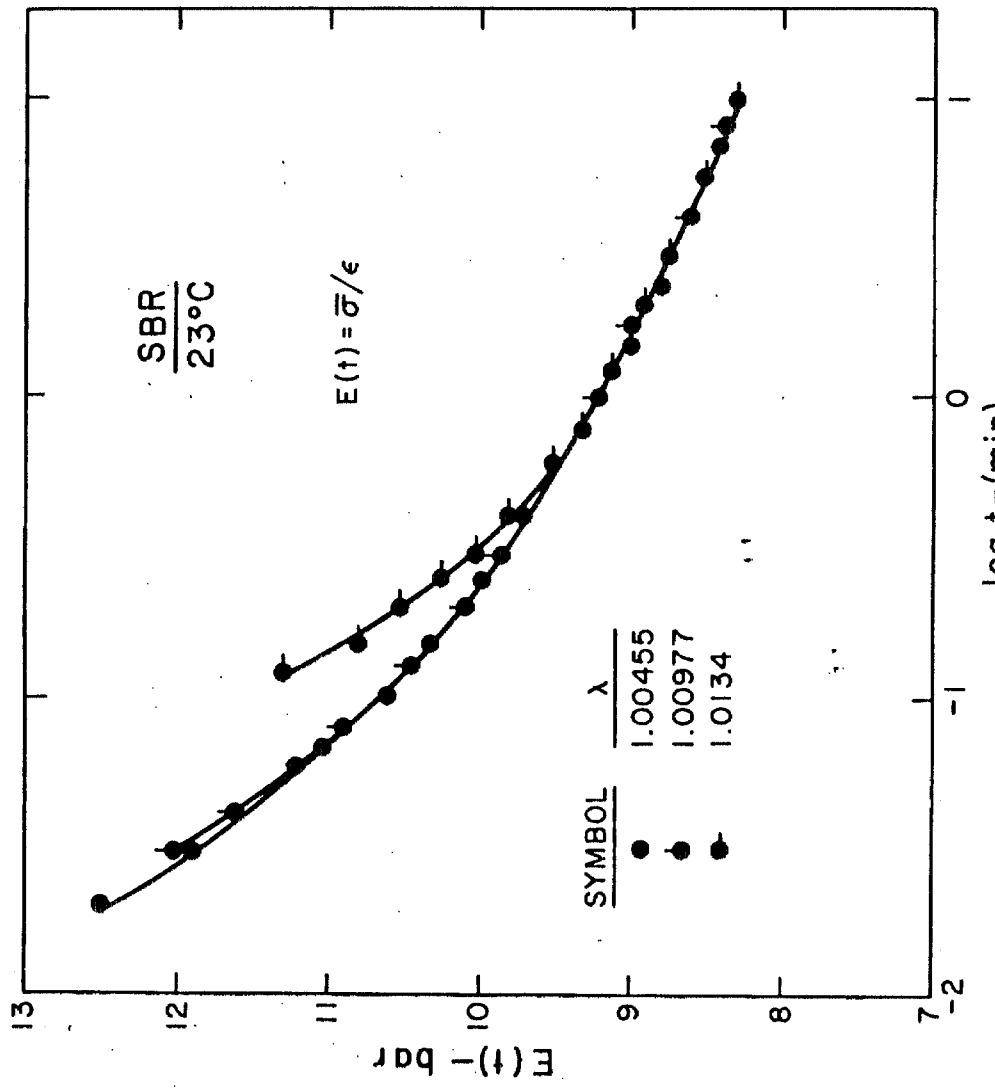

Figure 6 Relaxation modulus of unplasticized SBR at 23°C for three stretch ratios as function of time.

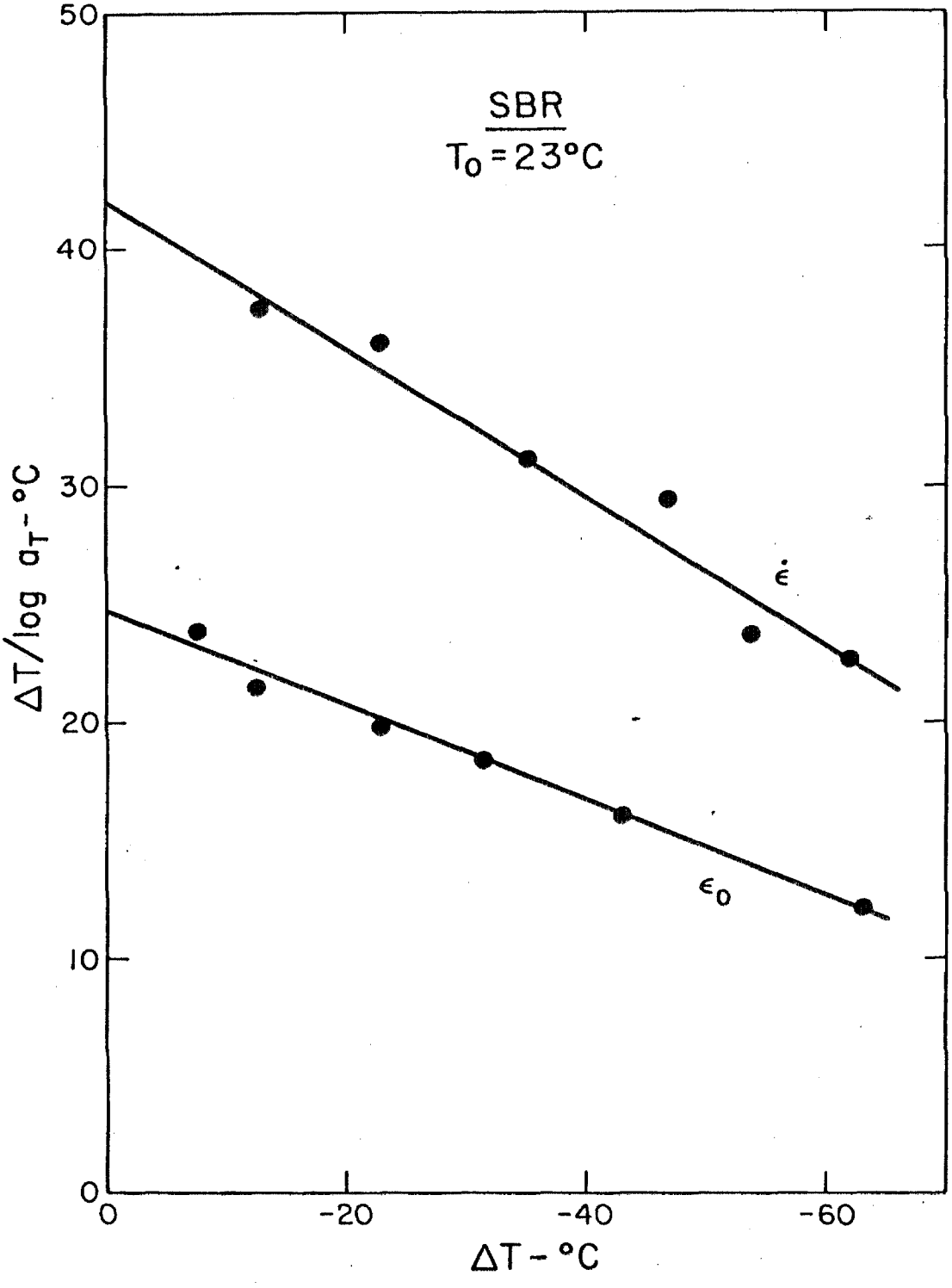

Figure 7 Linearized WLF plots for unplasticized SBR referred to 23°C.

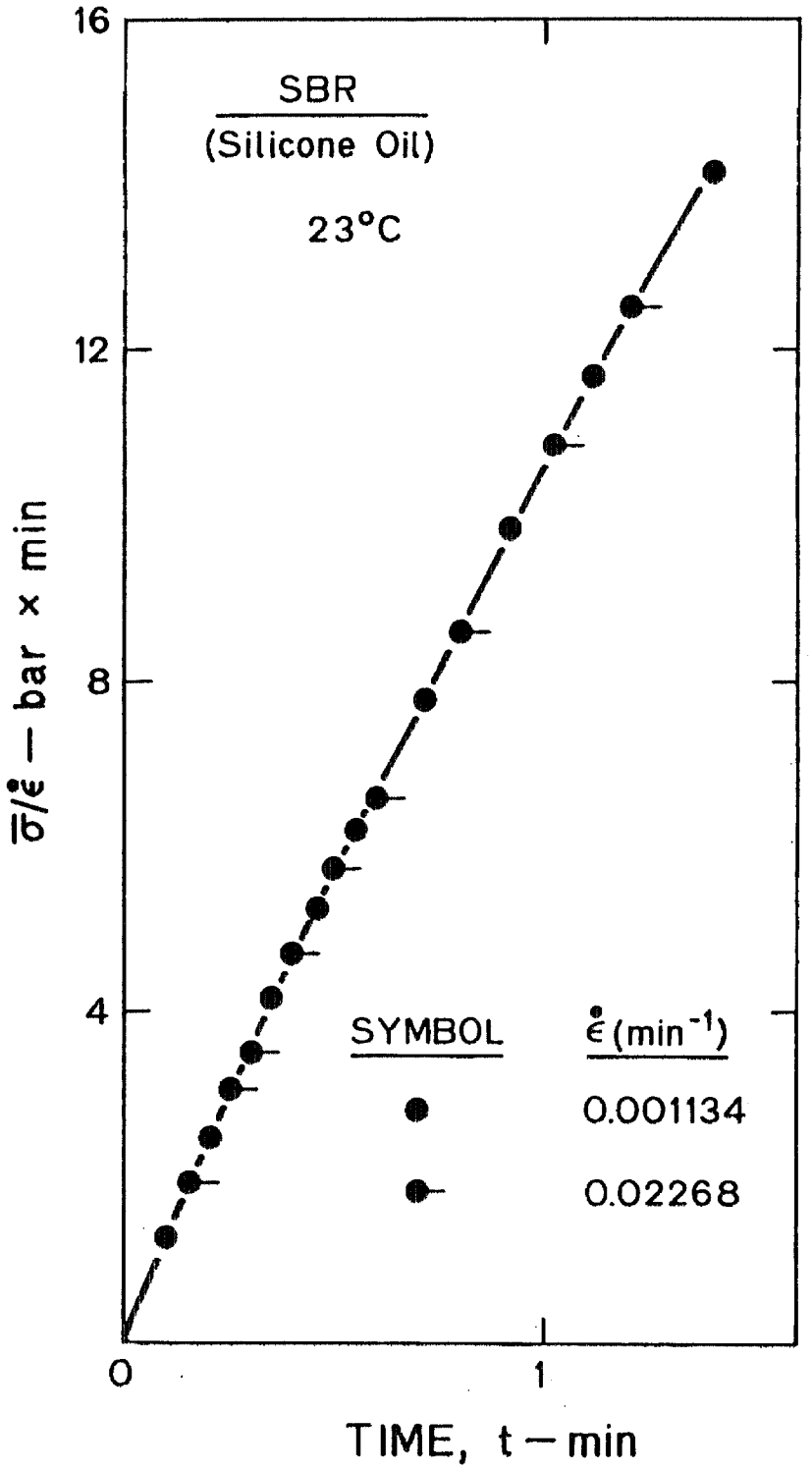

Figure 8 Response of plasticized SBR at 23°C for two ramp functions of strain as function of time.

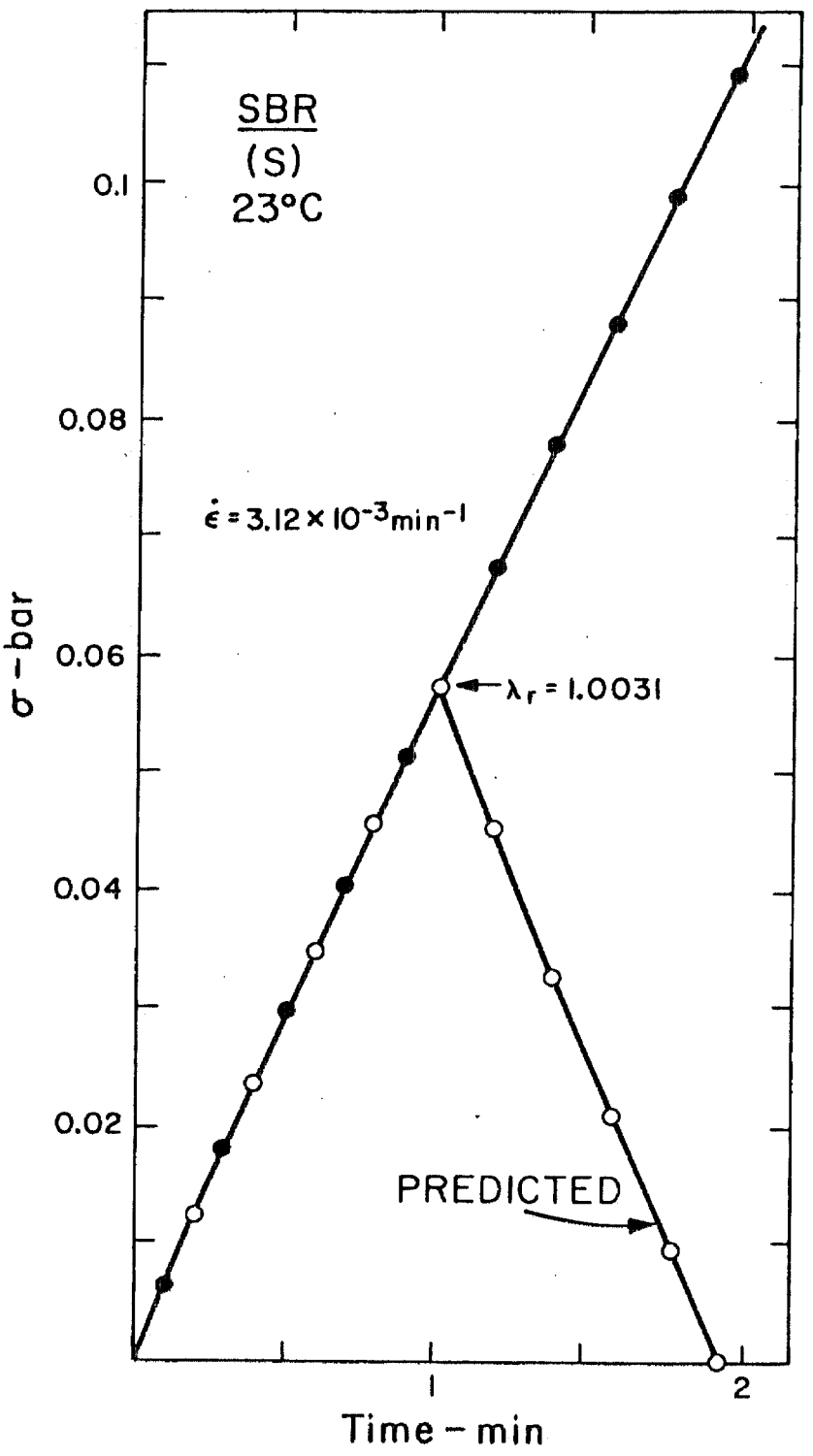

Figure 9 Response of sulfur crosslinked SBR at 23°C to a ramp function and to a triangular function of strain as function of time.

TABLE I

Preservation of Time Shift Invariance

Material	Crosslinking	q*	Treatment	T(°C)	Inv.
SBR 1502	peroxide	8.3		-40→23	no
			Tol. extr'd	23	no
			TEA extr'd	23	no
			1.5% Silicone Oil	-20→60	yes
			Tol. extr'd	23	no
		6.5	-	23	no
		1.7	-	23	yes
	peroxide	10.3	(cast)	0→23	yes
		6.2	(cast)	23	yes
	sulfur	6.9	Tol.+TEA extr'd	-20→23	yes
SBR 1500	peroxide	11.8	-	23	no
		5.2	-	23	no
		4.5	-	23	no
		3.5	-	23	no
Solprene 1204	peroxide	6.1	-	23	yes
NR	peroxide	17.2	Tol. extr'd	23	yes
		4.1	Tol. extr'd	-20→23	yes
PBD(cis)	peroxide	11.2	Tol. extr'd	23	yes
		3.4	Tol. extr'd	23	yes
PBD(trans)	peroxide	6.9	-	23	yes
				60	no
Butyl 305	sulfur	2.8	-	-20→23	yes
		3.6	Tol. extr'd	23	yes

*Swollen weight in toluene at 23°C per dry weight free of sol fraction.

TABLE II

Comparison of Butadiene-Styrene Copolymers[7]

	Solprene 1204	SBR 1500	SBR 1502
Method of Polymerization	Solution	Emulsion	Emulsion
Styrene (wt. %)	25	23.5	23.5
Fatty acid (wt. %)	0.5	-	2.9
Rosin acid (wt. %)	-	6.1	2.9
Ash (wt. %)	0.1	0.7	0.6
Water absorption (mg/sq. in.)	4	-	-
Monomer sequence	Random	Random	Random
Mol. wt. dist.	Narrow	Broad	Broad
Microstructure (diene portion)			
cis (%)	32	8	8
trans (%)	41	74	74
vinyl (%)	27	18	18

CHAPTER 4

VISCOELASTIC AND THIXOTROPIC BEHAVIOR IN CARBON BLACK FILLED SBR

INTRODUCTION

Rubbers are rarely used by themselves. In most industrial applications they are reinforced with a hard filler such as carbon black. Such applications include car tires, conveyor belts, motor mountings, etc. Addition of carbon black to the rubber lowers the cost while improving certain physical and chemical properties such as modulus, tensile strength, and ozone resistance.

We have obtained data in small and in moderately large tensile deformations on an uncrosslinked and a crosslinked styrene-butadiene rubber (SBR) filled with a high-structure carbon black. We call moderately large deformations those in which the relaxation spectrum in the response to a step function of strain is not changed by the level of strain. In carbon black filled rubbers the level of strain below which the deformation remains moderately large in this sense, is substantially lower than in the unfilled matrix rubber because of the presence of the filler. We developed and tested several models based on the assumption that time shift invariance is preserved in a moderately large deformation and that the observed nonlinear behavior can consequently be accounted for by stress-strain nonlinearity alone. Only one model (model HS) was even partly successful. The essential failure of the most general models, admitting a totally general, empirically determined strain function, indicates that time shift

invariance is not preserved even in moderately large deformations of structure black filled rubbers. Certain clues reported here suggest that this may be due to thixotropic effects arising from the time dependent destruction and reformation of a three-dimensional carbon black network held together by van der Waals forces.

THEORY

Our first aim is to develop suitable constitutive equations to describe the viscoelastic behavior of a carbon black filled elastomer as if we had no knowledge that it consists of filler and matrix. In simple tension the linear theory of visocelasticity provides the equation

$$\sigma(t) = \int_0^t E(t-u)d\varepsilon(u) \qquad (1)$$

where $\sigma(t)$ is the stress at the present time t, $E(t)$ is the relaxation modulus, and $\varepsilon(u)$ is the strain at the past time, u. Eq. (1) assumes that the material is isotropic and incompressible, apart from being homogeneous. The first assumption is justified because testing of specimens cut from the sample sheet with different orientations gave closely similar results. The second assumption is justified through the work of Shinomura and Takahashi[1] who showed that volume changes are negligible for strains less than 40% in simple tension at 25°C at the filler loadings (40-70 parts of filler per 100 parts of rubber) commonly used in carbon black filled elastomers.

As will be shown later, Eq. (1) is valid at most for strains below about 0.1% strain for compounds containing the usual filler loadings. We have shown elsewhere[2,3] that incorporation into Eq. (1) of a generalized strain measure characterized by a strain parameter n,

correctly predicts the viscoelastic behavior of unfilled crosslinked and uncrosslinked rubberlike (soft) materials in deformations which leave the distribution of relaxation times essentially unchanged[4,5].

Attempts to apply this theory to our filled samples were unsuccessful. It became clear that the n-measure of strain could not handle the relatively large curvature appearing in the isochronal stress-strain relation of carbon black filled rubbers at strains below about 10%. It is easy to show that, as a function of n at any strain for a given modulus, the single term potential of Blatz, Sharda, and Tschoegl[6] or Ogden[7] predicts a mimimum in the slope of the stress-strain relation which is not sufficient to account for the observed behavior. It follows that Ogden's linear combination of several n-measures of strain is to no avail. It is also clear that extension of the single term potential to the two-term potential of Blatz, Sharda, and Tschoegl[6] is futile because the second term does not contribute at small strains. We believe with Payne and Whittaker[8], Medalia[9], and Kraus[10] that the high curvature arises from the breakdown of the three-dimensional network structure formed by secondary aggregation of the primary structure aggregates (see next section) through van der Waals attraction. We therefore abandoned the n-measure of strain and attempted to describe the observed behavior through a more flexible generalized strain function $g(\lambda)$, where λ is the stretch ratio.

Our new approach is based on the empirical finding[11] that the response of filled systems to a step function of strain in simple

tension may be described by

$$\bar{\sigma}(t) = E(t)g(\lambda) \tag{2}$$

where $\bar{\sigma}(t)$ is the true stress. The function $g(\lambda)$ reduces to 1 as $\lambda \to 1$. $E(t)g(\lambda)/\varepsilon_o$ represents the secant modulus. Eq. (2) implies that the effects of time and strain can be factorized. This is commonly found to be true for unfilled elastomers up to about 150% strain in simple tension. We expect that the limit of applicability of Eq. (2) is reduced in filled systems, depending on the amount and nature of the filler.

We propose two models which are generalizations of the "solid" and "liquid" models we introduced elsewhere[3]. In simple tension the first (Model GS) takes the form

$$\bar{\sigma}(t) = \int_o^t E(t-u) \frac{dg[\lambda(u)]}{du} du \tag{3}$$

while the second (Model GL) becomes

$$\bar{\sigma}(t) = -\int_{-\infty}^t E(t-u) \frac{dg[\lambda(t)/\lambda(n)]}{du} du \tag{4}$$

We have here used a simplified notation for the generalized strain function[3,5] which is convenient to use in simple tension. The relation

between $g[\lambda(u)]$ and the function $\Phi[\lambda_\alpha(u)]$ is given, for $\lambda_1 = \lambda$, by

$$g[\lambda(u)] = \Phi[\lambda(u)] - \Phi[\lambda(u)^{-1/2}] \tag{5}$$

and an analogous relation applies to $g[\lambda(t)/\lambda(u)]$. To specialize Eqs. (3) and (4) to a particular form of excitation we follow the procedure used in the earlier papers[4,5]. For a step response both equations reduce to Eq. (2). For a ramp response (constant rate of strain experiment) Eq. (3) yields

$$\bar{\sigma}(t) = \dot{\varepsilon}\int_0^t E(t-u)g'[\lambda(u)]\,du \tag{5}$$

where $\dot{\varepsilon}$ is the strain rate and the prime denotes differentiation with respect to the argument, $\lambda(u)$. Eq. (4) gives

$$\bar{\sigma}(t) = \dot{\varepsilon}\int_0^t E(t-u)[\lambda(t)/\lambda^2(u)]g'[(\lambda(t)/\lambda(u)]\,du \tag{6}$$

For a small (theoretically infinitesimal) ramp superposed on a finite stretch λ_r at the time t_r we have

$$\lambda(u) = 1 + (\lambda_r - 1)h(u) + \dot{\varepsilon}(u-t_r)h(u-t_r) \tag{7}$$

where $h(u)$ is the unit step function. Expanding $g[\lambda(u)]$ in a Taylor series around λ_r and neglecting higher terms $g[\lambda(u)]$ becomes

$$g[\lambda(u)] = g(\lambda_r)h(u) + \dot{\varepsilon}(u-t_r)g'(\lambda_r)h(u-t_r) \tag{8}$$

If we define

$$\Delta\bar{\sigma}(t,t_r) = \bar{\sigma}(t) - \bar{\sigma}_r(t) \tag{9}$$

where $\bar{\sigma}(t)$ is given by Eq. (3) and

$$\bar{\sigma}_r(t) = E(t)g(\lambda_r) \tag{10}$$

we obtain

$$\Delta\bar{\sigma}(t,t_r) = \dot{\varepsilon}g'(\lambda_r)\int_o^{t-t_r} E(u)du = g'(\lambda_r)\dot{\varepsilon}(t-t_r)F(t-t_r) \tag{11}$$

for model GS, and

$$\Delta\bar{\sigma}(t,t_r) = \{[g'(\lambda_r)-1]E(t) + F(t-t_r)/\lambda_r\}\dot{\varepsilon}(t-t_r) \tag{12}$$

where

$$\lambda(t) = \lambda_r + \dot{\varepsilon}(t-t_r) \tag{13}$$

for model GL. The derivation of Eq. (12) follows that given in the appendix to reference (5). In Eqs. (11) and (12) F(t), the constant

strain rate modulus,[12] is defined by

$$F(t) = t^{-1}\int_0^t E(u)\, du = \sigma(t)/\dot{\varepsilon}t \tag{14}$$

for linear viscoelastic behavior. The constant strain rate modulus, $F_s(t,t_r)$, obtained in response to the superposed ramp function becomes

$$F_s(t,t_r) = \frac{\Delta\bar{\sigma}(t,t_r)}{\dot{\varepsilon}(t-t_r)} \tag{15}$$

Thus, for model GS

$$F_s(t,t_r) = g'(\lambda_r)F(t-t_r) \tag{16}$$

and for model GL

$$F_s(t,t_r) = [g'(\lambda_r)-1]E(t) + F(t-t_r)/\lambda_r \tag{17}$$

Both the GS and GL models predict the separability of strain and time effects in step response but not in ramp response. Model GS predicts separability in the response to a small ramp superposed on a finite stretch but model GL does not.

T.L. Smith[12] has proposed the equation

$$\sigma(t) = F(t)\Gamma(\lambda) \tag{18}$$

to describe the ramp response of unfilled elastomers. In our notation his equation becomes

$$\bar{\sigma}(t;\dot{\varepsilon}) = F(t)\hat{g}(\lambda)(\lambda-1) \tag{19}$$

where

$$\hat{g}(\lambda) = \lambda(\lambda-1)\Gamma(\lambda) \tag{20}$$

Extending this approach to a general response in simple tension we may write

$$\bar{\sigma}(t) = \hat{g}[\lambda(t)]\int_o^t E(t-u)\,\frac{d\lambda(u)}{du}\,du \tag{21}$$

We will call Eq. (21) the HS model. For a step response Eq. (21) reduces to

$$\bar{\sigma}(t;\varepsilon_o) = E(t)\hat{g}(\lambda)(\lambda-1)E(t) \tag{22}$$

For the superposition of a small ramp on a finite stretch, model HS

predicts

$$F_s(t,t_r) = \hat{g}'(\lambda_r)(\lambda_r-1)E(t) + F(t-t_r)\hat{g}(\lambda_r) \qquad (23)$$

The derivation is straightforward and follows the line of derviation of Eqs. (16) and (17). We note that model HS predicts the separability of strain and time effects in ramp and step response but not in the response to a small ramp superposed on a finite stretch.

MATERIALS

The work described in this paper was carried out on styrene-butadiene copolymer (Phillips® SBR 1502) and on cis-1,4-polybutadiene (B.F. Goodrich® CB 220).

Two carbon blacks were used in the study reported here: a medium thermal black (MT, ASTM designation N990) and a high abrasion furnace, high structure black (HAF-HS, ASTM designation N347). Thermal blacks have low structure, i.e. they consist[13] chiefly of single, spheroidal, relatively large particles (typically 270 nm). Furnace blacks have structure arising from the fusion of several spheroidal particles into primary structure aggregates of irregular shape. The size of the primary aggregates is roughly an order of magnitude smaller than that of the thermal black particles.

According to Kraus[10], the two most important physical characteristics of carbon blacks are their surface area and their maximum packing fraction. The surface area is measured by the absorption of surfactants such as cetyl trimethyl ammonium bromide (CTAB) or sodium di(2-ethyl hexyl) sulfosuccinate (Aerosol OT). The maximum packing fraction is obtained by determining the end point of the adsorption of dibutyl phthalate (DBP) or other oils by a specified amount of black which has first been subjected to a compacting procedure (compressed four times at 24000 psi).

The properties of our blacks[14]

Black	Surface Area	Oil Absorption
ASTM	CTAB (m^2/g)	DBP24M4 (cc/100g)
N990	8	40
N347	88	100

Sample Preparation

Samples were prepared according to the following recipes:

A.	SBR 1502	100 parts
	Antioxidant	1 part
	Dicumyl peroxide (crosslinker)	1 part
	N347 carbon black	40 parts
B.	SBR 1502	100 parts
	Antioxidant	1 part
	N347 carbon black	75 parts
C.	SBR 1502	100 parts
	Antioxidant	1 part
	N990 carbon black	5 parts
D.	CB 220	100 parts
	Dicumyl peroxide	1 part

The antioxidant was N-phenyl-2-naphthylamine. Hercules, Inc., Di-Cup® was used as the crosslinker. The ingredients were cold milled on a two-roll laboratory mill. The milled materials were placed in 15.2 x 15.2 x 0.2 cm (6 x 6 x 0.08 inch) molds and heated in a press at about 1750 bar (25000 psi) pressure for 15 minutes. Sample A was heated at 160°C (325°F), sample B and C at 112°C (240°F), and sample D at 126°C (260°F). Samples A and D became crosslinked under these conditions. The resulting samples had the following properties.

Sample	Sol fraction (weight %)	q*
A	4.0	2.66
B	25.0	5.53
C	99.5	(not detectable)
D	11.3	11.28

*Swollen weight in toluene at 23°C per sol free dry weight

A sample E was made by slowly casting an SBR block copolymer, Shell Kraton 101,® from solution in tetrahydrofurane (90%) and methyl ethylketone (10%).

Specimen Preparation

All experiments were made on tab bonded strip specimens. The strips were cut from the molded sheets using a knife-edged mill blade.

U-shaped phosphorus bronze tabs were glued to the ends using a poly-(cyano acrylate) adhesive (Devcon Corp. Zip Grip 10®).

Four kinds of specimen were used. Specimen I had dimensions of 12 x 0.5 x 0.2 cm. To minimize end effects[15], the area of contact between the strips and the tabs (i.e. the bonded area) was kept as small as possible. The length of overlap on each side at both ends of the strips was 1.5 mm. This specimen was used for samples A,B, and C.

Specimen II was used for sample E. It differed from specimen I only in its dimensions, 30 x 1 x 0.1 cm.

Specimen III had dimensions of 12 x 1 x 0.1 cm and was cut from sample D. It was modified to simulate filled systems by attaching an increasing number of steel washers using Zip Grip 10. The steel washers had outer diameters of 0.9525 cm (3/8"), inside diameters of 0.397 cm (5/32"), and thicknesses 0.118 cm (3/64"). These consecutive modifications are listed below.

Specimen	Number	Attachment	Remark
III_o	0	none	sample D only
III_3	3	steel washers	on one side
III_6	6	steel washers	3 on each side
III_9	9	steel washers	3 on one side, 6 on the other
III_{12}	12	steel washers	6 on each side
IV_o	0	none	sample D only
IV_6	6	magnets	3 on each side

Specimen IV was similar to specimen III but the attachments consisted of small magnets glued on so as to simulate attractive forces both in the length direction and perpendicularly to it.

Some specimens of sample A were plasticized by immersion in Dow Corning silicone oil (10 centistokes) for 24 hours. The reasons for the use of the silicone oil are given elsewhere[16].

RESULTS

We begin the presentation of our results by describing some simple experiments involving specimens III and IV. These specimens are anisotropic. We concentrate here only on their behavior in simple tension along the long axis. In Fig. 1 we plotted the constant strain rate modulus F(t) as a function of the time t in logarithmic coordinates for specimens III_N consisting of polybutadiene strips to which N steel washers had been glued. As shown in Fig. 1, attachment of the steel washers produces a stiffening of the specimen but leaves the relaxation spectrum of the polybutadiene unchanged, at least in the time interval from 0.1 to 2 minutes. Values of $\bar{\sigma}(t)/\dot{\varepsilon}t$ obtained on any specimen at different strain rates $\dot{\varepsilon}$ ranging from 0.04 to 0.0004 reciprocal minutes superposed within the experimental error (data not shown). Thus the true stress is a linear function of the strain, $\varepsilon=\dot{\varepsilon}t$.

The responses to step functions of strain were measured as a function of time on specimens III_{12} and IV_6. These responses (not shown)were parallel in logarithmic coordinates. In Fig. 2 we show a plot of

$$\tilde{g}(\lambda_r) = \frac{g(\lambda_r)}{\lambda_r - 1} = \frac{\bar{\sigma}(t_r)}{(\lambda_r - 1)E(t_r)} \tag{24}$$

versus $\lambda_r - 1$, again in logarithmic coordinates. For specimen III_{12} the

strain function $\tilde{g}(\lambda_r)$ is unity. For specimen IV_6, $\tilde{g}(\lambda_r)$ is a nonlinear function of the strain and is qualitatively similar to that obtained on carbon black filled rubbers as will be shown below. Both types of specimen may be considered to imitate the behavior of filled materials. The steel washers simulate an ideal filler which changes neither the relaxation behavior nor the linearity of the true stress-strain relation of the matrix. The magnets change the relaxation behavior of the matrix only slightly (data not shown) but greatly alter the linearity of the true stress-strain relation, evidently because of attractive forces between the "filler particles". Thus, these experiments demonstrate that attractive forces between particles may be responsible for nonlinear strain functions. As pointed out earlier, van der Waals forces provide similar attraction in carbon black filled rubbers between the primary structure aggregates.

We now turn to our experiments on carbon black filled materials. We will discuss essentially only isothermal data at 23°C. Our sample C with 5 phr of structureless thermal black showed linear viscoelastic behavior in the true stress up to about 6% strain, i.e. it followed Eqs. (1) and (14) provided that the true stress was used instead of the nominal stress. These data are not shown. Thus, the N990 (MT) black behaves as an ideal filler at this rather low loading.

The situation is quite different with the high structure black, N347 (HAF-HS). Fig. 3 shows the response of sample A to ramp excitations of strain followed by constant strain. The stress is normalized by the isochronal stress at t_r=10 minutes for convenience. Letting t_1

denote the time required for imposition of the ramp, the normalized stresses obtained for different strains collapse into a single curve at times longer than $10t_1$. Thus sample A obeys our basic assumption that the relaxation behavior is not affected by the magnitude of the strain. Similar behavior was obtained with sample B with which the experiments were carried to even longer times. The crossplot of the isochronal data for this sample is displayed in Fig. 4. we attempted unsuccessfully to fit the data points below λ_r=1.4 in the usual manner[4,5] to obtain the strain parameter n. The failure results from the strong curvature at small strains which is clearly seen in the insert. Over this range of stretch ratios unfilled crosslinked or uncrosslinked SBR is linear in the true stress[4,5]. The data obtained on sample A (not shown) failed in the same way.

Fig. 5 shows a plot of $\sigma(t)/\dot{\varepsilon}$ against t for sample A. The four curves at different strain rates would collapse into a single curve if the response of the material were linearly viscoelastic[16]. With sample A such a collapse occurs only below a strain rate of 4.348×10^{-3} reciprocal minutes. We used our lowest strain rate, 0.4348×10^{-3} reciprocal minutes, as our reference and denote it by $\dot{\varepsilon}_o$.

Because of the failure of the n-measure of strain with the carbon black filled materials, we must resort to the generalized strain function, $\tilde{g}(\lambda)$. The upper curve in Fig. 6 represents ramp response data on sample A, normalized by the linear constant strain rate modulus, $\sigma(t;\dot{\varepsilon}_o)/\dot{\varepsilon}_o$. This plot is based on model HS. At small strains we have

$$\lim_{\lambda \to 1} \bar{\sigma}(t) = \sigma(;\dot{\varepsilon}_o) = F(t)\dot{\varepsilon}_o t \tag{25}$$

because $\lambda - 1 = \dot{\varepsilon}_o t$. Hence

$$\frac{\bar{\sigma}(t;\dot{\varepsilon})/\dot{\varepsilon}}{\sigma(t;\dot{\varepsilon}_o)/\dot{\varepsilon}_o} = \hat{g}(\lambda) \tag{26}$$

The fact that the data for two times, t=0.5 and t=1.0 minutes, superpose, justifies this procedure.

We note that the data points along the bottom curve were obtained in random order. Since all experiments were made on the same specimen, the fact that all points lie on a smooth curve indicate that the specimen was not damaged irreversibly by the testing program and that adequate measures were taken to restore the specimen to its original condition between experiments.

The bottom curve in Fig. 6 represents the isochronal stress, $\bar{\sigma}_r = \bar{\sigma}(t_r)$, at t_r=10 minutes, divided by $\lambda_r - 1$. By Eq. (24) this is equal to $\hat{g}(\lambda_r)E(t_r)$. To obtain $E(t_r)$ we would have had to take data at exceedingly small strains. We could then have ascertained whether or not $\hat{g}(\lambda)$, based on the separability of ramp response data, and $\tilde{g}(\lambda)$, based on the separability of step response data, are identical. The two curves clearly superpose by an empirical vertical shift. Hence $\hat{g}(\lambda) \simeq \tilde{g}(\lambda)$, in agreement with model HS.

Both our models, GS and GL, predict that $\hat{g}(\lambda) \neq \tilde{g}(\lambda)$. To further test these models we turn to the most sensitive experiment we know, the

superposition of a small deformation on a finite stretch[4,5]. Fig. 7 shows $F_s(t,t_r)$ as a function of λ_r for sample A. We approximated[4] $\sigma_r(t)$ by $\sigma_r(t_r) = \sigma_r$. This approximation is entirely satisfactory for sample A under the conditions of the experiment, i.e. for t_r=10 and $t-t_r$ = 0.05 minutes. The strain rates were kept below 4.4×10^{-3} reciprocal minutes. As will be shown later, this ensures that the maximum strain remained within the linear region, i.e. that $\dot{\varepsilon}(t-t_r) << (\lambda_r - 1)$. The predictions of the two models, GS and GL, were calculated from Eqs. (16) and (17). The predictions of the HS model (not shown) are close to those of model GL for small values of λ_r and close to those of model GS for λ_r values. Clearly, neither model agrees with the data.

We next obtained data on sample A similar to those shown in Fig. 7, but at constant λ_r = 1.108, and varying t_r. The results are shown in Fig. 8 and compared with the predictions of the two models. Here, we did not use the approximation $\sigma_r(t) = \sigma_r(t_r)$. Not surprisingly, the data again contradict all three models.

The response in superposition depends also on the strain rate, $\dot{\varepsilon}$. This is shown for sample A in Fig. 9 in which $\Delta\sigma/\dot{\varepsilon}$ is plotted against the time, $t-t_r$, at constant λ_r = 1.327. In these experiments $\Delta\sigma/\dot{\varepsilon}$ is independent of t_r which ranged from 200 to 300 minutes. We see that the superposed ramp response is linear at strain rates below 4.4×10^{-3} reciprocal minutes for times less than 1 minute. It follows from the information presented in Fig. 9 that $(\Delta\bar{\sigma}/\dot{\varepsilon})/(\Delta\sigma/\dot{\varepsilon}_o)$ does not collapse into a single curve. Hence, these experiments reveal that in this material time and strain effects are not separable in the

superposition test. This contradicts the GS model but may be in agreement with models GL and HS. Figure 10 shows curve 2 of Fig. 5 replotted as log F(t) vs. log t, and curve 2 of Fig. 9 replotted as log $F_s(t,t_r)$ vs. log $(t-t_r)$. Now, from Eq. (16)

$$\log F_s(t,t_r) = \log g'(\lambda_r) + \log F(t-t_r) \tag{27}$$

By shifting F(t) to $F(t-t_r)$ and calculating $g'(\lambda_r)$ from Fig. 3, we obtain the predictions of model GS as displayed by the bottom line on Fig. 10. The experimental error does not allow any clear conclusion as to whether the two top curves are parallel or not. If they were parallel, strain and time effects would be separable in superposition. However, this proposition cannot be sustained in view of the arguments presented in the preceding paragraph.

On sample B we made only one superposition experiment. This confirmed that sample B and A behaved qualitatively in the same way. We determined $F_s(301, 300)$ to be 11.8 bar at $\lambda_r = 1.333$ and $\dot{\varepsilon} = 4.44 \times 10^{-4}$ reciprocal minutes. We also obtained F(1) = 5.14 bar from a ramp test at the same strain rate. Thus $F_s(301, 300)/F(1) = 2.29$. This ratio cannot be predicted by either model GS, GL, or HS using the data from Fig. 4 for $g(\lambda)$.

Finally, Figs. 11 and 12 show master curves of E(t) for the filled sample B and for the unfilled matrix, respectively. The isothermal segments were shifted empirically, using the shift factors displayed

in the inserts. The properties of the unfilled sample were described elsewhere[4]. This sample did not require vertical shifts[4,17]. The data were obtained in the linear region. For the master curve of sample B we used the smallest strains which we found experimentally convenient, $\varepsilon \simeq 0.015$. Even though these strains were small, they do not represent the linear region for this highly filled material.

DISCUSSION

We have tested experimental data on the viscoelastic behavior in simple tension of a crosslinked SBR filled with a high-structure carbon black (sample B) against five possible models: (1) and (2) the two models, S and L, based on our n-measure of strain; (3) and (4) our generalized solid and liquid models, GS and GL; and, finally, (5) model HS. Of these, models S, L, GS, and GL failed generally except that model GL predicted a weak dependence of $F_s(t,t_r)$ on t_r, insufficient to account for the observed behavior. Model HS agrees with the experimental observation that $\tilde{g}(\lambda) \simeq \hat{g}(\lambda)$. Thus, it can handle data reduction in simple ramp and step response. However, it fails in the more sensitive superposition test, as do all the other. Thus we have not succeeded in presenting a usable constitutive equation for the viscoelastic behavior of carbon black filled systems.

Perhaps the most significant result obtained in this study is the experimental demonstration, illustrated in Fig. 7, of a time-dependent increase in the small deformation constant strain rate modulus. We interpret this as a reflection of the time-dependent reformation of a three-dimensional network resulting from the secondary aggregation of primary structure aggregates. The superposition of a small deformation on a finite stretch may be considered to act as a probe exploring the rebuilding, in the new configuration, of the carbon black structure which existed in the undeformed specimen and which was destroyed by the

imposition of the finite stretch. The rebuilt structure is unlikely to be identical with that in the undeformed sample because of orientation effects. This is clearly shown by the fact that our experiment on sample B showed that $F_s(301,300)>F(1)$ beyond any possible experimental error. The observed phenomenon is akin to the thixotropy often found in fluid dispersions such as, e.g., hydrocarbon gels[18], paints[19] clay suspension[20], and wheat flour dough[21].

The rebuilding of the structure in thixotropic systems can be characterized by a *thixotropic retardation (or rebuilding[18]) time*, or distribution of retardation times. Our data displayed in Fig. 7 are adequate only for a rough estimate of a single retardation time, θ. From the equation

$$F_s(t,t_r) - F_s(t,o) = F_s(t,\infty)(1-\exp-t_r/\theta) \tag{28}$$

we obtain $\theta \simeq 15$ minutes for sample A.

We note that the procedure discussed here represents a useful technique for the characterization of thixotropic phenomena in carbon black filled elastomers. This technique was demonstrated in detail on a single system only. Much further work is needed to correlate the thixotropic behavior with carbon black structure, volumetric loading, the properties of the matrix, effect of temperature, etc. A successful constitutive equation for carbon black filled elastomers must await the incorporation of the thixotropic character of these systems into the mathematical model.

Changes in the carbon black network structure in filled elastomers

must have an effect not only on the time dependent behavior but also on the stress-strain relations. It is evident that a simple stress or strain amplification factors[22,23] would not be able to handle this problem successfully. The two concepts may be formulated as

$$\sigma_\phi = X_\sigma(\phi)\sigma_o \tag{29}$$

and

$$\varepsilon_\phi = X_\varepsilon(\phi)\varepsilon_o \tag{30}$$

where X_σ and X_ε are the stress and the strain amplification factors, respectively, ϕ is the volume fraction of carbon black, and the subscripts, ϕ and o refer to the composite and the matrix respectively. X_ε is generally preferred to X_σ. It has been shown by Mullins and Tobin [23] that Eq. (30) is useful with structureless thermal blacks over a wide range of volumetric loadings and strains. It is less successful with structure blacks.

Figures 13 and 14 show isochronal stress-strain curves, plotted as $\log \bar{\sigma}_r$ vs $\log(\lambda_r-1)$ for samples A and B. The data on sample A displayed in Fig. 13 were replotted from the bottom part of Fig. 6. They are here compared with the unfilled crosslinked SBR sample which we have described elsewhere [4]. All data are isochronal data at t_r=10 minutes. The amount (in phr) of DCP was the same in both samples and

they were crosslinked under the same conditions. Since the presence of carbon black modifies the crosslinking reaction[10] the two samples could not have contained the same amount of covalent crosslinks. They can, nevertheless, be compared qualitatively. Below a true stress of about 3 bars Eqs. (29) and (30) clearly fail. At higher true stresses, or, more appropriately, at strains higher than about 15%, both equations would hold within the apparent experimental error.

This fact was utilized by Kraus[24] whose ingenious shifting procedure takes the form

$$\sigma_{a\phi} = X(\lambda, a\phi; a\phi_r)\sigma_{a\phi_r} \tag{31}$$

in our notation, where ϕ_r denotes a small reference loading, and $\underline{a}$ is a carbon black structure parameter which can be obtained[24] from dibutyl phthalate absorption.

We note that Eq. (31) differs from Eq. (29) in that X is a function of λ in the former but not in the latter. We note further that, if the relaxation spectrum of the rubber is not changed appreciably by the incorporation of varying amounts of carbon black, we have

$$X(\lambda, a\phi) = \hat{g}(\lambda, a\phi) \tag{32}$$

and Kraus's procedure can then be viewed as being based on an extension of model HS to various volumetric loadings and carbon black structures.

Fig. 14 displays data on sample B replotted from Fig. 4. These are compared with the uncrosslinked SBR described elsewhere [5]. All data are at t_r=1 minute. Here, equations (29) and (30) might hold below about 10% strain but certainly fail above it. We believe that the difference between the stress-strain behavior of samples A and B is due primarily to the difference in carbon black content (40 and 75 phr, respectively).

The data on samples A and B were obtained at constant isochronal time. Thus, the data represented by each curve are referred to the same state of viscoelastic relaxation but almost certainly not to the same state of network reformation because the extent of destruction of the original network depends on the magnitude of the finite stretch, i.e. on λ_r. The strain function $g(\lambda_r)$ is independent of the path imposed to attain a given λ_r in a tensile experiment and can therefore be used as the basis of an elastic potential. We satisfied ourselves on this point by comparing the response to the "double ramp" excitation with the response to the "single ramp" excitation illustrated in Fig. 15. Beyond about $t=6t_4$ the two responses were identical.

We conclude this paper by comparing the small deformation tensile relaxation modulus determined on sample B with the modulus found for the corresponding unfilled rubber. The curve shown in Fig. 12 represents E(t) for the uncrosslinked SBR. At the low end of the time span covered, i.e. at $\log t/a_T = -7.5$, E(t) is leaving the transition region and enters a short entanglement plateau located at about

log t/a_T = -4.5. The plateau region is followed by the terminal region characteristic of uncrosslinked polymers.

The E(t) curve, shown in Fig. 11, for sample B containing 75 phr of carbon black, is displaced upwards, as a whole, in comparison with that in Fig. 12 because of the reinforcing effect of the filler. At the same time the entanglement plateau is shifted to shorter times, lying now at about log t/a_T = -6.5. It is followed by a pseudo-flow region which appears to be leveling off into the rubbery plateau to be expected from the crosslinking effect of chain adsorption unto the carbon black aggregates. The pronounced pseudo-flow region is probably explained by the presence of a relatively large (25%) sol fraction.

The shapes of the two curves are quite different. There appears to be no satisfactory way at present to predict the relaxation modulus of carbon black filled uncrosslinked (gum) rubbers from the relaxation modulus of the matrix.

References

1) T. Shinomura and M. Takahashi, *Rubber Chem. Tech.* 43, 440 (1971).

2) W.V. Chang, R. Bloch, and N.W. Tschoegl, *Proc. Natl. Acad. Sci.* U.S.A. (in press).

3) W.V. Chang, R. Bloch, and N.W. Tschoegl, submitted to *Rheol. Acta.*

4) R. Bloch, W.V. Chang, and N.W. Tschoegl, submitted to *Trans. Soc. Rheol.*

5) W.V. Chang, R. Bloch, and N.W. Tschoegl, submitted to *J. Polym. Sci.*

6) P.J. Blatz, S.C. Sharda, and N.W. Tschoegl, *Trans. Soc. Rheol.* 18, 145 (1974).

7) R.W. Ogden, *Rubber Chem. Tech.* 46, 398 (1973).

8) A.R. Payne and R.E. Whittaker, *Rubber Chem. Tech.* 44, 307 (1971).

9) A.I. Medalia, *Rubber Chem. Tech.* 46, 877 (1973).

10) G. Kraus, *Advances in Polym. Sci.* 8, 155 (1971).

11) E.B. Bagley and R.E. Dixon, *Trans. Soc. Rheol.* 18, 371 (1974).

12) T.L. Smith, *Trans. Soc. Rheol.* 6, 61 (1962).

13) M. Morton, Introduction to Rubber Technology, Rheinhold, New York, 1968.

14) G. Kraus, Phillips Petroleum Co., private communication (1974).

15) R. Bloch, Ph.D. Dissertation, California Institute of Technology, (1976) Appendix 2, Pasadena, California 91125.

16) R. Bloch, W.V. Chang, and N.W. Tschoegl, submitted to *Trans. Soc. Rheol.*

17) W.V. Chang, R. Bloch, and N.W. Tschoegl, submitted to *Macromolecules*.

18) B. Järse, *Kolloid Zeitschrift* 178, 35 (1961).

19) J. Pryce-Jones, *Kolloid Zeitschrift* 129, 96 (1952).

20) A. Weiss, *Rheologica Acta* 2, 292 (1962).

21) J.R. Smith, T.L. Smith, and N.W. Tschoegl, *Rheol. Acta.* 9, 239 (1970).

22) E. Guth, P.E. Wack, and R.L. Anthony, *J. Appl. Phys.* 17, 347 (1946).

23) L. Mullins and N.R. Tobin, *J. Appl. Polym. Sci.* 9, 2993 (1965).

24) G. Kraus, *Polym Letters* 8, 601 (1970); *Rubber Chem. Tech.* 44, 199 (1971).

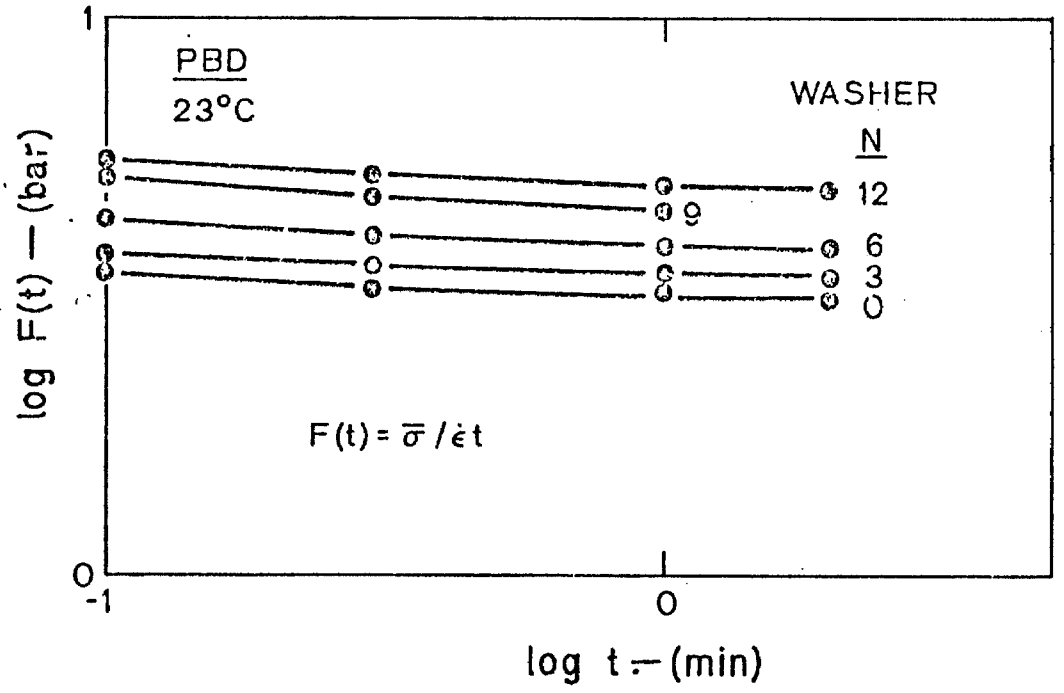

Figure 1 Response to a ramp function of strain of a polybutadiene specimen at 23°C to which N steel washers were attached sequentially.

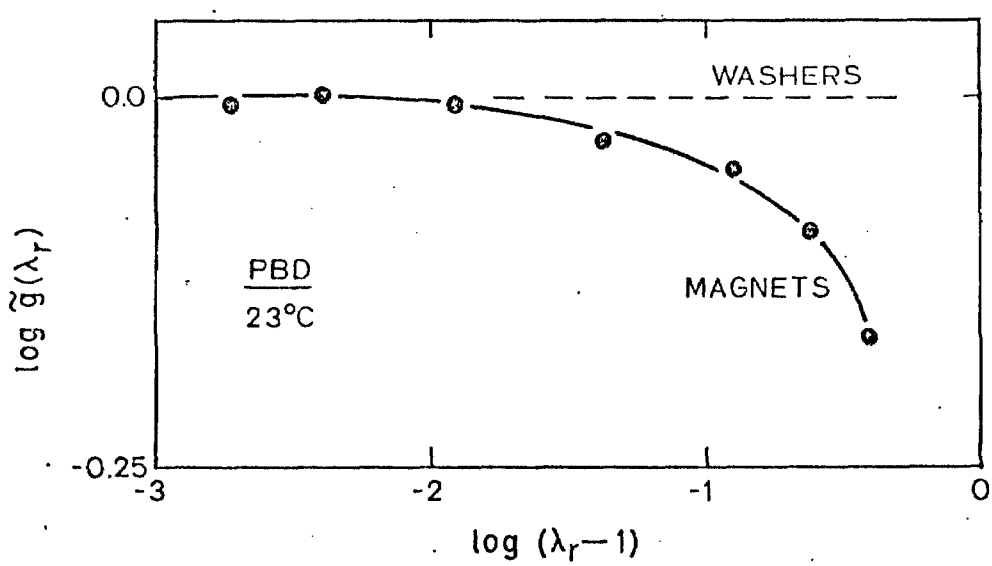

Figure 2 Comparison of the strain function $\tilde{g}(\lambda_r)$ for two polybutadiene specimens at 23°C to which 12 washers or 6 magnets were attached.

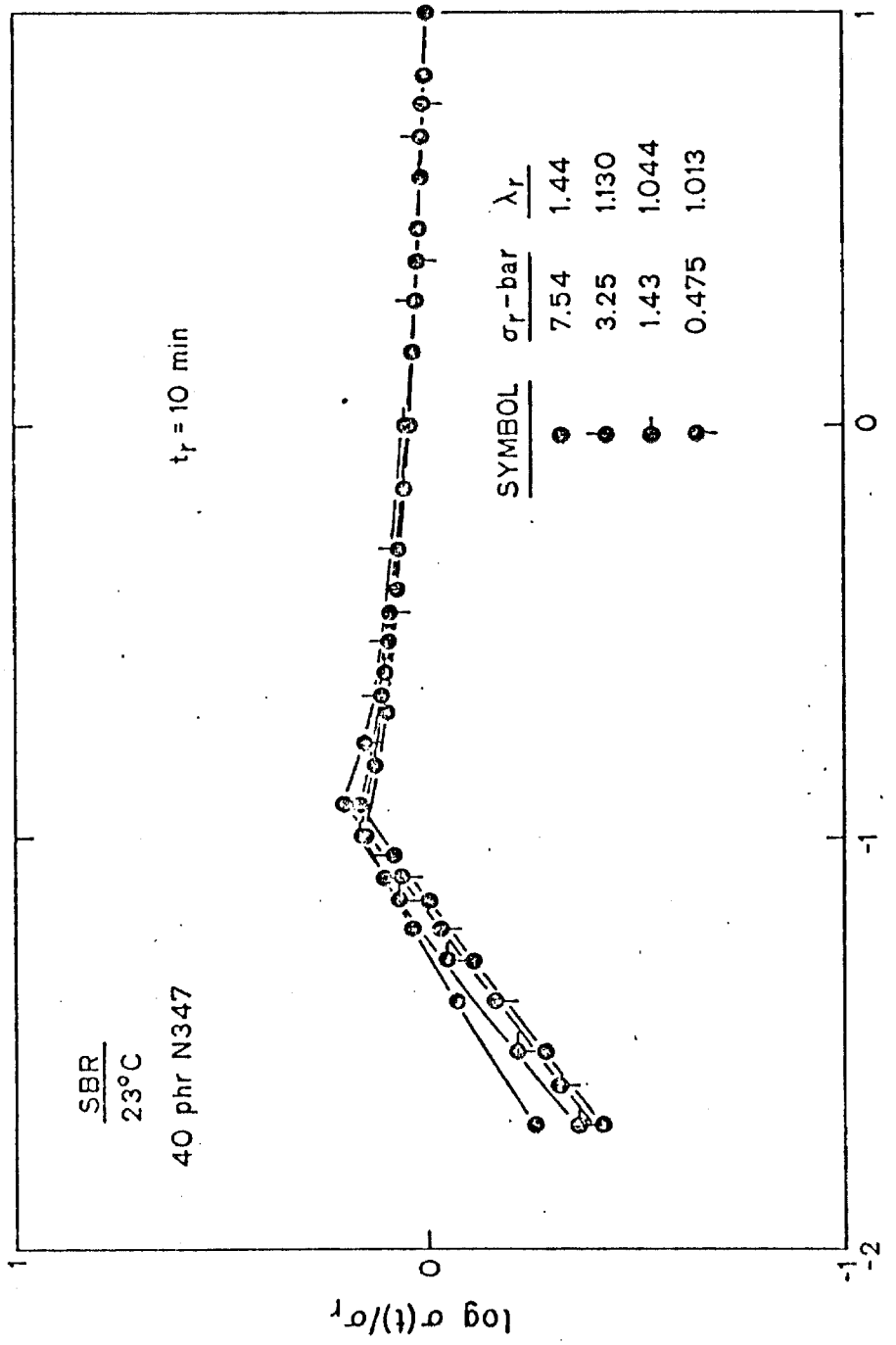

Figure 3 Response to various ramp functions followed by constant strains for SBR filled with 40 phr N347 at 23°C.

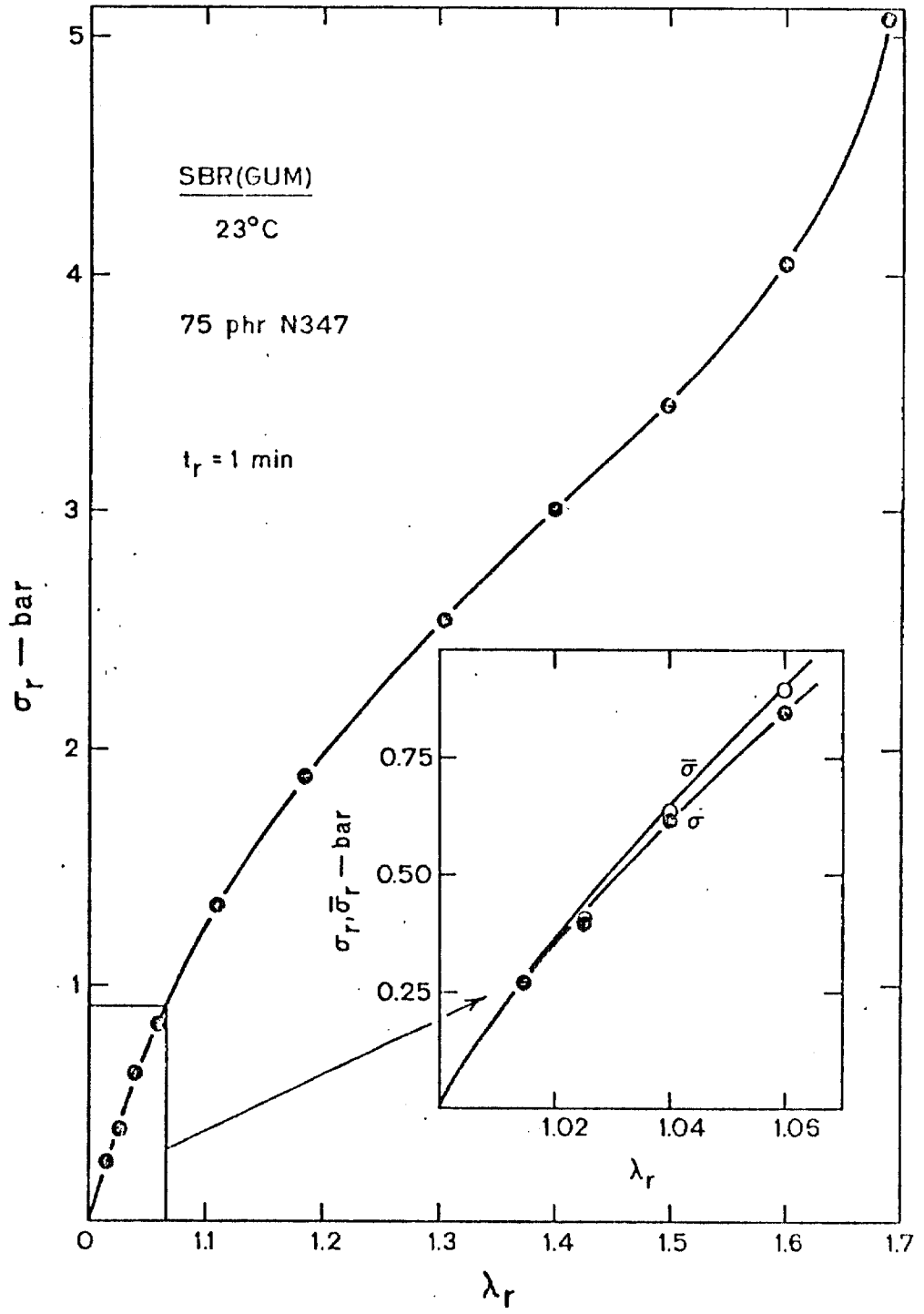

Figure 4 Isochronal stress-strain curve for SBR (GUM) filled with 75 phr N347. Response to step functions of strain at an isochronal time of 1 min. at 23°C.

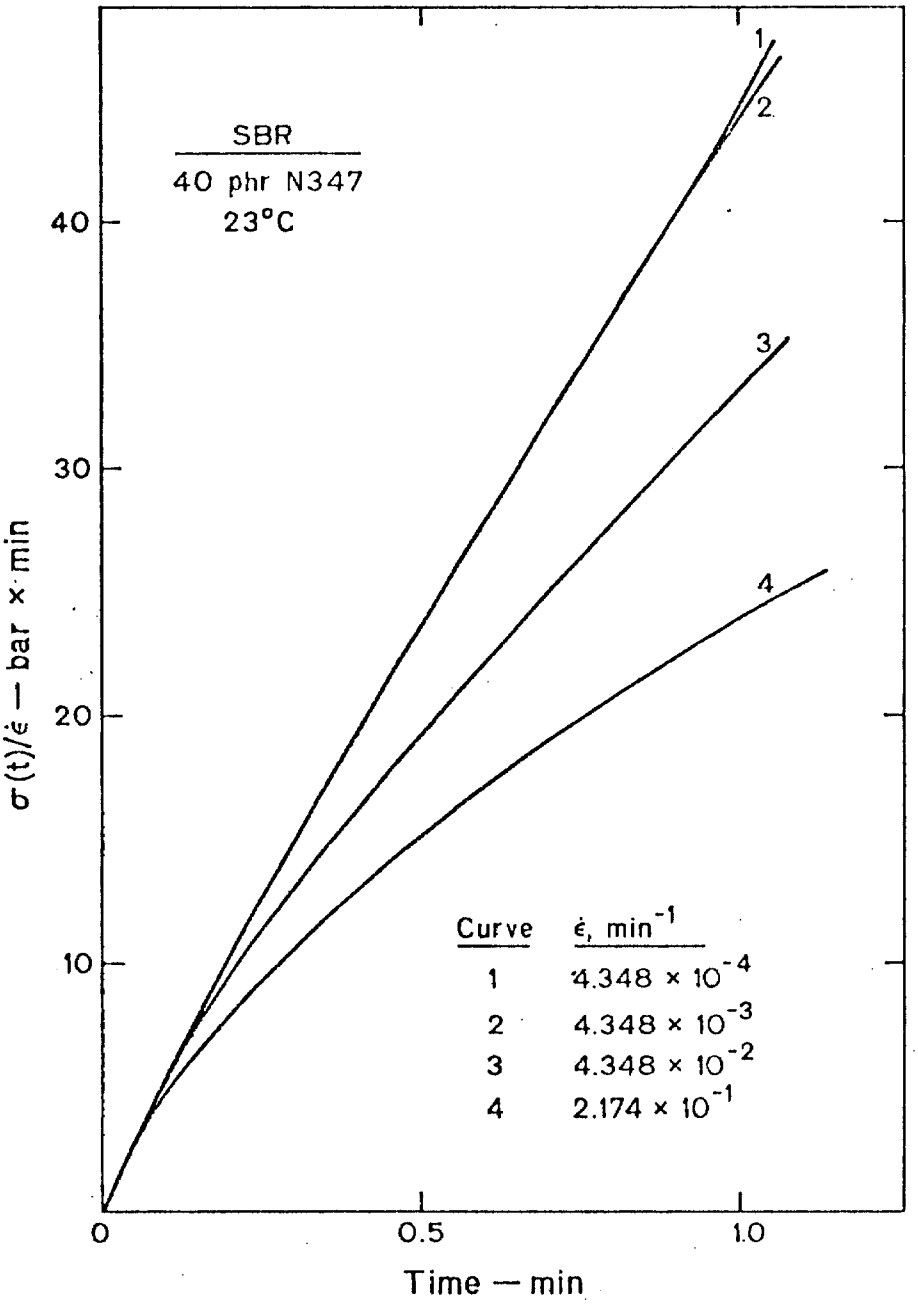

Figure 5 Response to ramp functions of strain at various strain rates for SBR filled with 40 phr N347 at 23°C.

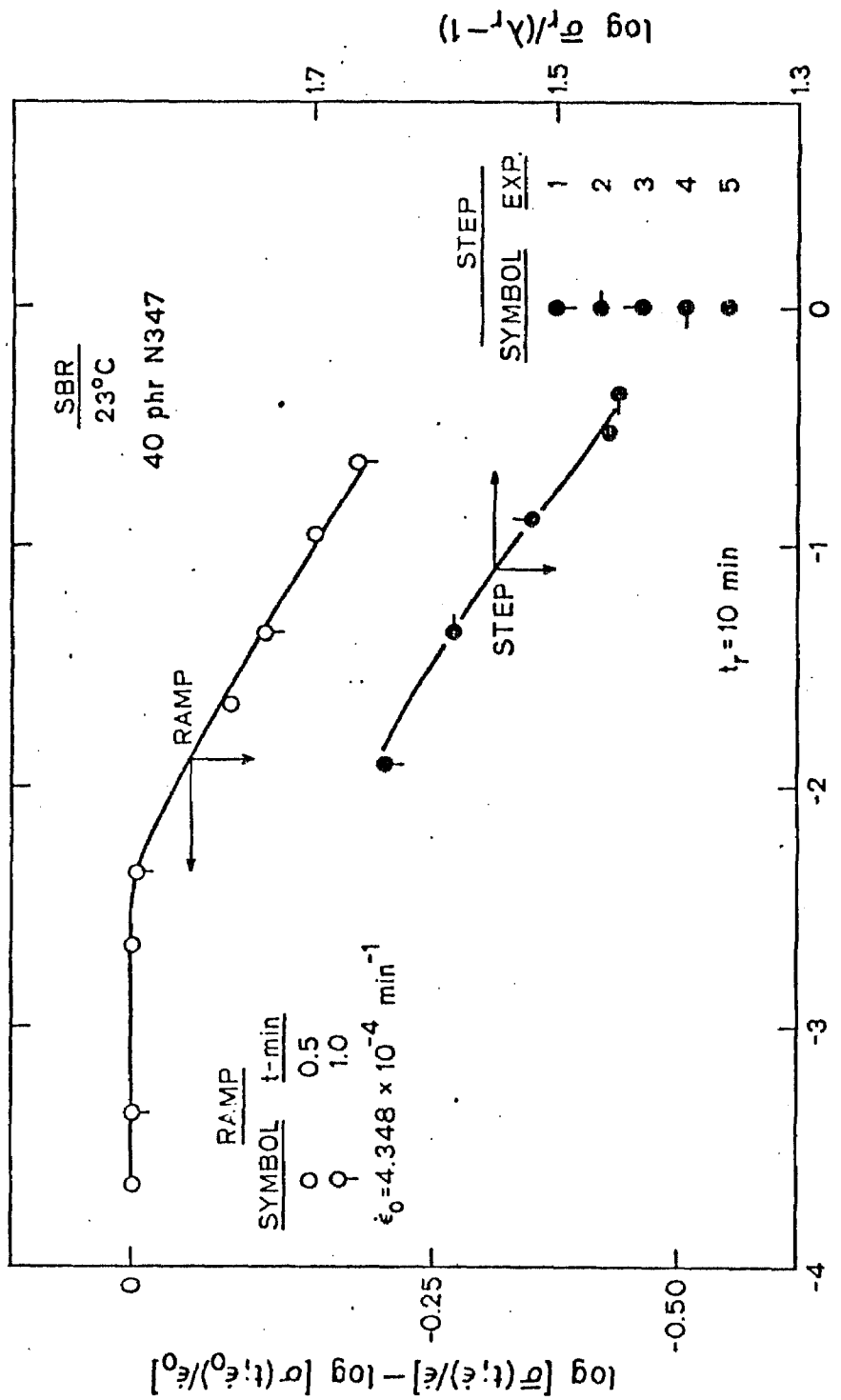

Figure 6 Comparison of $\hat{g}(\lambda)$ as determined from the response to ramp functions of strain with $\tilde{g}(\lambda_r)$ as determined from the response to step functions of strain for SBR filled with 40 phr N347 at 23°C.

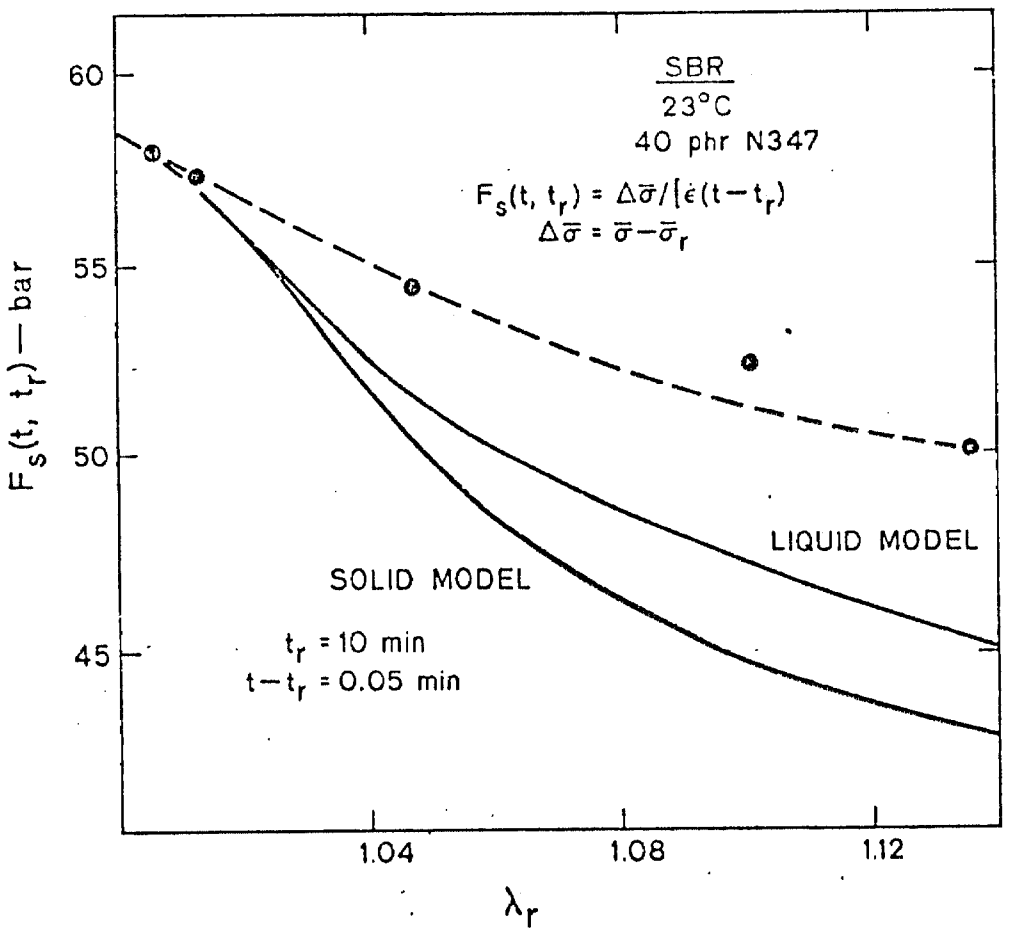

Figure 7 Comparison of the response of SBR filled with 40 phr N347 at 23°C to small ramps superposed on a finite stretch with the predictions of the generalized liquid and solid models. The data was obtained at constant t_r and $t-t_r$ for various λ_r.

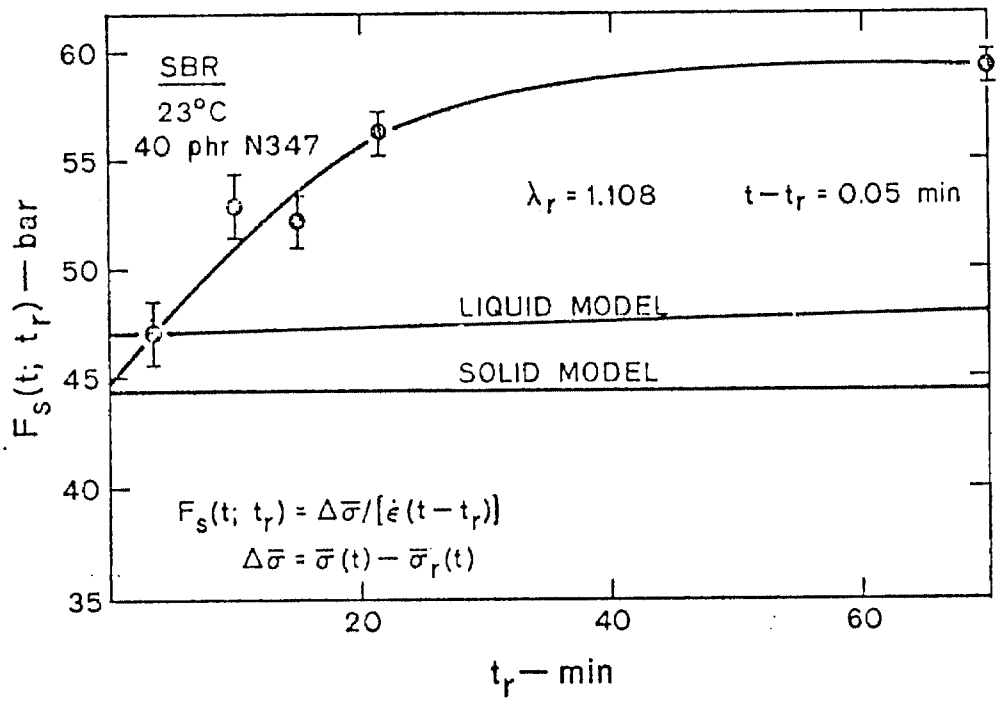

Figure 8 Comparison of the response of SBR filled with 40 phr N347 at 23°C to small ramps superposed on a finite stretch with the predictions of the generalized liquid and solid models. The data were obtained at constant λ_r and $t-t_r$ for various t_r.

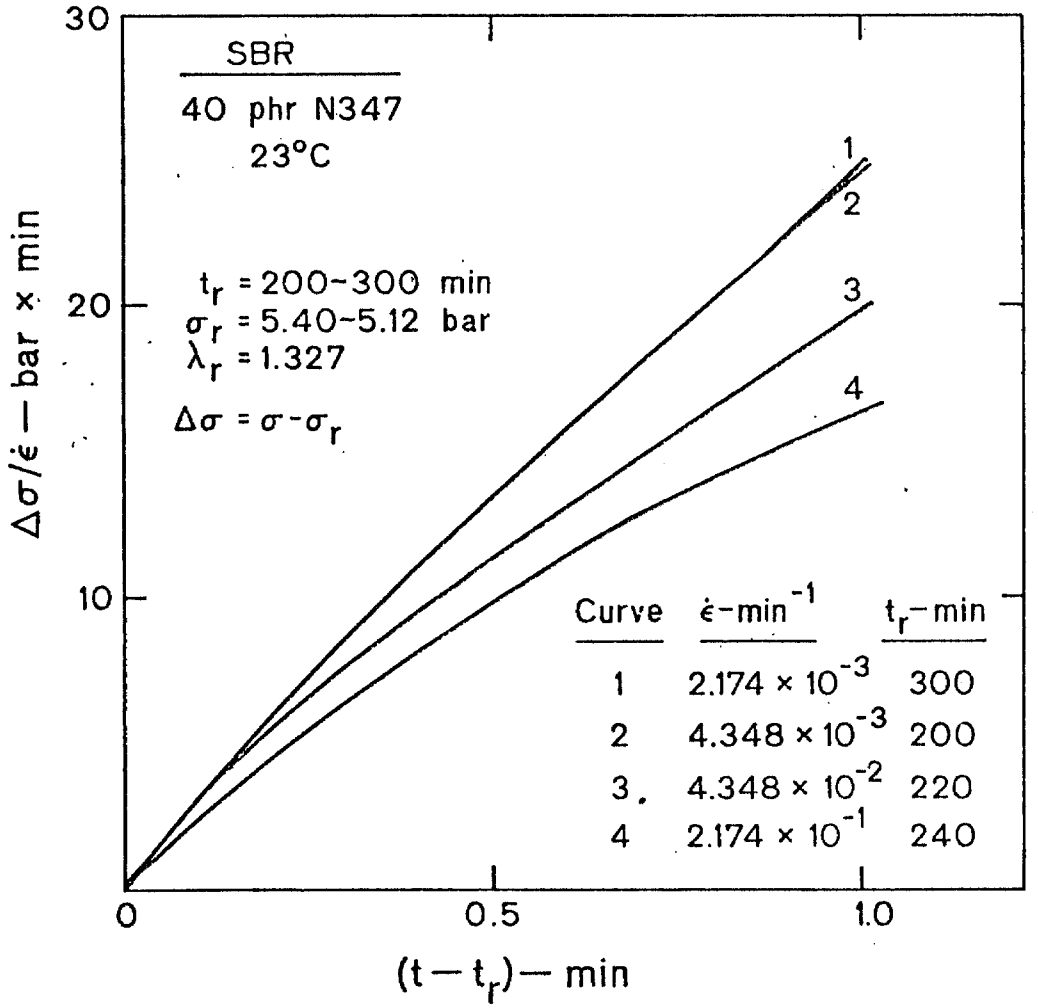

Figure 9 Response to ramp functions of strain superposed on a finite stretch. Data at λ_r=1.327 for SBR filled with 40 phr N347 at 23°C.

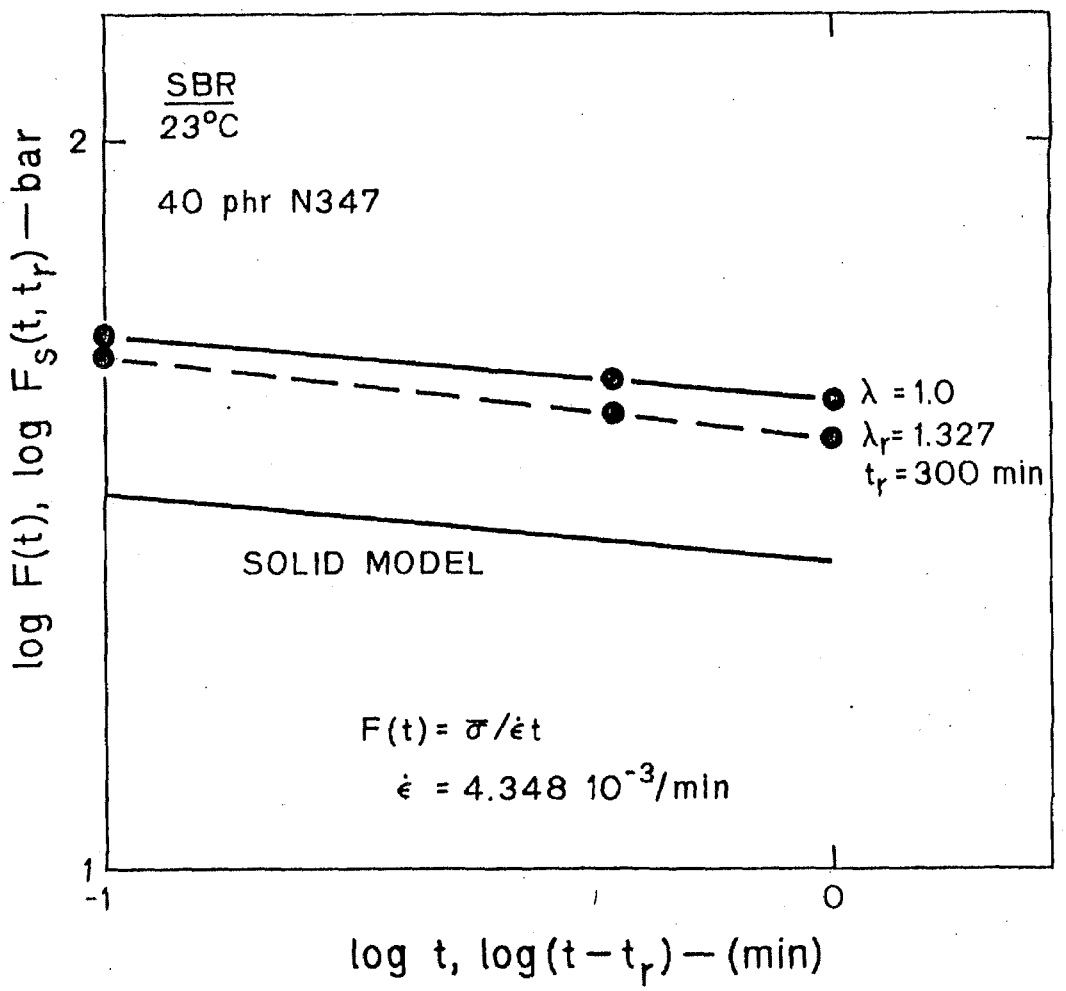

Figure 10 Comparison of the response to a small ramp superposed on a finite stretch and the response to an identical ramp imposed on the unstretch state with the predictions of the generalized solid model for the superposition experiment.

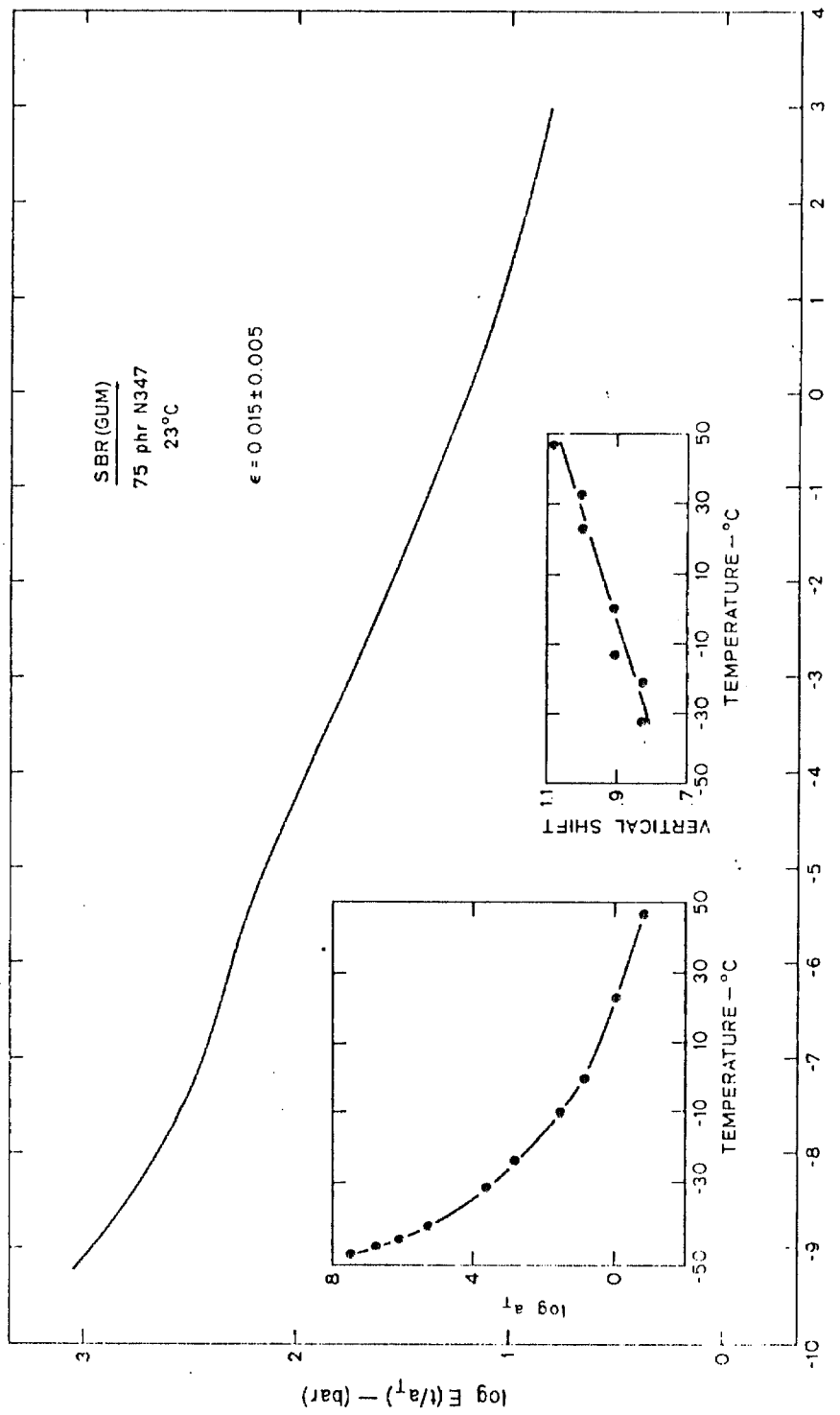

Figure 11 Master curve of SBR (GUM) filled with 75 phr N347 referred to 23°C.

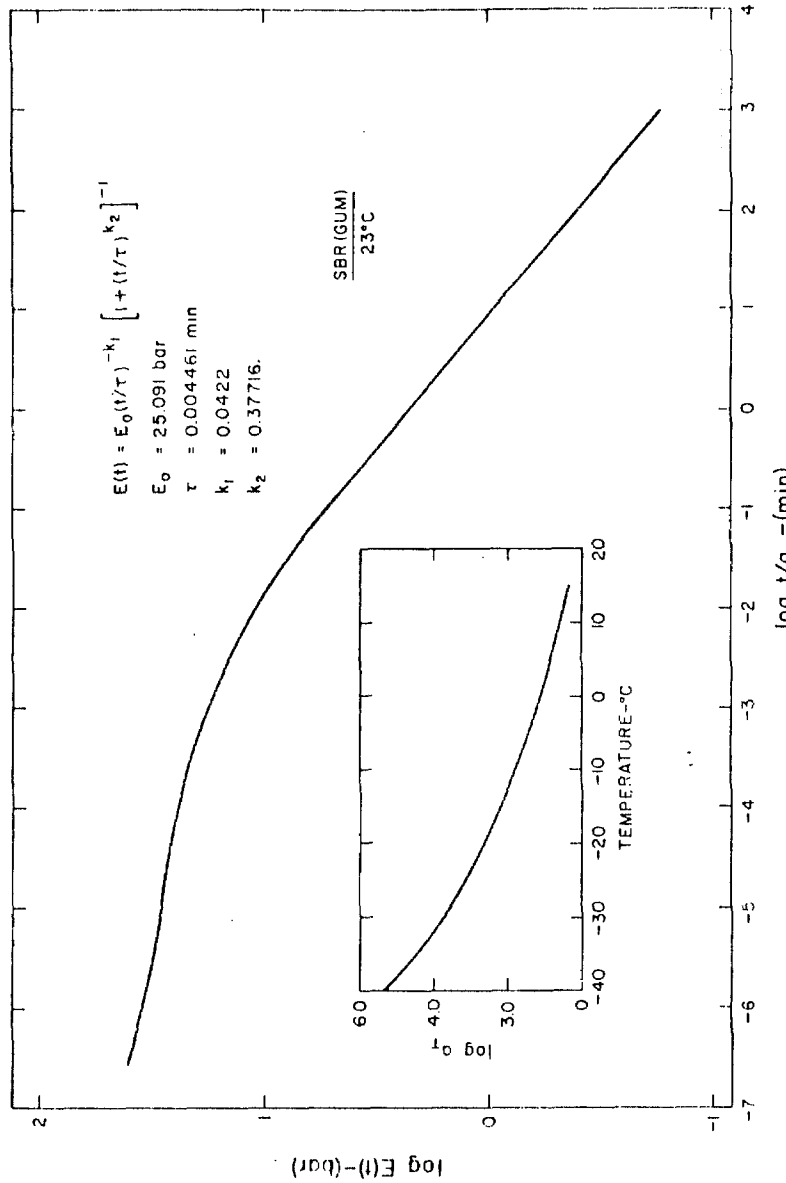

Figure 12 Master curve of SBR (GUM) referred to 23°C. Taken from Reference 5.

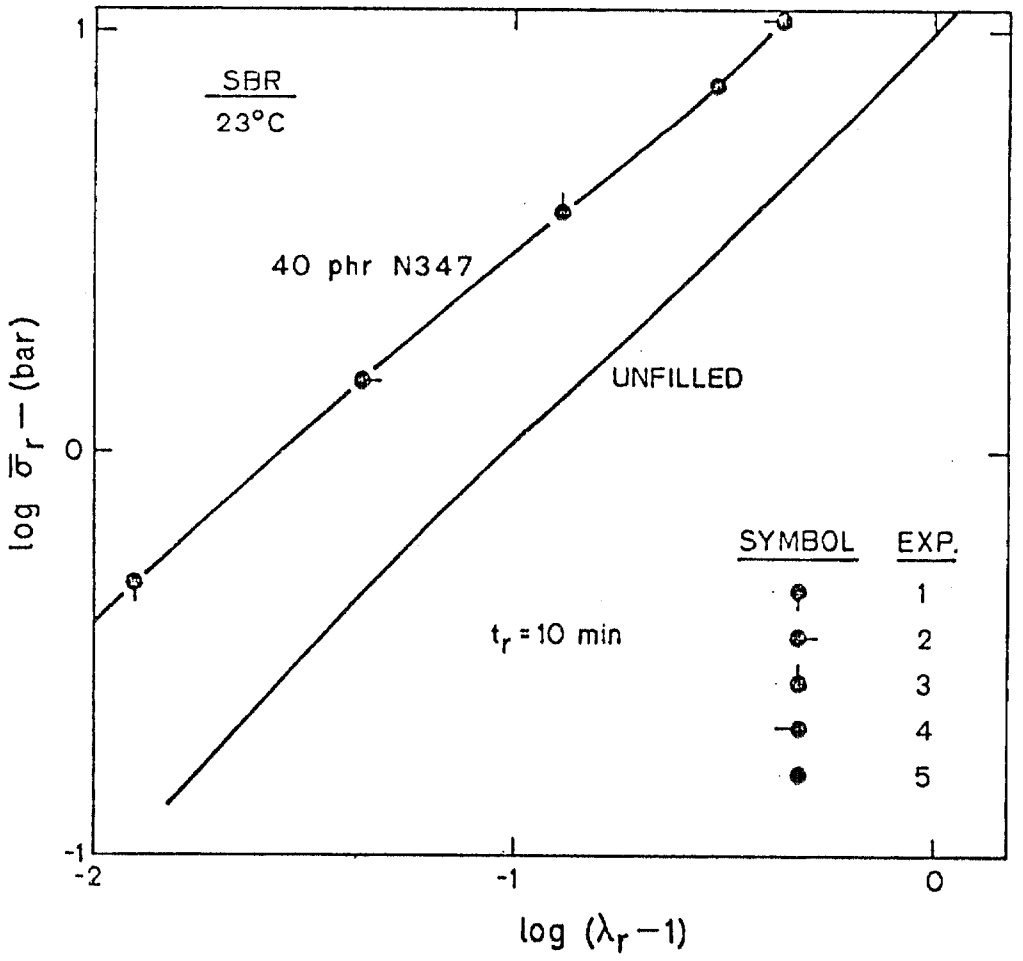

Figure 13 Isochronal stress-strain curves in logarithmic coordinates for unfilled SBR taken from Reference 4, and for the same material filled with 40 phr N347 carbon black, both at 23°C.

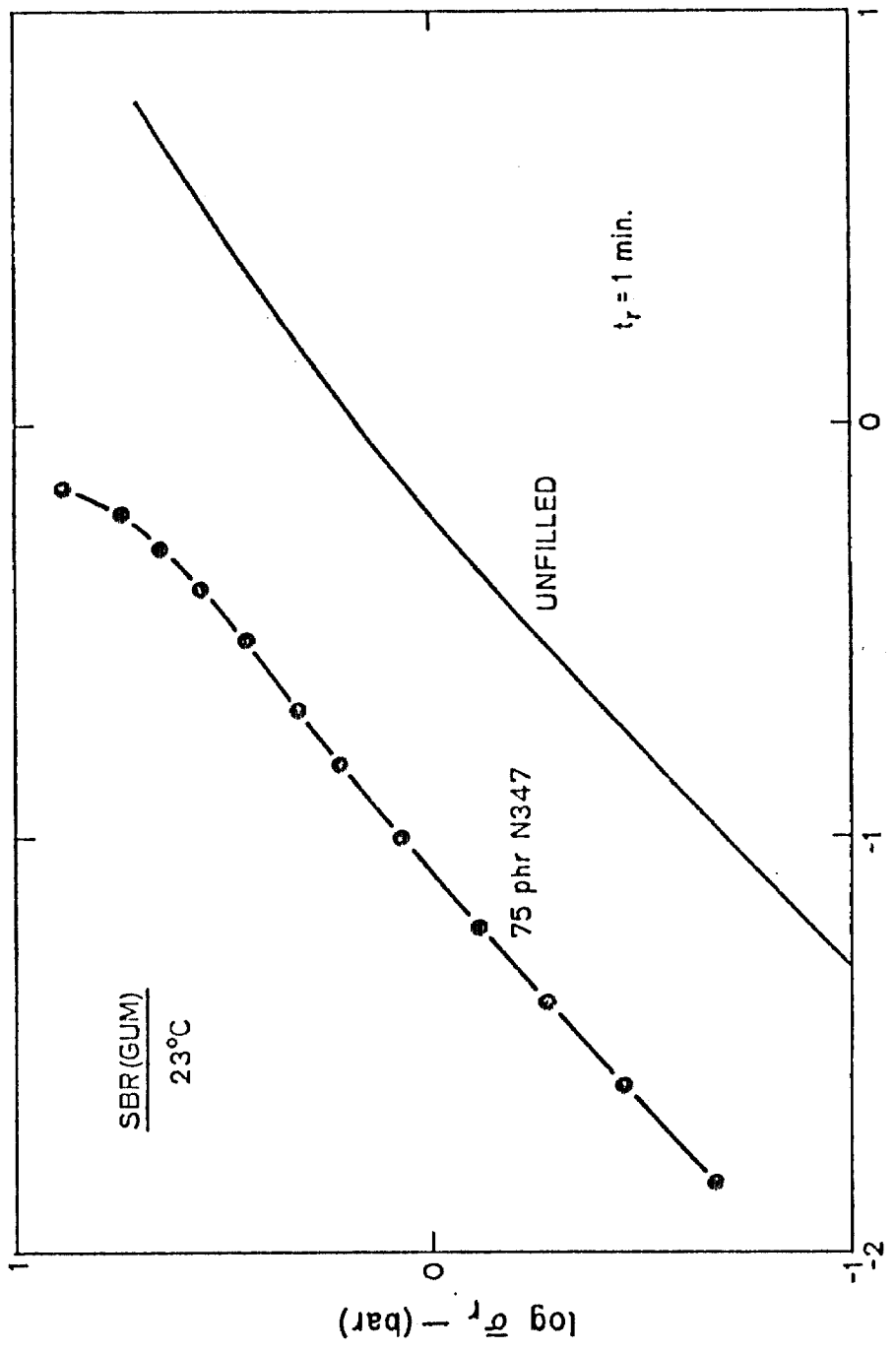

Figure 14 Isochronal stress-strain curves in logarithmic coordinates for uncross-linked unfilled SBR taken from Reference 5, and for the same material filled with 75 phr N347 carbon black both at 23°C.

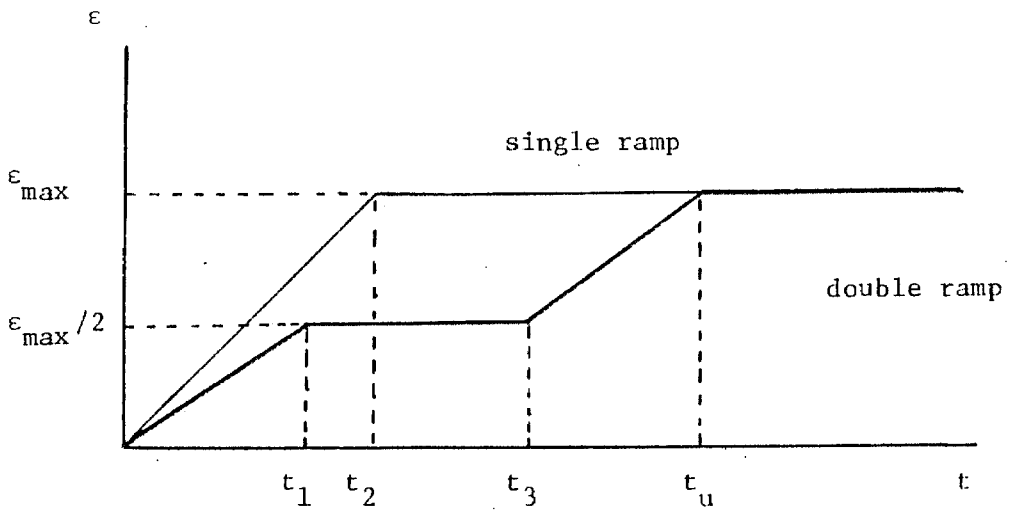

Figure 15 Single ramp and double ramp excitations.

APPENDIX I

THE TIME-DEPENDENT RESPONSE OF SOFT POLYMERS IN MODERATELY LARGE DEFORMATIONS - A NEW APPROACH

W.V. Chang, R. Bloch, and

N.W. Tschoegl

Accepted for Publication in Proc. Nat.

Acad. Sci., April 1976.

ABSTRACT

A new theory successfully describes the time-dependent mechanical behavior of soft incompressible isotropic polymers in moderately large deformations. The theory is based on the introduction of a generalized measure of strain into the Boltzmann superposition integral.

In a polymeric material the ratio of stress at time t to that at an arbitrary reference time t_r in a stress relaxation experiment is usually independent of strain. For stress relaxation in simple tension this behavior was observed by Tobolsky and Andrews (1) on styrene-butadiene rubber (SBR), by Guth et al. (2) on natural rubber (NR), and by us on 1,4-polybutadiene (PBD). Chasset and Thirion (3) studied the stress relaxation behavior of NR and SBR specimens which were prepared with different crosslinking agents. They concluded that the observation holds generally for various network structures. The same behavior was also seen in carbon black and starch xanthide reinforced SBR by Bagley and Dixon (4).

Similar observations have been made in other deformation fields. Our own unpublished data as well as the data of Bergen (5) on carbon black filled SBR and on PVC samples containing various amounts of plasticizer, the data of Gent (6) on SBR, of Valanis and Landel (7) on silica filled poly(dimethyl siloxane) rubber, and by Kawabata (8) on NR and SBR all indicate that the phenomenon is not restricted to simple tension.

This behavior suggests that a constitutive equation containing only a single integral might be more appropriate for the description of time-dependent mechanical properties than one containing multiple integrals. Indeed, several one-dimensional modified Boltzmann integrals have been proposed (e.g. 2,9-12). These attempts can be divided into two classes. One generalizes the integral by replacing the true stress by an experimentally determined function of the tensile stress (12,13). The other replaces the infinitesimal strain of the classical Boltzmann integral

by replacing the true stress by an experimentally determined function of the tensile stress (12,13). The other replaces the infinitesimal strain of the classical Boltzmann integral by a finite strain measure such as the Cauchy or Green strain (9,11,13). Leaderman (14) concluded from multiple step creep and creep recovery experiments that the first approach is inadequate. Hence, it is ruled out from our considerations.

The observations we have cited strongly intimate that the non-linear mechanical response of soft (i.e. rubberlike) materials results from strain non-linearity while time shift invariance is essentially preserved (i.e. the normalized modulus density on relaxation time remains unchanged), at least in moderately large deformations. The term "moderately large" will be made more precise further on.

To introduce our formalism we first consider the purely elastic deformation of an incompressible isotropic soft material. We write our constitutive equation as

$$t^{k}_{\ell} = -p\delta^{k}_{\ell} + 2Gb^{k}_{\ell} \qquad [1]$$

where t^{k}_{ℓ} is the (mixed) Cauchy stress tensor, p is an arbitrary hydrostatic pressure, δ^{k}_{ℓ} is the Kronecker delta, G is the shear modulus, and

$$b^{k}_{\ell} = (\bar{c}^{-1k}_{\ell} - \delta^{k}_{\ell})/2 \qquad [2]$$

is a (mixed) strain tensor defined in terms of Finger's deformation tensor whose contravariant form is

$$\overset{-1}{c}{}^{k\ell} = G^{KL} x^{k}{}_{,K} x^{\ell}{}_{,L} \tag{3}$$

In Eq. 3 the $\{x^k\}$ are the spatial (deformed) coordinates, the comma denotes partial differentiation with respect to the material (undeformed) coordinates $\{X^K\}$, and G_{KL} is the metric tensor of the material system.

Rotation to principal axes yields

$$t_\alpha = \nu^\alpha{}_k \, t^k{}_\ell \, \nu^\ell{}_\alpha \qquad \text{(no summation on } \alpha\text{)} \tag{4}$$

and

$$\overset{-1}{c}{}_\alpha = n^\alpha{}_k \, \overset{-1}{c}{}^k{}_\ell \, n^\ell{}_\alpha \qquad \text{(no summation on } \alpha\text{)} \tag{5}$$

where α=1,2,3, and the $\{\nu^k\}$ and $\{n^k\}$ are the eigenvectors of the stress tensor and the deformation tensor, respectively. For purely elastic isotropic materials, these eigenvectors are identical. Substituting Eqs. 4, 5, and 2 into 1 gives

$$t_\alpha = - p + 2Gb_\alpha \tag{6}$$

where

$$b_\alpha = (\overset{-1}{c}{}_\alpha - 1)/2 = (\lambda_\alpha{}^2 - 1)/2 \tag{7}$$

In Eqs. 4 through 7 the $\{t_\alpha\}$, $\{b_\alpha\}$, and $\{\overset{-1}{c}{}_\alpha\}$ are the principal components of the respective tensors, and the $\{\lambda_\alpha\}$ are the principal stretch

ratios. We note that $b_\alpha = E_\alpha$ where the $\{E_\alpha\}$ are the principal components of the Lagrangean strain tensor, and that $t_\alpha = \bar{\sigma}_\alpha$ where the $\{\bar{\sigma}_\alpha\}$ are the true stress components. This establishes the connection with the notation we have used in preceding publications (19-21). The principal components (i.e. the eigenvalues) of the two tensors, $b^k{}_\ell$ and $E^K{}_L$, are identical. We have replaced $E^K{}_L$ by a strain tensor in spatial coordinates for convenience in extending the treatment to viscoelastic behavior.

To generalize the strain measure, Eq. 7, we now write

$$\underline{b}_\alpha = (\bar{\underline{c}}_\alpha^{-1\, n/2} - 1)/n = (\lambda_\alpha^n - 1)/n \qquad [8]$$

where the underscore distinguishes the generalized tensor components from the classical ones. We prefer $\underline{b}_\alpha$ because the strain exponent, n, will then be positive definite for a rubberlike material. We note that n, a material parameter, has nothing to do with the eigenvectors, n^k.

The idea of a generalized measure of strain is not new. Its earlier history has been reviewed by Truesdell and Toupin (15). Some new measures were proposed by Karni and Reiner (16). Seth (17, 18) applied it to transition field problems such as elastic-plastic transitions, creep, boundary layers, and shocks. Blatz, Sharda, and Tschoegl (19-21) and Ogden (22) independently adopted the idea of a generalized strain measure to predict equilibrium stress-strain relations for crosslinked SBR and NR samples under various modes of deformation. The agreement between the predictions of their theories and the experimental results was unprecedentedly good.

We now adapt the idea to the problem of time-dependent (viscoelastic) deformations by introducing our generalized strain, Eq. 8, into the Boltzmann superposition integral. We obtain

$$\bar{\sigma}_{\alpha}(t) = - p + 2\int_{o}^{t} G(t-u)\frac{d\underline{b}_{\alpha}(u)}{du}du \qquad [9]$$

where t is the present time, u is the past time, and G(t) is the shear relaxation modulus in small (theoretically infinitesimal) deformation. Excluding the glassy and upper transition regions of the viscoelastic response from consideration, we may replace 3G(t) by E(t) where the latter is the tensile small deformation relaxation modulus. Introducing, in addition, the second of Eqs. 8 into Eq. 9 we obtain

$$\bar{\sigma}_{\alpha}(t) = - p + (2/3n)\int_{o}^{t} E(t-u)\frac{d\lambda^{n}_{\alpha}(u)}{du}du \qquad [10]$$

Eq. 10 is limited to moderately large deformations for both theoretical and experimental reasons to be discussed elsewhere. Under a moderately large deformation we understand one which requires only the first term of the elastic potential functions of Blatz, Sharda, and Tschoegl and of Ogden for the description of their mechanical response in purely elastic deformations. In our present notation this single term potential function becomes

$$W = (2G/n)\ I_{\underline{b}} \qquad [11]$$

where $I_{\underline{b}}$ is the first invariant of the generalized strain tensor $\underline{b}^{k}_{\ell}$. Typically, in a moderately large deformation of an unfilled crosslinked rubber the stretch ratio would not exceed about 2.5 in simple tension.

Equation 10 is neither the only admissible form nor is it the most general one. Other admissible forms and their relations with mechanical models will be discussed in a separate paper. The equation reduces to the classical Boltzmann superposition integral for infinitesimal deformations, and it reduces to the stress-strain relations given by Blatz, Sharda and Tschoegl (20) in purely elastic deformations. In particular, the response to a step function of strain in simple tension becomes

$$\bar{\sigma}(t) = (2/3n)(\lambda^{n}-\lambda^{-n/2})E(t) \qquad [12]$$

We note that this relation is true for all times, and, hence, also for a specific isochronal time.

The only material information needed to apply Eq. 10 is a relaxation function and the strain exponent n. The relaxation function can be constructed, utilizing the time-temperature superposition principle, by conducting stress relaxation tests at different temperatures in small deformations. The exponent n can be found, using non-linear least squares fitting, from isochronal stress-strain relations cross-plotted from stress relaxation measurements in simple tension at different values of strain in moderately large deformations. The exponent n, its variation with temperature, crosslink density, nature of material, etc., will be discussed in another forthcoming publication.

As an example, we show here the application of Eq. 10 to constant rate of strain experiments. The experiments were made on specimens of dicumyl peroxide cured SBR 1502 having a 100 minute tensile modulus of 7.55 bar at 23°C. The specimens were slightly swollen (about 1.5%) in silicone oil. The reasons for this are irrelevant to the present discussion and will be presented elsewhere. The strain exponent, n, was 1.22 for this sample at 23°C.

For constant rate of strain, $\dot{\varepsilon}$, Eq. 10 specializes to

$$\bar{\sigma}(t) = (2\dot{\varepsilon}/3) \int_0^t E(t-u)[\lambda^{n-1}(u) + 0.5\lambda^{-n/2-1}(u)]du \qquad [13]$$

where $\lambda(u) = 1 + \dot{\varepsilon}u$. Fig. 1 shows data at four strain rates. The filled circles and the lines represent the experimental data and the theoretical predictions, respectively. Fig. 2 embodies the results of an experiment in which the specimen was first extended at the indicated rate of strain to a predetermined strain, left to relax ($\dot{\varepsilon}=0$), and then brought back to zero stress at a different strain rate 10 minutes after the first stretch was begun (t_r).

We have examined numerous literature data as well as our own. In all cases the agreement between theory and experiment was within experimental error. We have extended our treatment to uncrosslinked materials with similarly good results. These studies will be presented in a series of papers now in preparation.

This work was supported in part by NSF Grant number DMR75-08076.

References

1. Tobolsky, A.V. & Andrews, R.D. (1945) *J. Chem. Phys.* 13, 3-27.
2. Guth, E., Wack, P.E. & Anthony, R.L. (1946) *J. Appl. Phys.* 17, 347-351.
3. Chasset, R. & Thirion, P. (1965) in *Proceedings International Conference on Physics of Noncrystalline Solids* ed. Prins. J.A. (North-Holland, Amsterdam) pp. 345-359.
4. Bagley, E.B. & Dixon, R.E. (1974) *Trans. Soc. Rheol.* 18, 371-394.
5. Bergen, J.T. (1960) in *Viscoelasticity-Phenomenological Aspects*, ed. Bergen, J.T. (Academic Press, New York), pp. 109-132.
6. Gent, A.N. (1962) *J. Appl. Poly. Sci.* 6, 433-448.
7. Valanis, K.C. & Landel, R.F. (1967) *Trans. Soc. Rheol.* 11, 243-256.
8. Kawabata, S. (1973) *J. Macromol. Sci.-Phys.* B8, 605-630.
9. Staverman, A.J. & Schwarzl, F. (1956) in *Die Physik der Hochpolymeren*, Vol. IV, ed. Stuart, H.A. (Springer-Verlag, Berlin) pp. 138-140.
10. Leaderman, H. (1962) *Trans. Soc. Rheol.* 6, 361-382.
11. Halpin, J.C. (1965) *J. Appl. Phys.* 36, 2975-2982.
12. Findley, W.N. & Lai, J.S.Y. (1967) *Trans. Soc. Rheol.* 11, 361-380.
13. Leaderman, H. (1943) *Elastic and Creep Properties of Filaments and Other High Polymers* (The Textile Foundation, Washington D.C.).
14. Leaderman, H., McCrackin, F. & Nakada,). (1963) *Trans. Soc. Rheol.* 7, 111-123.
15. Truesdell, C. & Toupin, R. (1960) "Principles of Classical Mechanics and Field Theory", in *Encyclopedia of Physics*, ed. Flügge, S.

(Springer-Verlag, Berlin), Vol. III, part 1, section 33.

16. Karni, Z. & Reiner M. (1964) in *IUTAM Symp.*, eds. Reiner, M & Abir, D. (McMillan, New York), pp 217-227.

17. Seth, B. (1964) in *IUTAM Symp.* eds. Reiner, M. & Abir, D. (McMillan, New York), pp. 162-172.

18. Seth, B.R. (1970) *Bull. Cal. Math.* 62, 49-58.

19. Blatz, B.P., Sharda, S.C. & Tschoegl, N.W. (1973) *Proc. Nat. Acad. Sci., USA*, 70, 3041-3042.

20. Blatz, P.J., Sharda, S.C. & Tschoegl, N.W. (1974) *Trans. Soc. Rheol.* 18, 145-161.

21. Sharda, S.C., Blatz, P.J. & Tschoegl, N.. (1974) *Letters Appl. Eng. Sci.*, 2, 53-62.

22. Ogden, R.W. (1973) *Rubber Chem. Tech.* 46, 398-416.

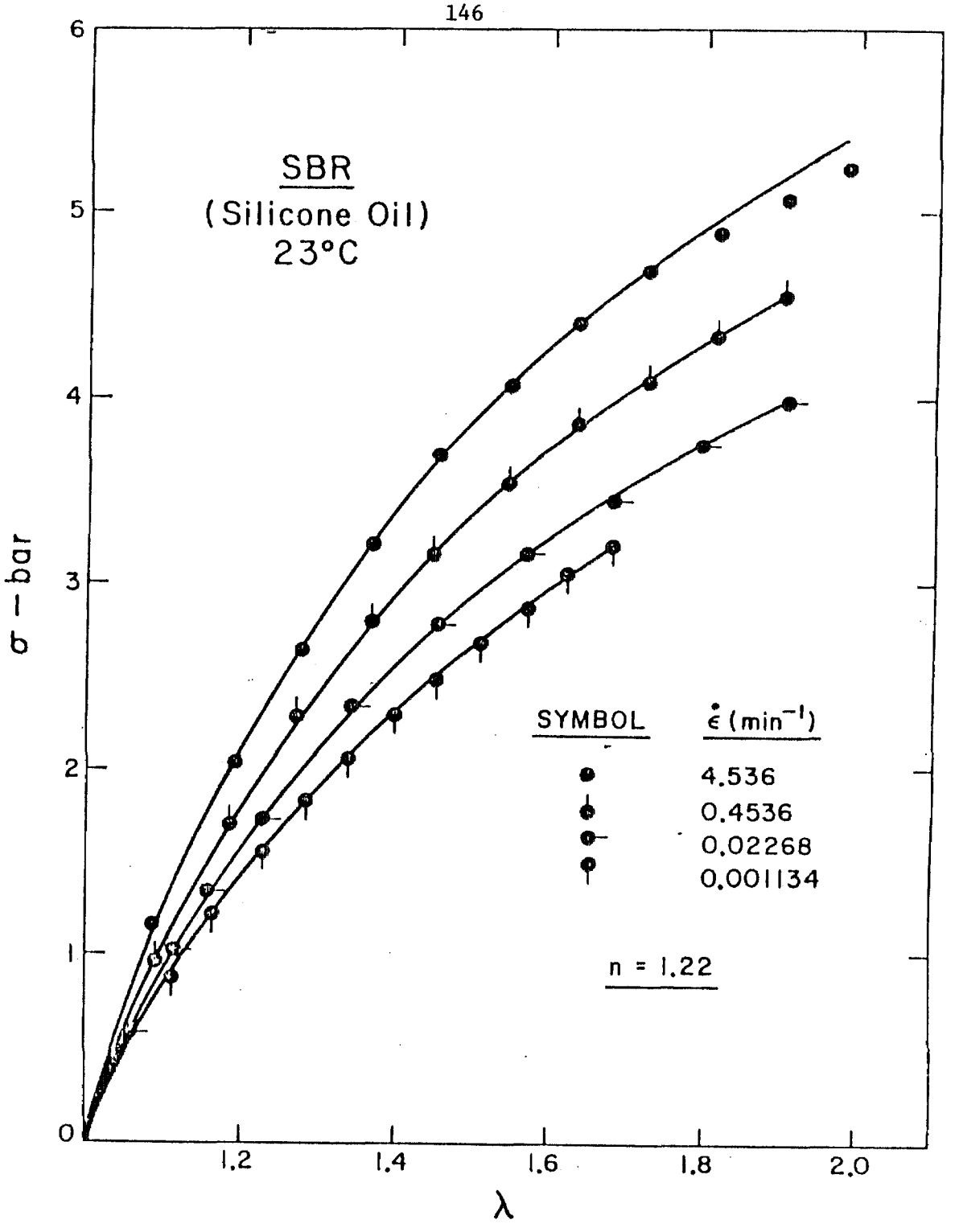

Figure 1. Stress-strain curves on styrene-butadiene rubber at different rates of extension fitted by Eq. 13.

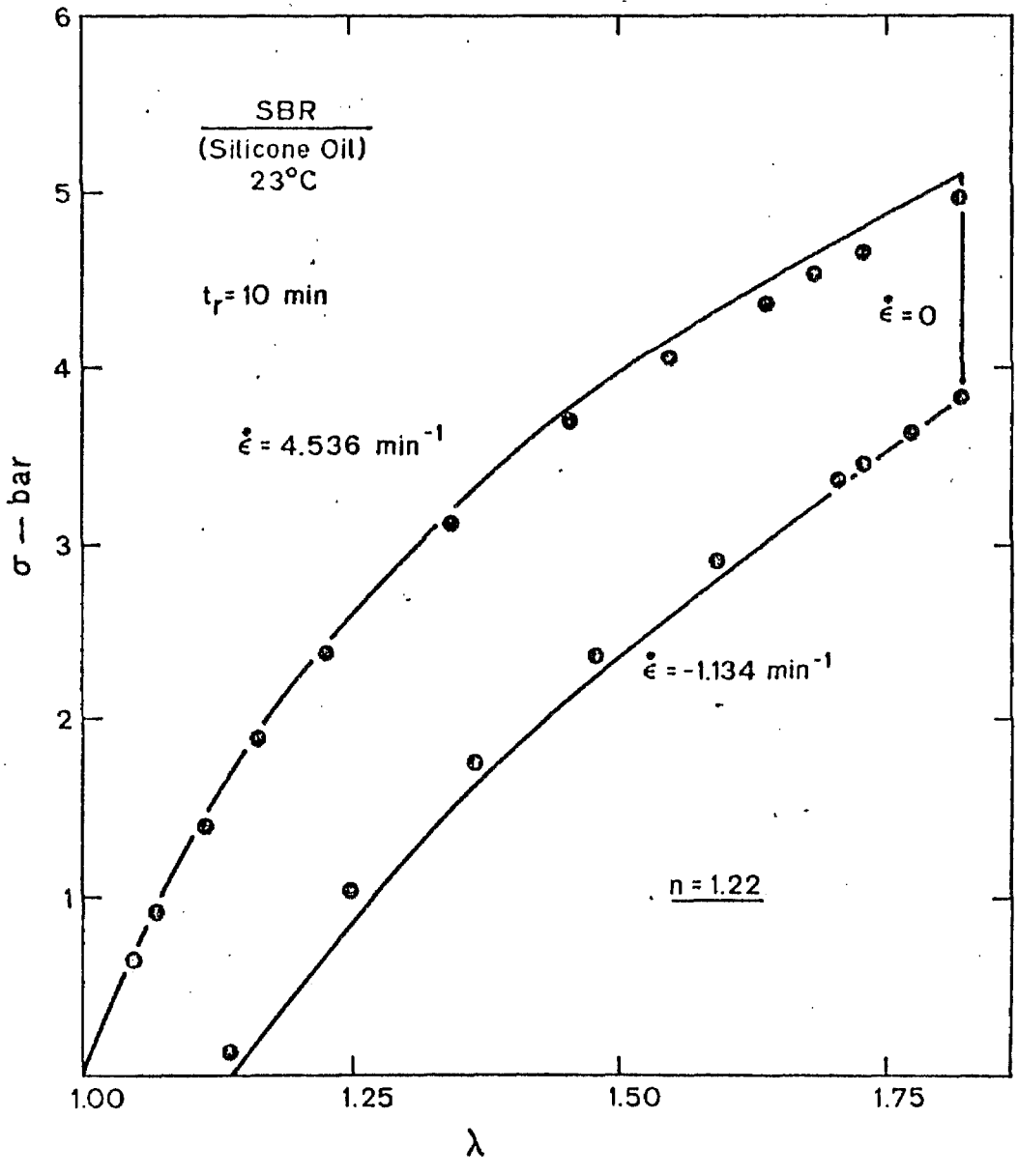

Figure 2. Response to a trapezoidal strain excitation fitted by Eq. 13.

APPENDIX 2

EXPERIMENTAL PROCEDURES

In this appendix some of the experimental procedures followed in the course of this work are presented. We will discuss first the specimen preparation and then we will describe how its mechanical properties are obtained and the types of errors involved in these measurements.

Specimen Preparation

In this work a large variety of specimens were used. However a detailed preparation procedure for such specimens is given only for the most common materials, such as crosslink Styrene Butadiene Rubber (SBR).

The following materials and their corresponding quantities were used

Material	Quantity
SBR	100 parts
N phenyl 2-naphthylamine	1 part
Dicumyl Peroxide (DCP)	variable
Carbon black (different types)	variable

where N phenyl 2-naphthylamine is an antioxidant and DCP is a cross-linking agent.

These substances were mixed using a water cooled roll mill and were added in the following sequence:

A. The SBR was mixed until an even spread was obtained on the rolls. This process took about 10 minutes.

B. The antioxidant and the carbon black were then added slowly to the mill over a period of about 30 minutes while the mixing process was in progress. This time depended on the amount of black incorporated. To obtain a higher homogeneity, the mixture was passed a few times through the rolls while the distance between the rolls was reduced. The final mixture appeared to be homogeneous, although under a microscope (X 100) it was not.

C. The DCP was added last to avoid crosslinking during the mill. This was discussed in detail in chapter 3.

D. The rolls were adjusted to obtain a mixture of desired thickness. After this mixing process was completed the final mixture, now in a sheet form, was allowed to recover in creep at room temperature. This recovery took about 8 hours. The next step was to mold the mixture by means of a hot press into 6" x 6" sheets. This molding process was done as follows:

1. To standardize the process the mold, in the press, was preheated to the desired temperature, usually around 300°F.
2. Then the mixture was quickly loaded into the mold and placed in the press.

3. The pressure in the press was increased and decreased several times from atmospheric pressure to 25000 psi. The reason for this pressure variation was to reduce bubbles in the final sheet. This is the most important problem of the molding process and it is most common when the material has a low crosslink density. The mixture was placed in the mold in a single sheet and not in pieces for the same reason.
4. Afterwards the pressure was raised to 25000 psi and the mixture was allowed to crosslink (cure) for about 15 minutes.

The hot mold, with the sheet, was then rapidly cooled to about room temperature. Then the sheet was removed from the mold and labeled. The molded sheet was isotropic (within 2%) as was determined by its swelling behavior.

The sheets were then wrapped in paraffined paper and placed in the refrigerator (0°C). This temperature was chosen since SBR can be easily oxidized at air and room temperature, and cooling reduces the oxidation process.

Strips were cut from the sheets by a knife-edged mill blade discarding the outer 1/2" of the sheet. To facilitate the cut, the sheets were bonded to the surface of a polyethylene sheet. It was noticed that the bonding and debonding process, using double sticking tape, create some substantial stresses at the surface. These stresses

were found to be significant for some materials (uncrosslinked ones) because it allowed some premature break. However, no significant effects were noticed in the mechanical properties (modulus, n etc.) and since the purpose of this thesis was not to include the study of rupture effects this problem was neglected.

The strips had dimensions of 12 cm x 0.5 cm x 0.2 cm. Phosphorous-copper tab ends were bonded to the specimens ends with Devcon Zip Grip 10®, a poly(cyano-acrylate) adhesive, as shown in Fig. 1. In the following we will call specimens these strips. To minimize end effects, the tab ends were made to extend over the specimen for no more than 1 to 2 mm. End effects are nonlinear quantities in the stress strain field caused by the binding technique and will be discussed in the next paragraphs. Before their mechanical testing the specimens were allowed to relax at room temperature. This was done sometimes under vacuum conditions to remove any moisture. This storage procedure did not alter the mechanical properties of the specimens.

Measurements of Mechanical Properties

A floor model INSTRON testing machine (Model TTB) was used in the experiment. This machine allows tests under several modes of tensile deformation. Several of these are discussed in Chapter 2. The force measuring system uses load cells with an accuracy of $\pm$ 0.25 percent.

The crosshead provides a constant rate of specimen deformation independent of the load, with speeds varying from 0.002 in/min. to 20 in./min. The machine is also equipped with a load-elongation recording apparatus. The chart of the recorder is driven synchronously over a wide range of speeds independent of the speed of the crosshead.

This Instron tester is equipped with a Missimers temperature control chamber. The temperature of the specimen is kept constant within about $\pm$ 0.1°C over the temperature range used in our experiments by circulating air of the required temperature through the chamber.

The design of the Instron environmental chamber used at Caltech (Missimers) allows a large current of air to hit the grip which holds the specimen. This air current causes oscillations in the forces measured. These oscillations are fast (100 or more per minute) and their effect on the relaxation curves was found to be small but not negligible in some instances. In order to improve the data, baffles were used to reduce the air currents.

Variations in temperature were found to be negligible for the measurement of the force response to a step function of strain excitation. However, higher accuracy was necessary for superposition experiments, therefore in these cases a bath (silicone oil) was used to keep the specimen at a constant temperature. This was done at conditions where the swelling by silicon oil was negligible. Therefore, the bath does not alter the mechanical behavior. At very low temperatures there was some problem with the temperature controller and

because of this, data for T<-60°C was not obtained. At high temperatures (above 50°C), a visible oxidation of the SBR was observed and therefore no experiments were done at these temperatures. Most of the work was done below 23°C. This oxidation was apparent by the pink color that appears on the specimen, which may be caused by the anti-oxidant.

The Instron load cell measures force within a 1/4% accuracy, which can be reached if the following precautions are kept. First, the internal voltage of the battery is kept at 1 volt, this increases the stability of recorded force. Second, the calibration is repeated as often as possible. This step is needed because some drift was noticed in the "balance zero" of the Instron.

The speeds of the recorder chart were checked and found in good agreement with the specified ones. Similar checks were performed to the range of force switch. The speed of the crosshead is not achievable instantaneously, because of inertia, therefore there is a lag of time in the response. This lag of time depends on the desired speed and makes the data for $t<0.01$ min useless. Therefore, the Instron is restricted for $0.01 \leq t \leq 1000$ min. The upper limit is due to the drifts already discussed.

A problem that should be avoided is to achieve the maximum speed of pen (full scale in 1.5 sec). An example of such response is shown in fig. 2. This problem can be avoided by a proper use of the force range switch. In fig. 2 we plot the stress, σ, versus the strain $(\lambda-1)$

for the same specimen at the same strain rate. The full-circles represent an experiment in which the maximum speed of the pen was achieved. Therefore the pen was not able to follow the force response. The semi-full and empty circles represent correct experiments.

Since the specimen has a large length and a small cross sectional area it can not withstand compressive forces without bending or buckling. This bending is detectable even by a simple inspection and should be avoided by illuminating all compressive forces.

Still some bending may exist due to slight misalignment of the specimen, specially if the specimen is attached with rigid connectors. For this purpose pin connectors were used which allow free rotation of the specimen and reduce this misalignment. In spite of all these precautions this problem cannot be completely eliminated. This is presented in fig. 3 which shows the correct response to a ramp with strain rate of 4.3×10^{-4} min^{-1} and the response of the same specimen, but with some small bending, to the same strain rate. The dotted line represents a procedure, used sometimes, to obtain useful data when this problem occurs. The curve for the bent specimen shows an apparent strain hardening, since the materials used in this study do not possess such a behavior whenever this happened we used the extrapolation procedure already discussed to obtain the zero strain stress point (the reference state).

The stress and strain field are not homogeneous in the specimen due to the cross section area variations in the specimens. This error

is unavoidable in our molding procedure. Therefore we use the average cross sectional area as a measure. However, we think that this error is negligible because the experiments in which the bench marks distances (which will be discussed in the next paragraph) show that in these specimens the deformation field is near homogeneous. The areas measured at different positions are within $\pm$ 2%.

The variation between specimens was reduced by choosing specimens from the center of one sheet only. We used few specimens (less than 5) for each material and for each series of superposition experiments only one specimen was used, because these experiments are very sensitive to variations of conditions. In simple tension it is assumed that

$$\sigma_{22} = \sigma_{33} = 0 \tag{1}$$

$$\sigma_{ij} = 0 \qquad i \neq j \tag{2}$$

$$\varepsilon_{11} = \varepsilon \tag{3}$$

$$\varepsilon_{22} = \varepsilon_{33} = \varepsilon_{ij} = 0 \tag{4}$$

At the bonded edges these assumptions cannot be met. Therefore, we have a complex stress and strain field at such points. If the geometry is adequate this effect can be neglected. In order to find

such a geometry a small experimental study was performed. Before we describe in detail this study, let us consider a brief review of the literature. We found that various experimental studies were performed earlier by Lindsey et al.[1], Gent and Lindley[2], and Moghe and Neff[3], Lindsey et al. performed an experimental and theoretical study. They considered the compression of poker-chips (large diameter cylinders) and found by a detail stress-strain linear elastic analysis that:

- The end-effects introduced by the bonding depends on the aspect ratio (Diameter/height for cylinders) and the higher the aspect ratio the higher the apparent modulus.
- This end-effect is a function of the Poisson ratio, and is more important for uncompressible or near uncompressible (ν = 0.49 to 0.5) materials. Since rubbers are near uncompressible this effect is important.

These authors[1,2,3] found that

$$E_{apparent} = E_{real}\,[f(s)] \tag{5}$$

E = Young's modulus,

f(s) = a function of the aspect ratio

s = aspect ratio

$f(s) \to 1$ as $s \to o$.

The following study was performed in order to find f(s) approximately for the geometry and bonding process chosen in our work.

Therefore we prepared specimens with various aspect ratios and the values which were bonded in such a way that s varies between 1/20 to 1/3. For the specimen with aspect ratio 1/20 a very small area was bonded at the edge of the strip. For the one with aspect ratio 1/4 a large area is bonded (20% of the total area of the specimen). In order to be able to determine the stress strain distribution in the specimen we drew lines (bench marks) on its surface. To obtain thin lines the specimen was prestretched, the line was drawn and then the specimen was released. After relaxation was completed the specimen was pulled to a given position and then the bench to bench marks distances were measured, using a cathetometer. These measurements also included the end to end distance.

In Fig. 4 we present a comparison of the strain $[y=(\lambda-1)_{CENTERS}]$ as measured from the bench marks near the center of the specimen to the strain $[x=(\lambda-1)_{ENDS}]$ as measured by the Instron recorder or by the cathetometer from the two ends of the specimen. The data in the figure is for unfilled SBR at 23°C for a specimen with a aspect ratio s=0.37. The fact that the data do not fall in the diagonal (y=x) indicates that the end-effects produce a nonhomogeneous strain field for a given stress. For very small strains a linear relation (y=1.55x) was obtained between the two strains x and y. Fig. 5 present similar data as Fig. 4 for SBR filled with 40 phr N326 (phr stands for parts per hundred of rubber). This specimen had an aspect ratio s=0.17. We

can see that the deviation from the diagonal are smaller than in the previous figure. We ascribe this to the lower aspect ratio.
At small strains we again found a linear relation between strains x and y (y=1.15x). We performed similar experiments using other aspect ratios (not shown here) and found similar results in all cases. By comparing these experiments we found that the following approximate rule holds

$$1 \leq x/y \leq 1+ks^2 \tag{6}$$

where k≃4 eq. (6) represents a special form of eq (5), which is valid for our bonding technique, we use eq (6) to select the aspect ratio of our specimen.

The specimens used in the present work had an aspect ratio of 1/20 which gives an end-effect error of approximately 1% as calculated from eq. (6). Therefore the strain as measured by the end to end distance is the same (within 1%) as that measured anywhere in the specimen. If we accept this error, bench marks are not needed. In this case we measure the stretch ratio λ by the end to end distance which can be obtained either from the Instron displacement gauges or from the Instron force-time recorder. The displacements can be obtained by gauges on the recorder of the Instron which measure cross-head displacement.

Another result of the experiments presented above was that the dimensions were not time dependent functions. This can be taken to imply that the Poisson ratio of the material and the parameter k in eq (6) are not time dependent functions. The experiments were done

at 23°C within a time range from 0.1 min to 100 min using carbon black filled SBR and unfilled SBR.

Furthermore we study briefly the problems caused by the slipping of the specimen from the mechanical grips of the Instron or by the debonding of the glue. When any of these problems occur they happen very fast. Therefore they are easily detectable from the force-time Instron recorder. In fig. (6) we show that the cathetometer measurements as well as the force measurements of the recorder were not able to detect any changes (the data falls on the diagonal) before the slipping. Whenever this happens all the data obtained before the slipping is accurate and can be used without double checking. Slipping makes it harder to obtain data because rebonding is needed. In Fig (6) we show the strain for a specimen that slips $[(\lambda-1)_{SLIP}]$ versus the strain for a specimen correctly placed which did not slip $[(\lambda-1)_{COR}]$ at the same level of stress. This data was obtained in SBR at 23°C for a strain rate of 0.11 min^{-1}. The balance between the slipping of the specimen and the inhomogeneous stress-strain distribution was achieved by an aspect ratio of 1/20 for the work presented in this thesis. However we remark that for thermoelastic measurements this aspect ratio has to be reduced to 1/50 (because of the extra precision needed[4]). This can be achieved by our bonding technique if the dimensions of the specimen are changed.

We found that when different specimens were used there was an appreciable scatter in the measured mechanical data. To reduce this scatter we used the same specimen for a variety of tests. Such

sequential testing could be done only when no appreciable damage occured in the specimen due to previous tests. In order to verify this assumption in viscoelastic materials we have to account for the relaxation of the material.

We consider the following strain (ε) excitation:

$$\varepsilon = h(t)\varepsilon_1(t) + h(t-t_2)\varepsilon_1(t-t_2) \tag{7}$$

where $h(t)$ is the unit step function, $\varepsilon_1(t)$ is a strain history applied at $t=0$ and $\varepsilon_1(t) = 0$ at $t = t_1$. The strain $\varepsilon_1(t-t_2)$ is the same as $\varepsilon_1(t)$ only applied at later time t_2.

For materials in which no permanent damage occurs (fading memory) the response of the second term in the excitation given by eq (7) will be identical to the response of the first term in the same equation when $t_2 >> t_1$.

In practice the excitation given by Eq. (7) is difficult to be achieved because our experimental technique does not allow for the compressive forces that appear at $t \simeq t_1$. Therefore, we consider the excitation given by Fig. (7), where t_{10} was chosen so that the stress response at that time is close to zero (still positive). The same considerations apply to t_{11}, t_{12} etc. The time t_2 was selected when both the stress and the strain were close to zero (i.e. for case 1 ε at t_2 is less than $\varepsilon_1/100$). We found for case 1 that the response for times past t_2 was within experimental error identical to the

response in the $0-t_o$ interval. We noticed that $t_2 \simeq 5t_{10}$ for crosslinked SBR and $t_2 \simeq 10t_{10}$ for uncrosslinked SBR. For case 2 when $\varepsilon_2 = 10\varepsilon_1$ we found that we can permit some large deviations from zero strain at t_2 (i.e. ε at t_2 was about $\varepsilon_1/20$) this strain will not produce a significant effect in the response part t_2. When this happened we noticed that for uncrosslinked SBR $t_2 \simeq 4t_{10}$. For case 3 when $\varepsilon_3 = 0.1\ \varepsilon_1$ we found that we cannot permit large deviations from zero strain at t_2 (i.e ε at t_2 was about $\varepsilon_1/1000$). This small strain was found not to produce a significant effect in the response part t_2. We notice that for uncrosslinked SBR $t_2 \simeq 40\ t_{10}$.

From these tests we conclude that reproducibility can be achieved if care is taken to permit sufficient relaxation time between experiments. However, the sequential experiments shown in case 3 should be avoided because it requires very long waiting time. This is more important if data at $(t_3-t_2) > 10t_{10}$ is needed.

Reproducibility is not obtained when the strain at any time exceeds a limit. We determine this limit to be about: 250% for SBR, 70% for SBR filled with 40 phr HAF-HS black. Therefore each material has a critical value of strain. A specimen which did not exceed at any time the strain limit discussed above is called "virgin specimen". If the strain is larger than this limit, a permanent damage occurs and the data is no longer reproducible, when it is compared to the virgin state. However, the new "damaged" state is reproducible when it is compared with tests done after the initial damage. This is true when

the strain levels in the subsequent tests do not exceed (approximately) the strains that cause the initial damage. If strains larger than the one that caused the initial damage are applied a new "damaged" material will be obtained. This process can be repeated until rupture.

In this thesis we consider only virgin specimens in order to avoid vacuoles which appear as damage occurs in filled elastomers. Vacuoles are micro-separations between the filler and the rubbery matrix.

References

1. G.H. Lindsey, R.A. Shapery, M.L. Williams and A·R. Zak. The Triaxial tension failure of viscoelastic materials ARL 63-152, Sept. 1963.
2. A.N. Gent, and P.B. Lindley, *Proc. Inst. Mech. Eng.* 173, 111 (1959)
3. S.R. Moghe, H.F. Neff, *J. Appl. Mech.* 38, 393 (1973).
4. W.V. Chang, R. Bloch, and N.W. Tschoegl submitted to *Macromolecules*.

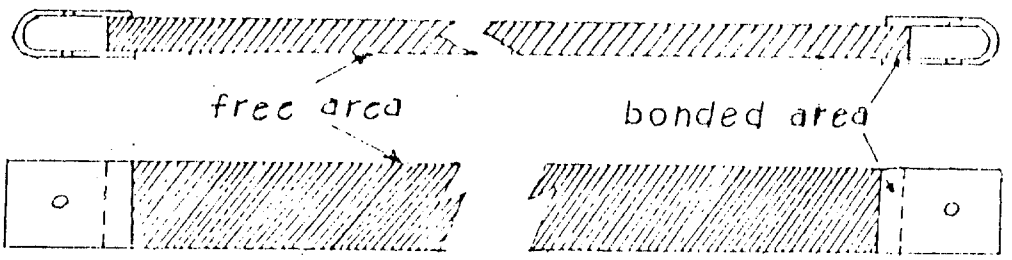

Figure 1 Tab end bonded specimens, side and front view.

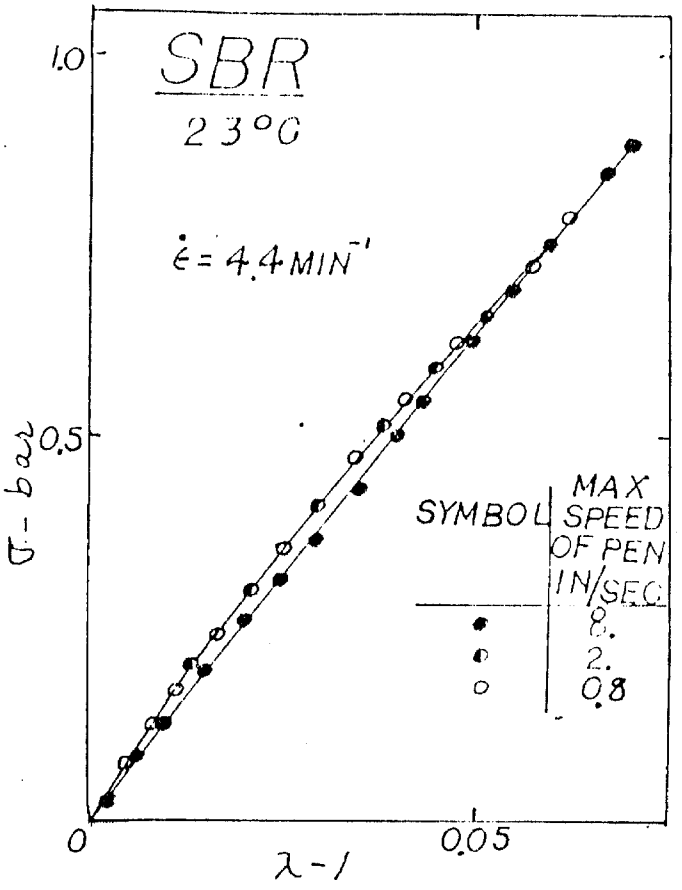

Figure 2 The response of SBR to a ramp function of strain at a fast rate. An example of the error that can be invoked by the slow response of the Instron recorder pen.

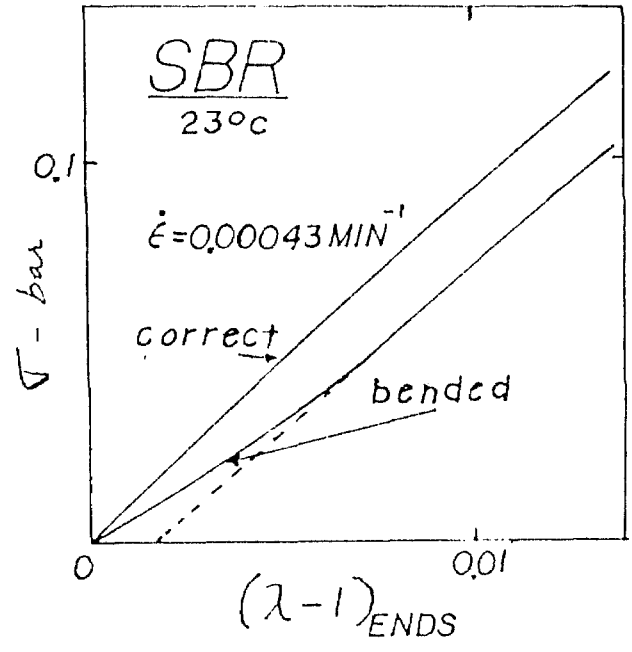

Figure 3 The response of SBR to a ramp function of strain at a slow rate. Comparison of a correctly placed specimen to the same specimen slightly bent.

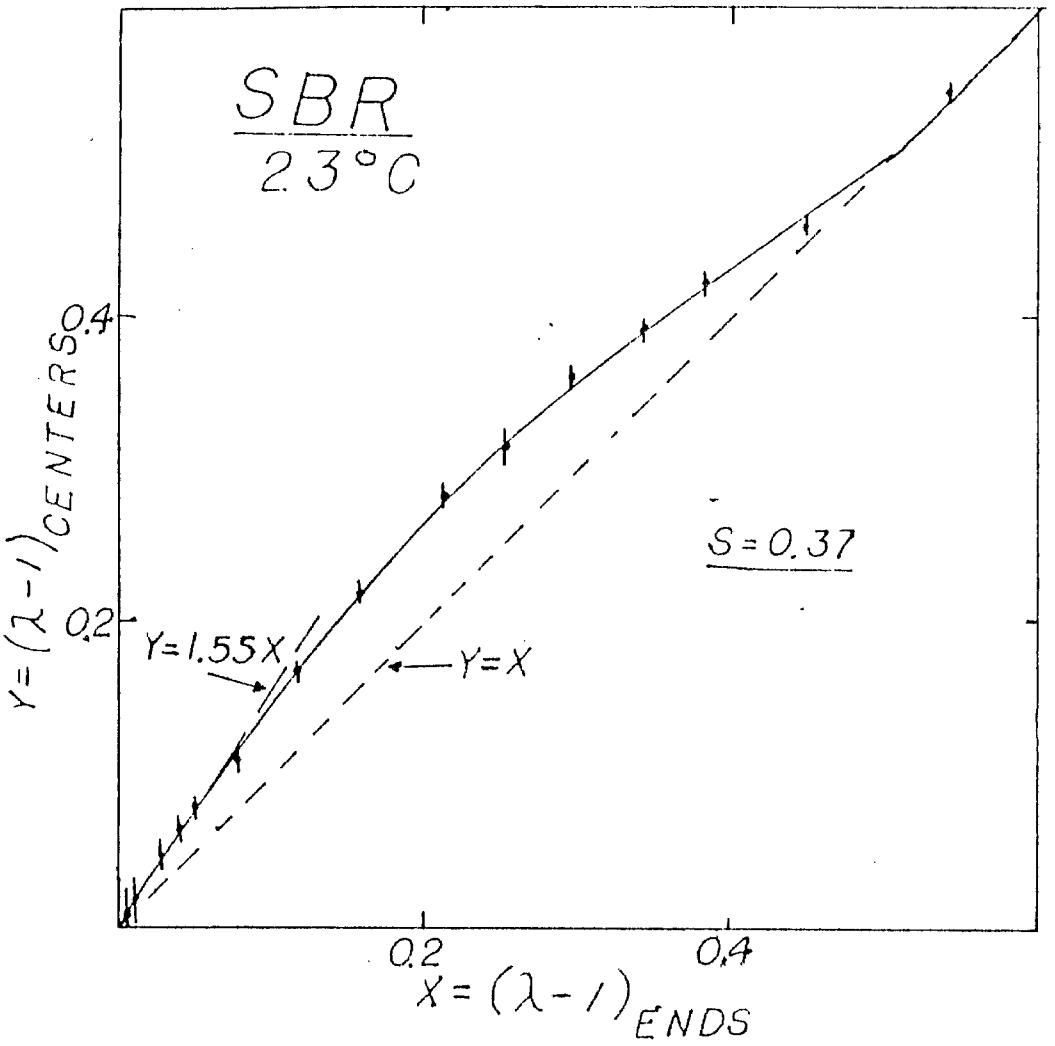

Figure 4 Comparison of the strain as measured near the center of the specimen to the strain as measured from end to end of the specimen, for a specimen with aspect ratio 0.37.

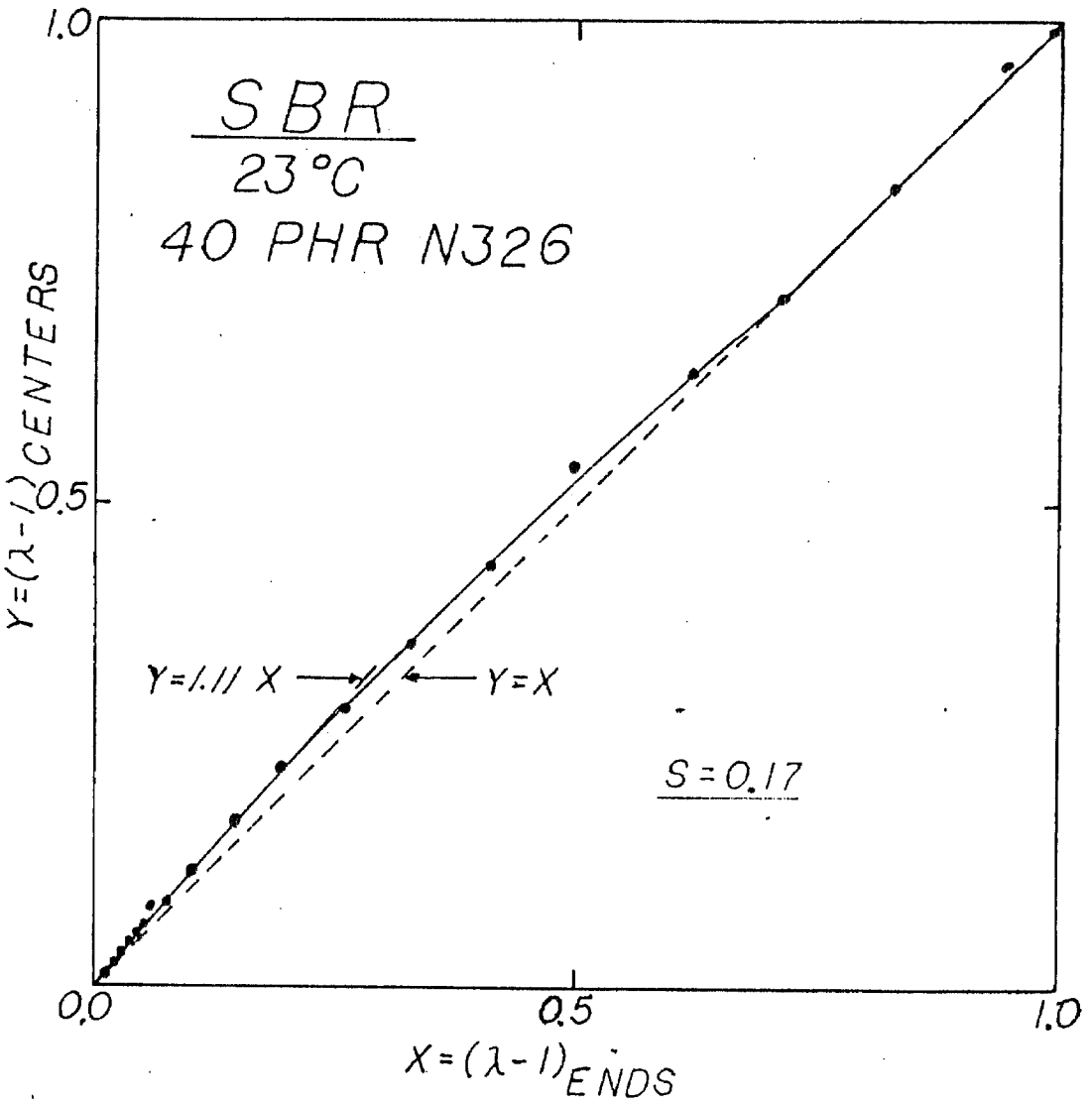

Figure 5 Comparison of the strain as measured near the center of the specimen to the strain as measured from end to end of the specimen, for a specimen with aspect ratio 0.17.

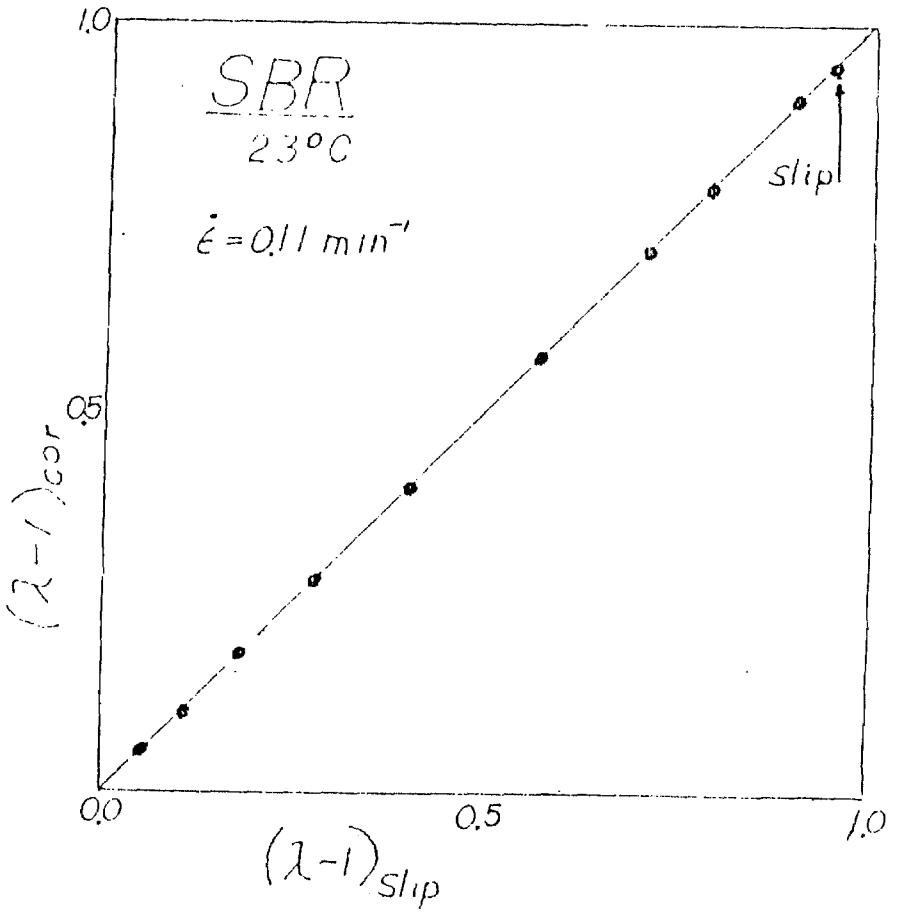

Figure 6. Comparison of the strain at the same stress for the same specimen when no slip occurs and when slip occurs.

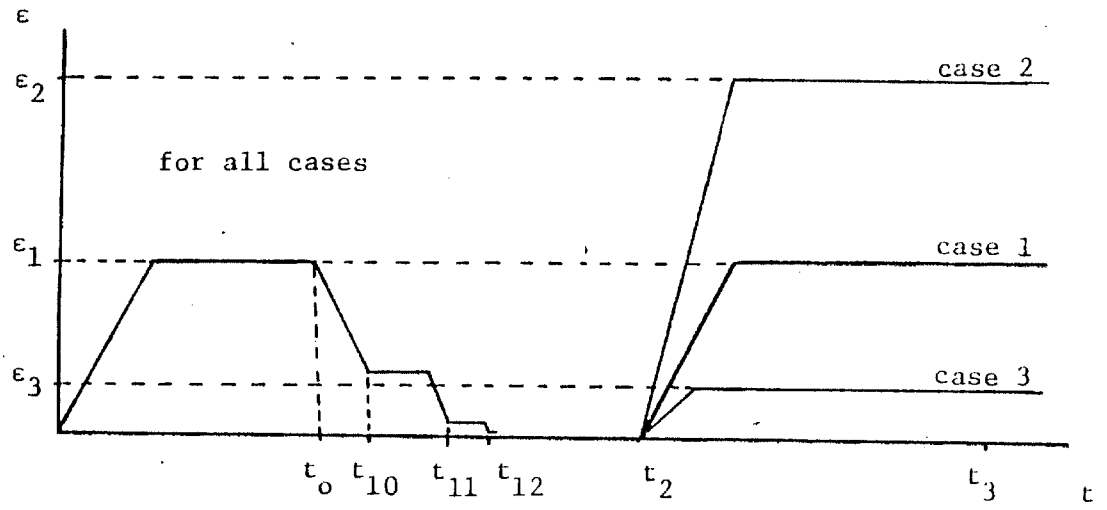

Figure 7 Case 1 is the strain history used to check the reproducibility. Case 2 represents an optimal strain history for sequencial experiments and case 3 is a procedure not recommended.